CALCULATION OF THE ROTATION PERIOD OF MAIN BELT ASTEROIDS

Chrysoula Avdellidou

Department of Physics

Section of Astrophysics, Astronomy and Mechanics

Aristotle University

Supervisors: Professor John H. Seiradakis,

Assistant Professor Kleomenis Tsiganis

To my beloved grandfather
and brother.

Acknowledgements

In order to fulfil this Diploma Thesis many people helped me in different ways during the last two years.
First of all I would like to thank Professor John H. Seiradakis for giving me this subject. He is the most reasonable, kind and clever person that I have ever met and I feel lucky for being his student. With his tolerance and faith I finally managed to conclude this Diploma Thesis.
Simultaneously I want to thank Assistant Professor Kleomenis Tsiganis, for formulating the details of the project. Moreover he helped a lot with the preparation of the observing proposal for Skinakas Observatory.
Also my former fellow student, John Antoniadis, for his precious help at the beginning.
Very helpful was the Director, Mr. G. Panourgias, and the stuff of the Aristotle University's Forest "Vrastamon-Taxiarchis" at Mt. Holomon in Chalkidiki, administered by the Department of Forestry, where we spent many months observing at Holomon Astronomical Station.
Visiting the Skinakas Observatory was a new experience for me. I thank the Time Allocation Committee for accepting my proposal. Special thanks to Associate Professor Iosif Papadakis for his welcome and trust.
Finally, I want to thank my Mom and Dad for their financial help during all these years at the Department of Physics.
I wouldn't have been able neither to undertake the observations that I needed nor to have the psychological encouragement if my fellow student and boyfriend, Panos Ioannidis, was not every minute by my side.

Abstract

This Diploma Thesis is the result of a two-year effort observing and calculating the rotation period of main belt asteroids. The interest for the small bodies in our Solar System has been growing during the last decades. New theories for the Solar System formation are published and every day new objects in Earth's neighbourhood are discovered. These observations were undertaken at the Aristotle University's Astronomical Station at Mt.Holomon and also at Skinakas Observatory in Crete. The rotation period or parts of it was extracted for almost every target that was selected. Moreover the behaviour of the orbit of a Mars-crosser asteroid was predicted.

The Diploma Thesis is divided in four chapters. In the First Chapter (Introduction) the main Solar System regions which host small bodies are described along with their evolution in time. In the Second Chapter there is a discussion of the reasons for which the study of asteroids is necessary and essential for understanding the evolution of the whole Solar System. Some of the most acceptable theories are presented together with the regions of present orbits and the potential hazardous asteroids. Apart from the orbital elements, the size, mass, composition and spin characteristics are equally important for further classification. Studying their light-curves, we are able to reveal significant information related to the previous aspects. All these are described in the Third Chapter while in the final Fourth Chapter all the observations are presented step by step, followed by photometry, light-curve and phase period extraction. Simultaneously there is a summary of the theoretical proper procedure of target selection, observation and photometry of minor planets.

Nomenclature

General Symbols

a	semi-major axis
e	eccentricity
i	inclination
Ω	longitude of the ascending nodes
ω	argument of perihelion
q	perihelion distance
H	absolute magnitude
P	period
p	geometric albedo
$\mathrm{M}_\oplus$	Mass of Earth

Subscripts

p	proper element

Acronyms

TNO	Trans-Neptunian Object
SDO	Scattered-Disk Object

KBO Kuiper Belt Object

NEO Near Earth Object

NEA Near Earth Asteroid

NEC Near Earth Comet

MBA Main Belt Asteroid

LHB Late Heavy Bombardment

$MOID$ Minimum Orbit Intersection Distance

SNR Signal-to-Noise Ratio

RMS readout noise

Contents

List of Figures

List of Tables

Chapter 1

Introduction

1.1 Regions of Small Bodies

As more and more objects are discovered in the Solar System, the need for a more accurate classification was born. The category of Small Bodies includes objects such as the Main Belt asteroids, centaurs and *Trans-Neptunian Objects* (TNOs). These bodies orbit around the Sun, however, they neither have spherical shape nor have "cleaned" their neighbourhood from other objects. These are the main reasons why they cannot be called planets or even dwarf planets.

1.1.1 TNOs

A Trans-Neptunian Object is every object that orbits the Sun with a *semi-major axis* (a) grater than Neptune's (Figure 1.4). The first body that was detected was Pluto. Although at the beginning it was thought to be a regular planet, after over seventy years it was placed in a different group of bodies, the dwarf planets. The reason was that Pluto does not applies to all statements that characterise a solar system body as a planet. According to the *International Astronomical Union* (IAU), it has not cleaned its neighbourhood, but it has spherical shape.

TNOs are divided in three areas. The Oort cloud, the scattered disk and the Kuiper Belt.

Oort Cloud

The Oort cloud is the outermost limit of the Solar System. It is considered to be a remnant of the Sun's protoplanetary disk. Also, it is the main reservoir of comets with extremely long elliptic or parabolic orbits, as a result of gravitational interactions with giant planets.

Jan Hendrik Oort assumed the existence of this cloud for two major reasons. Fist of all, because of their composition of volatiles. As comets orbit the Sun, they lose part of their matter and make a crust on the surface which prevents farther outgassing. As a result, they should have formed in the outer Solar System. The second reason is that there is a limit in their orbits, as the most isotropic comets have the aphelion at 20.000 AU.

The Oort cloud is consisted of two regions. An outer spherical and an inner disc (Hills disk). It is located about 1 ly far from the Sun, almost at the 1/4 of the distance between the Sun and the Proxima Centauri.

Scattered Disk

The scattered disk is another subgroup of TNOs. It is placed far from the Sun and hosts small bodies with perihelia greater than 30 AU, big *eccentricities* (e) and *inclinations* (i) around 40^o. This disk was probably formed with Small Bodies after perturbations with Neptune.

The scattered disc was created when Neptune migrated outward into the proto-Kuiper belt, which at that time was much closer to the Sun, and left a wake population of dynamically stable objects which could never be affected by Neptune's orbit (the Kuiper Belt proper), and a population whose perihelia are close enough that Neptune can still disturb them as it travels around the Sun (the scattered disc).

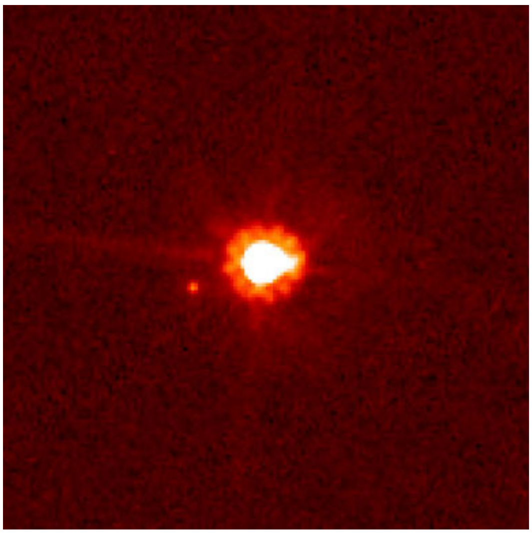

Figure 1.1: The dwarf planet Eris with its satellite Disnomia

Because the scattered disc is dynamically active and the Kuiper Belt relatively dynamically stable, the scattered disc is now seen as the most likely point of origin for periodic comets which slowly migrates to the inner solar system. The outer limits are farther above and below the ecliptic. That is happened because perturbations with the giant planets lead them to move closer to the Sun. The first *scattered-disk object* (SDO) was found in 1996 from Mauna Kea in Hawaii, and until now over than 200 SDOs were detected. (136199) Eris is an SDO dwarf planet and was found in 2005 (Figures 1.1-1.2).

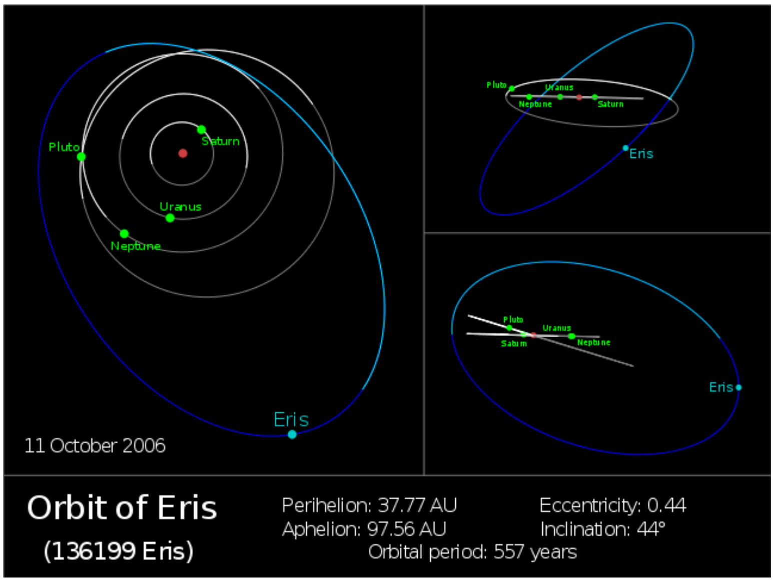

Figure 1.2: The extreme orbit of Eris, with e=0.43 and i=43.8^o

Right after the scattered disk, another area for small bodies is located. The contents of that zone are detached objects, which means that they are not affected by the gravitation of Neptune or any other planet of Solar System. Those objects have even larger perihelia, larger than Neptune's aphelion. Their semi-major axes are up to a few hundreds AU. Only a few objects were found in that area and the best known is Sedna.

Kuiper Belt

Kuiper Belt, also called as *Edgeworth-Kuiper Belt*, is a region beyond the Neptune's orbit, from 30 to 50 AU from the Sun and was discovered in 1992. It is consisted mainly of remnants of planetary formation, the *Kuiper Belt Objects* (KBOs). That area is dynamically stable, and the true origin of comets is the scattered area. The composition of Small Bodies is of frozen volatiles like ammonia, water and light hydrocarbons. Three well known dwarf planets are placed there, such as Pluto, Makemake and Haumea. Moreover it is believed that some planet moons are originated from that region (Figure 1.3).

Although theoretically the Kuiper Belt and the scattered disc have the same number of object, observations do not confirm that. Since the belt was discovered, the number of known KBOs has increased to over a thousand, and more than 70,000 KBOs over 100 km in diameter are believed to exist. At approximately 42–48 AU, the gravitational influence of Neptune is negligible, and objects can exist with their orbits essentially unmolested. This region is known as the classical Kuiper Belt, and its members comprise roughly two thirds of KBOs observed to date. Because 1992 QB1 is the first modern KBO that was discovered and is considered as the prototype of this group, classical KBOs are often referred to as cubewanos. The guidelines established by the IAU demand that to classical KBOs should be given names of mythological beings associated with creation.

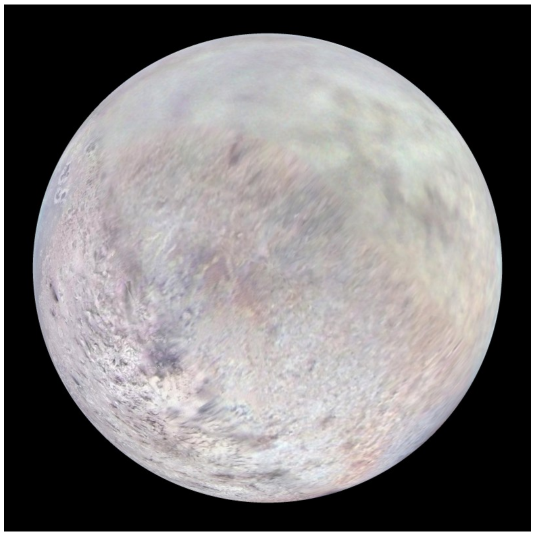

Figure 1.3: Triton is one of the moons which are originated from Kuiper Belt

The classical Kuiper Belt appears to be a composition of two separate populations. The first, known as the "dynamically cold" population, has orbits much like the planets, nearly circular, with an orbital eccentricity of less than 0.1 and with relatively low inclinations up to about 10^o (they lie close to the plane of the Solar System rather than at an angle). The second, the "dynamically hot" population, has orbits much more inclined to the ecliptic, by up to 30^o. The two populations have been named this way not because of any major difference in temperature, but from analogy to particles of their gas, which increase their relative velocity as they become heated up. The two populations not only possess different orbits, but different compositions. The cold population is markedly redder than the hot, suggesting it formed in a different region. The hot population is believed to have formed near Jupiter, and to have been ejected out by movements among the gas giants. The cold population, on the other hand, is believed to have formed more or less in its current position although it may also have been later swept outwards by Neptune during its migration. Despite its vast extent, the collective mass of the Kuiper belt is relatively low. The total mass range is estimated between a 10 $M_\oplus$ and 25 $M_\oplus$, with some estimates placing it at a 30 $M_\oplus$. Since the year 2000, a number of KBOs with diameters between 500 and 1,500 km, more than half that of Pluto, have been discovered.

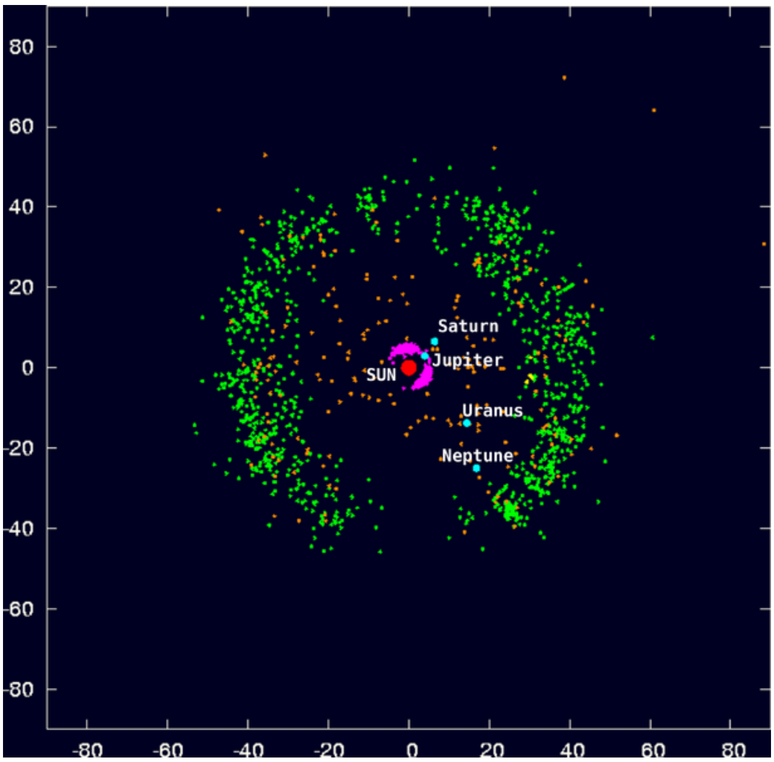

Figure 1.4: Small bodies in the Outer Solar System. We are able to distinguish the KBOs with green and centaurs with orange colour.

1.1.2 Centaurs

Centaurs are an unstable orbital class of minor planets that behave with characteristics of both asteroids and comets. There is no clear orbital distinction between centaurs and comets. They are named after the mythological race of beings, centaurs, which were a mixture of horse and human. Centaurs have transient orbits that cross or have crossed the orbits of one or more of the giant planets, and have dynamic lifetimes of a few million years. It has been estimated that there are around 44,000 centaurs in the Solar System with diameters larger than 1 km. The *Minor Planet Center* (MPC) and the *Jet Propulsion Laboratory* (JPL) defines centaurs as having a perihelion beyond the orbit of Jupiter and a semi-major axis less than that of Neptune (Figure 1.5).

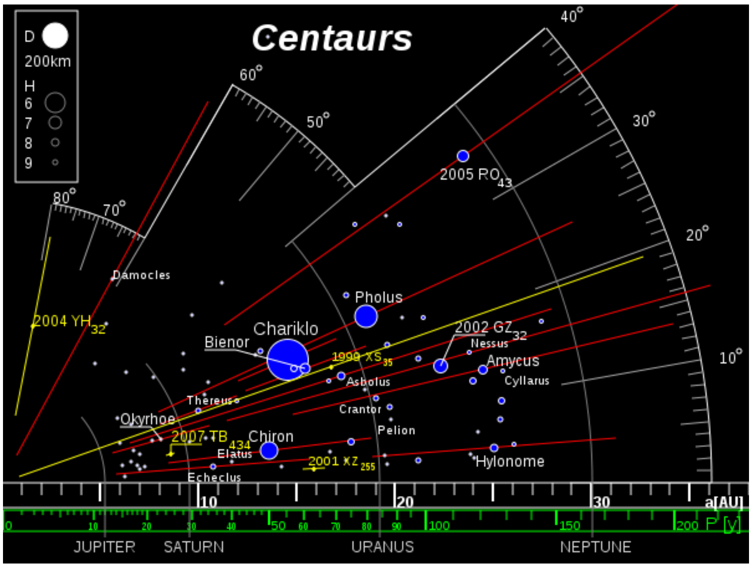

Figure 1.5: Centaurs' distribution in semi-major axis and inclination

The first centaur-like object which was discovered was (944) Hidalgo in 1920. Some KBOs can be perturbed, resulting in the object's expulsion so that it becomes a centaur. Scattered disk objects would be dynamically the best candidates for such expulsions, but their colours do not fit the bicoloured nature of the centaurs. Plutinos are a class of Kuiper-belt object that display a similar bicoloured nature, and there are suggestions that not all plutinos' orbits are as stable as initially thought, due to perturbations with Pluto. Centaurs' orbits are characterised by a wide range of eccentricities, from highly eccentric (Pholus, Asbolus, Amicus, Nessus) to more circular (Chariklo and the Saturn-crossers: Thereus, Okyrhoe).

1.1.3 Trojans

A *Trojan* is a planet, a minor planet or a natural satellite (moon) that shares an orbit with another planet or larger moon, but does not collide with it because it orbits around one of the two Lagrangian points of stability, L4 and L5, which lie approximately 60^o ahead of and behind the larger body, respectively. Trojan objects are one type of co-orbital object. In this arrangement, the massive star and the smaller planet orbit about their common barycenter. A much smaller mass located at one of the Lagrange points is subject to a combined gravitational force that acts through this barycenter. As a consequence, the mass can follow a circular orbit around this point with the same period as the planet, and the arrangement can remain stable over time.

In 1772, Joseph-Louis Lagrange predicted the existence and location of two groups of Small Bodies that were located near a pair of gravitationally stable points along Jupiters orbit. The term originally referred to the Trojan asteroids orbiting around Jupiter's Lagrangian points, which are by convention named after figures from the Trojan War of Greek mythology. The asteroids orbiting Jupiter's L4 point are named after the heroes from the Greek side of the war, while those at L5 are from the Trojan side (Figure 1.6). The two exceptions, the Greek-themed 617 Patroclus and the Trojan-themed 624 Hektor, are actually assigned to the wrong sides. Astronomers estimate that the Jupiter Trojans are comparable in number to the asteroids of the main belt.

The Trojans are far distant and it is harder to observe them. Also, their spectra does not have the clear features that main belt asteroids have and they are more reddish. For this reason it is assumed that they consist of organic molecules. Their rotational properties seem to be similar to the Main Belt asteroids'. The origin and the evolution of the Trojans are connected to the evolution of Jupiter. According to this theory, as the gaseous envelope collapsed and accreted onto Jupiter's core increasing its mass, the regions in L4 and L5 rapidly expanded.

Because of this expansion many planetesimals were captured in these two Lagrangian points. So the more massive the Jupiter became, more planetesimals were captured. In the end, the planetesimals with large libration amplitudes escaped, leaving the Lagrangian areas almost as it is today.

In addition, small objects have been found orbiting the Lagrangian points of Neptune (8 asteroids), Mars(3 or 4 asteroids), and Earth(1 asteroid).

The Earth trojan, 2010TK7, was confirmed in 2011 and is located in L4. It is a 300 m in diameter asteroid, which was found using the WISE satellite. It has an orbital period of 365.389 d with a chaotic character, so we cannot make long term predictions. It is believed that 1,500 years ago it was in L5 and jumped to L4 via L3.

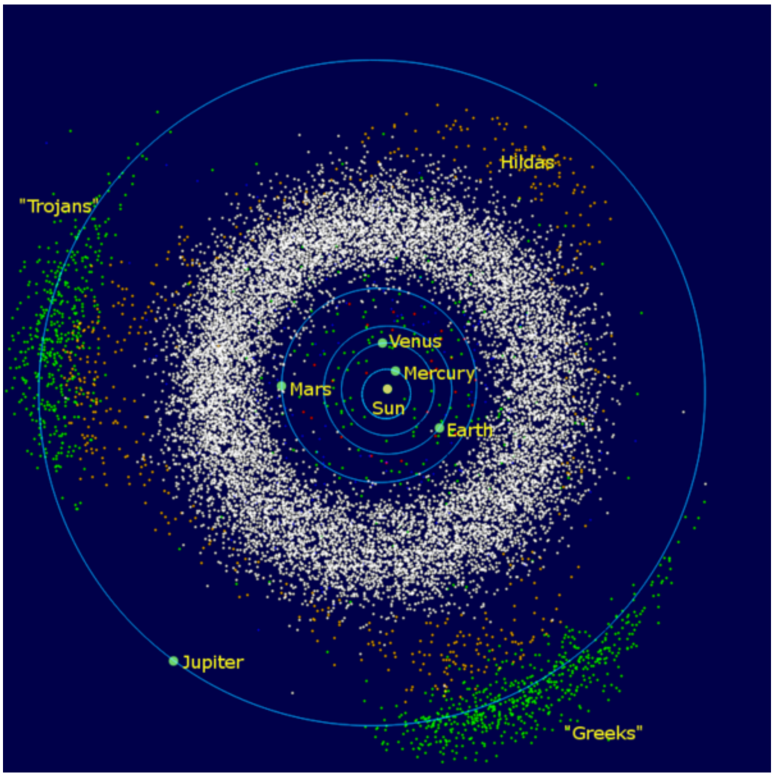

Figure 1.6: The distribution of Trojans, Hildas and Main Belt asteroids.

1.1.4 Main Belt

Between the orbits of Mars and Jupiter exists the Main Belt. This region contains small bodies which are called asteroids or minor planets. According to the JPL's recent catalogue, this zone contains approximately 529,612 objects and expands from 2 to 3.3 AU.

In 1766 and 1768, Johann Titius and Johann Bode respectively, extracted the same pattern for the calculation of planets' semi-major axis, known as Titius-Bode law. According to this law each semi-major axis is calculated from the following equation:

$$a = 4 + n\,, \qquad n = 0, 3, 6, 12, 24, 48 \tag{1.1}$$

Each value of n > 3 is twice the previous value. With this way all semi-major axes were found correctly, but a gap between the orbits of Mars and Jupiter was existed. At that time that result was interesting but none gave it the appropriate notice. In 1781 Uranus was discovered at almost the exact position, which Titius-Bode law predicted. After this success Bode started a research for the fifth in the raw planet.

In 1800 the astronomer Baron Franz Xaver von Zach recruited 24 of his fellows into a club, the Vereinigte Astronomische Gesellschaft ("United Astronomical Society") which he informally dubbed the "Lilienthal Society" for its meetings in Lilienthal, a small city near Bremen. Determined to bring the Solar System to order, the group became known as the "Himmelspolizei", or Celestial Police. Notable members included Herschel, the British Astronomer Royal Nevil Maskelyne, Charles Messier, and Heinrich Olbers. The Society assigned to each astronomer a 15 region of the zodiac cycle to search for the missing planet. Only a few months later, a non-member of the Celestial Police confirmed their expectations. On January 1, 1801, Giuseppe Piazzi, Chair of Astronomy at the University of Palermo, Sicily, while working on his star catalogue, found a tiny moving object in the shoulder of Taurus, in an orbit with exactly the radius predicted by the TitiusBode law. He dubbed it Ceres, after the Roman goddess of the harvest and patron of Sicily. Piazzi initially believed it is a comet, but its lack of a coma suggested it was a planet.

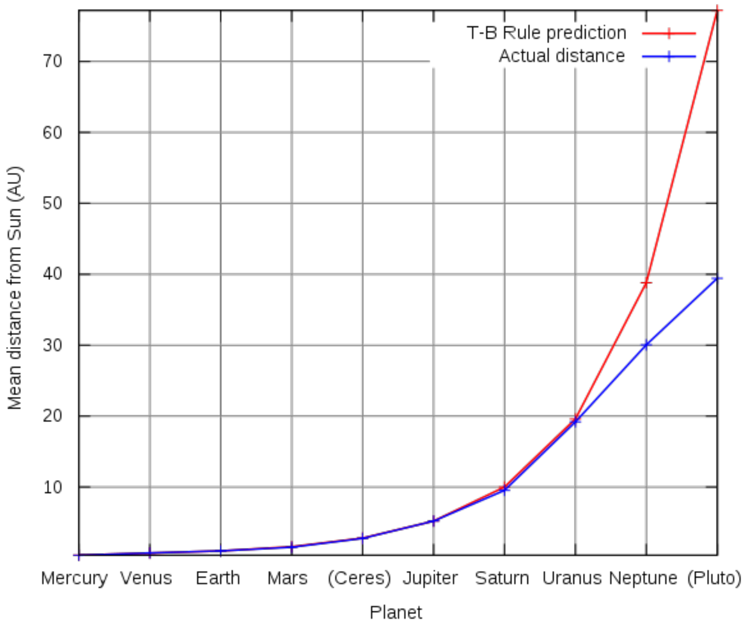

Figure 1.7: The incompatibility of Titius-Bode empiric law with the real distances of the outer solar system.

Fifteen months later, Olbers discovered a second object in the same region, Pallas. Unlike the other known planets, that objects remained points of light even under the highest telescope magnifications, rather than resolving into discs. Apart from their rapid movement, they appeared indistinguishable from stars. So in 1802 William Herschel suggested that they should be placed into a separate category, named asteroids, after the Greek asteroeides, meaning ”star-like”.

The sequence was destroyed after the discovery of Neptune in 1846. Unfortunately, that planet did not seem to satisfy Titius-Bode law (Figure 1.7). Apart from the failure of the universality of the law, a great step was done towards to the discovery of the asteroids Main Belt.

Chapter 2

Main belt asteroids

2.1 History facts

Piazzi (Figure 2.2) was not informed about the plans of the Astronomical Society to search for the missing planet, according to the Titius-Bode law. Independently, on January 1, 1801 while studying his star catalogue, he discovered a new tiny "star". On the next night he saw that this star had changed its position in the sky. At first, he thought that it must be a mistake, but 2 days later he realised that it was about a moving object, maybe a comet. Immediately he published in the press his comet detection.

Piazzi continued to observe his target (Figure 2.1) and after a few days he decided to write to his friends Oriani and Bode. In the letter which was written for Bode, Piazzi refers to the object as a comet without a nebula around. The following months a continuous debate was held in central Europe.

Beobachtungen des zu Palermo d. 1. Jan. 1801 von Prof. Piazzi neu entdeckten Gestirns.

1801		Mittlere Sonnen-Zeit	Gerade Aufstg. in Zeit	Gerade Aufsteigung in Graden	Nördl. Abweich.	Geocentrische Länge	Geocentr. Breite	Ort der Sonne + 20" Aberration	Logar. d. Distanz ☉ ♂
		St ' "	St ' "	° ' "	° ' "	Z ° ' "	° ' "	Z ° ' "	
Jan.	1	8 43 27,8	3 27 11,25	51 47 48,8	15 37 43,5	1 23 22 58,3	3 6 42,1	9 11 1 30,9	9,9926156
	2	8 39 4,6	3 26 53,85	51 43 27,8	15 41 5,5	1 23 19 44,3	3 2 24,9	9 12 2 28,6	9,9926317
	3	8 34 53,3	3 26 38,4::	51 39 36,0	15 44 31,6	1 23 16 58,6	2 58 9,9	9 13 3 26,6	9,9926324
	4	8 30 42,1	3 26 23 15	51 35 47,3	15 47 57,6	1 23 14 15,5	2 53 55,6	9 14 4 24,9	9,9926418
	10	8 6 15,8	3 25 32,1::	51 23 1,5	16 10 32,0	1 23 7 59,1	2 29 0,6	9 20 10 17,5	9,9927641
	11	8 2 17,5	3 25 29,73	51 22 26,0	....	....	.....	....	.....
	13	7 54 26,2	3 25 30,30	51 22 34,5	16 22 49,5	1 23 10 27,6	2 16 59,7	9 23 12 13,8	9,9928490
	14	7 50 31,7	3 25 31,72	51 22 55,8	16 27 5,7	1 23 12 1,2	2 12 56,7	9 24 14 13,5	9,9928809
	17	......	....	......	16 40 13,0	....	.....	....	.....
	18	7 35 11,3	3 25 55,::	51 28 45,0	....	....	.....	....	.....
	19	7 31 28,5	3 26 8,15	51 32 2,3	16 49 16,1	1 23 25 59,2	1 53 38,2	9 29 19 53,8	9,9930607
	21	7 24 2,7	3 26 34,27	51 38 34,1	16 58 35,9	1 23 34 21,3	1 46 6,0	10 1 20 40,3	9,9931434
	22	7 20 21,7	3 26 49,42	51 42 21,3	17 3 18,5	1 23 39 1,8	1 42 28,1	10 2 21 32,0	9,9931886
	23	7 16 43,5	3 27 6,90	51 46 43,5	17 8 5,5	1 23 44 15,7	1 38 52,1	10 3 22 22,7	9,9932348
	28	6 58 51,3	3 28 54,55	52 13 38,3	17 32 54,1	1 24 15 15,7	1 21 6,9	10 8 26 20,1	9,9935062
	30	6 51 52,9	3 29 48,14	52 27 2,1	17 43 11,0	1 24 30 9,0	1 14 16,0	10 10 27 46,2	9,9936332
	31	6 48 26,4	3 30 17,25	52 34 18,8	17 48 21,5	1 24 38 7,3	1 10 54,6	10 11 28 28,5	9,9937007
Febr.	1	6 44 59,9	3 30 47,2::	52 41 48,0	17 53 36,3	1 24 46 19,3	1 7 30,9	10 12 29 9,6	9,9937703
	2	6 41 35,8	3 31 19,06	52 49 45,9	17 58 57,5	1 24 54 57,9	1 4 1,5	10 13 29 49,9	9,9938423
	5	6 31 31,5	3 33 2,70	53 15 40,5	18 15 1,0	1 25 22 43,4	0 54 23,9	10 16 31 45,5	9,9940751
	8	6 21 39,2	3 34 58,50	53 44 37,5	18 31 23,2	1 25 53 29,5	0 45 5,0	10 19 33 33,3	9,9943276
	11	6 11 58,2	3 37 6,54	54 16 38,1	18 47 58,8	1 26 26 40,0	0 36 2,9	10 22 35 11,4	9,9945823

Figure 2.1: First observations of Ceres

There was the belief that this "comet" was eventually a planet, but without more observing nights it was not possible to established this idea. During the summer it was not possible to observe, because the object was next to the Sun. In December 1801, more observations were undertaken in order to fill more points in the trajectory of the moving object. After this, Gauss was able to calculate with the best approximation the orbit of the planet, which was elliptical. Shortly before, Burckhardt, had tried to obtain the orbit using only the initial data, obtaining at first a circular orbit and after three days an elliptical. Meanwhile, Piazzi had also tried to calculate it, without success.

German astronomers decided to name the new planet after the Greek goddess Hera. However Piazzi was not pleased about this because he had already named the planet, Ceres Ferdinandea. Ceres the Roman goddess was the protector of Sicily and Ferdinandea was in honour of King Ferdinand of Bourbon. After exchanging a few letters with other astronomers he was convinced to name it just Ceres.

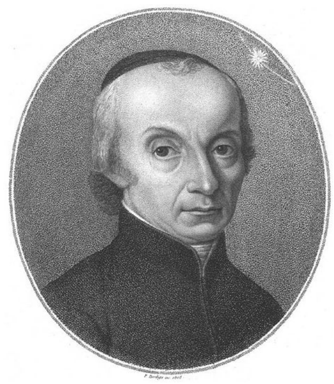

Figure 2.2: Giuseppe Piazzi (1746-1826)

Piazzi was accused several times for withholding his data for so long from the Astronomical community until the fist release. For that reason they were not able to re-observe quickly the target in order to determine the nature of the object and its trajectory.

A few months later, on 28 March 1802, another small body was detected, Pallas. It seemed to have similar features with Ceres but larger inclination and eccentricity. Two years later, on September 1, 1804 Juno was detected too. Until then, the most acceptable theories explained that these objects were fragments of a larger planet who disrupted because of natural forces or a catastrophic impact with a comet. But soon after the new discovery, Hofrath Huth proposed a new explanation. In the area between the orbits of Mars and Jupiter must be many more small planets of a similar size, of the same origin and age as the others in the Solar System.

A few years later, in 1807, Olders found another asteroid and Gauss gave it the name Vesta. This fact strengthen Olders belief about their origin as fragments of a larger planet. Unfortunately in the following 40 years no other asteroid was found until Hence found Astrea in 1845. The major reason for this was Olders' misleading theory and as a result they covered with observations only a small area in the sky.

2.2 Why do we study asteroids?

Studying asteroids helps understanding the origins of our Solar System. Their physical nature, origin, distribution in the Solar System and evolution during billion years are fundamental in the effort to know how the planets were formed. But the most ultimate question which needs to be answered is the creation of life.

Asteroids and comets are the most primitive remnants of the birth of the system. The asteroids that have survived have experienced collisions, dynamical and thermal events which have given them their present state and orbital elements. Although their total mass is very small compared with the total mass of the rest of the Solar System, their large number, variety in composition and orbital distribution can give useful information about planet formation.

Studies of the terrestrial planets (in the inner Solar System) and their moons reveals that the Solar System, in the beginning, was dynamically unstable. The orbits of the small bodies populations were dynamically affected from the gas and ice giant planets. This fact caused changes in the inner Solar System too.

The questions which demand an answer are many. How did the primordial asteroid belt look like? From what parent bodies are the present fragments originated? Which were the first steps of the planet formation and evolution? What do craters tell us about the sizes in the asteroid belt? Are there any hazardous objects in the sky which threaten Earth with collision, like in the past? Are they large enough to produce severe or catastrophic damage to human civilization?

Along with the minor planet study, important information may be obtained from the detection and observation of other star systems that can be found in many and different evolution stages.

2.3 Planetary Migration

Before studying the current orbits of minor planets it is necessary to investigate the theory of planetary migration to understand the way planets and small bodies affected each other.

The planetary migration is the procedure where a planet interacts with a disk of gas or other planetesimals resulting in the alteration of the planet's orbital elements, for example its semi-major axis.

Migration may happen because of interaction with either the primordial gas disk or with planetesimals. In the first case, planets having the mass of the Earth or greater, while orbiting, they transfer angular momentum to the gas and as a result move inwards approaching the Sun. In the other case there is a chaotic gravitational interaction between planets and planetesimals. Angular momentum is exchanged too and there is migration either inwards or outwards.

There are two types of migration. Both begin and end in a similar way but differ in the intermediate stages. According to Type I migration the terrestrial planets produce, while orbiting, spiral density waves in the gas or planetesimal disk. This imbalance is followed by a loss of the angular momentum because the outer waves affect the planet more than the interior. As a result the planet moves inwards. Super Earths begin migration Type I but because of their mass they clean their neighbourhood. A gap of matter is created in both sides of the orbit. However, new material enters the external gap pushing the planet to migrate inwards again. That consists the Type II migration and according to this we are able to explain the existence of hot Jupiters.

Apart from the two main migration types another possible mechanism which can lead a planet to migration is the gravitational scattering. That means that smaller planets change their orbits due to close encounters with bigger planets.

But how the planetary migration theory explains the Solar System? How it is related to the Minor Planets? It is believed that at the early Solar System, after the end of dissipation of gas and dust of the planets, the giants Jupiter, Saturn, Uranus and Neptune were orbiting in a relatively narrow area between 5.5 AU and 17 AU. Moreover their orbits were nearly circular. After the last planet a dense disk of rocky and icy planetesimals was extended until the 35 AU. The total mass of that region was about 35 $M\oplus$. This means that today's Kuiper Belt was much denser and closer to the Sun.

After the formation of the Solar System, the orbits of all the giant planets continued to change slowly [Levison et al., 2008], influenced by their interaction with

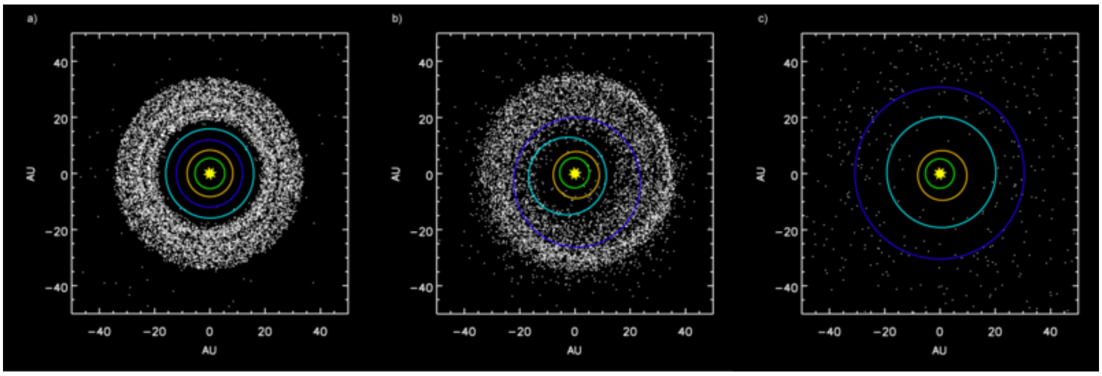

Figure 2.3: a) Before Jupiter/Saturn 1:2 resonance b) Scattering of KBOs into the Solar System after the orbital shift of Neptune c) After ejection of KBOs by Jupiter

the large number of remaining planetesimals via gravitational encounters. The planets scatter inwards the majority of the small icy bodies that they encounter, exchanging angular momentum with the scattered objects so that the planets move outwards in response, preserving the angular momentum of the system (Figure 2.3). After 500–600My Jupiter and Saturn fell into a 2:1 orbital resonance [Tsiganis et al., 2005]. This resonance increases their orbital eccentricities, destabilizing the entire planetary system. This resonance created a gravitational push against the outer planets, causing Neptune to surge past Uranus and go into the dense planetesimal belt. This relocation causes mutual gravitational encounters between Saturn and the two ice giants, which propel Neptune and Uranus onto much more eccentric orbits. The planets scattered the majority of the small icy bodies inwards, while themselves were moving outwards. These planetesimals then scattered off the next planet they encountered in a similar manner, moving the planets' orbits outwards while they were moving inwards. This process continued until the planetesimals interacted with Jupiter, whose immense gravity sent them into highly elliptical orbits or even ejected them outright from the Solar System. This caused Jupiter to move slightly inward. This disruption almost entirely scatters the primordial disk, removing 99% of its mass.

The outer two planets of the Solar System, Uranus and Neptune, are believed to have migrated outward in this way from their formation in orbits near Jupiter and Saturn to their current positions, over hundreds of millions of years. Eventually, friction within the planetesimal disc made the orbits of Uranus and Neptune circular again.

In contrast to the outer planets, the inner rocky planets are not believed to have migrated significantly over the age of the Solar System, because their orbits have remained stable.

Jupiter Trojans were planetesimals that formed near Jupiter and captured while Jupiter was growing. But how do they have large distribution in their inclinations, with a maximum of 40^o? After Jupiter and Saturn 2:1 mean motion resonance, the gravitational influence of the migrating giant planets destabilized quickly the pre-existing Trojan groups in the L4 and L5 Lagrange points of Jupiter and Neptune. During this time, the Trojan regions were termed "dynamically open". But this phenomenon may happen reversed. The planetesimals leaving the disrupted disk cross this region in large numbers, are able temporarily to inhabit it. When the period of orbital instability ended and the system Jupiter- Saturn passed the 2:1 mean motion resonance, the Trojan regions were "dynamically closed". The present Trojan populations are then these acquired scattered planetesimals of the primordial asteroid belt. This simulated population matches the libration angle, eccentricity and the large inclinations of the orbits of the Jupiter Trojans. A similar mechanism generated the Neptune Trojans [Morbidelli et al., 2005].

Considering the above model, the lack of water and organics in Trojans can also be explained: Some planetesimals before being captured in Trojan regions had very eccentric orbits, which brought them close to the Sun. So it is possible that their surfaces could have been volatilized.

A large number of planetesimals would have also been captured in the outer asteroid belt, at distances greater than 2.6 AU, and in the region of the Hildas family. These captured objects would then have undergone collisional erosion, grinding the population away into smaller fragments that could have then acted upon by the solar wind and the YORP effect, removing more than 90% of them [Bottke et al., 2006]. The size–frequency distribution of this simulated population following this erosion are in excellent agreement with observations. This suggests that the Jupiter Trojans, Hildas and some of the outer asteroid belt, all spectral D-type asteroids, are the remnant planetesimals from this capture and erosion process, possibly also including the dwarf planet Ceres.

2.4 The Late Heavy Bombardment

The *Late Heavy Bombardment* (LHB) is a short period at the early life of our Solar System about 700My after the planet formation. According to this hypothesis, all inner Solar System planets and the Moon suffered numerous impacts by a very large number of asteroids. It is called "late" because it happened after the planet formation and could not be explained from planetary formation theories.

The main evidence are the craters on the Moon. The age of most impact melt rocks, which were collected from the basins around the landing area of Apollo expeditions, are dated in a short period of time at the beginning of the Solar System. The majority of these rocks are believed to have formed during asteroid and comet collisions. The study of crater size distribution suggest that bodies of the same family struck the Moon and Mercury. They were projectiles of tens of kilometres in diameter.

However, the LHB hypothesis can be explained from the Nice model and the planetary migration [Gomes et al., 2005]. After Jupiter and Saturn reached the 2:1 orbital resonance, Neptune expanded its orbit beyond the orbit of Uranus and became the last planet of the Solar System reaching the area of the planetesimals. The result was the ejection of a large number of planetesimals towards the inner Solar System. When they reached Jupiter they were pushed deeper. Eventually they behaved like bombshells making collision to the rocky planets. Apart from the contribution of comets of the outer, massive, icy disk, asteroids of the Main Belt also took part in the LHB. After the 2:1 Jupiter-Saturn resonance, secular resonances were created through the Main Belt. Because of those resonances, asteroids were pushed to orbits with larger eccentricities and inclinations and moved into the inner Solar System. From simulations it was extracted that asteroids with Earth-crossing orbit behave in two ways. A part of them were trapped in secular resonance with Saturn and went directly to Earth-crossing orbits. The other part stayed in the Main Belt with unstable orbits which slowly evolve, reaching trajectories in the inner Solar System.

2.5 Kirkwood Gaps in Main Belt

An orbital resonance is a state where two orbiting bodies are connected with gravitational interaction with each other. In order to show this bound we usually use a simple ratio of their orbits around the Sun. For example when we said that Jupiter and Saturn fell into 2:1 resonance we mean that Jupiter orbits twice the Sun in the same time as Saturn orbits once.

The resonances may be classified in several types. They combine one or more orbital parameters as eccentricity and semi-major axis, they can also be secular or not.

A mean motion resonance either stabilize or destabilize the small bodies. The regions with stable orbits are located in 3:2, 4:3 and 1:1 resonances with Jupiter. In the first region we meet the Hildas family, in 4:3 the (279) Thule and in 1:1 the Jupiter Trojans (Figure 2.4).

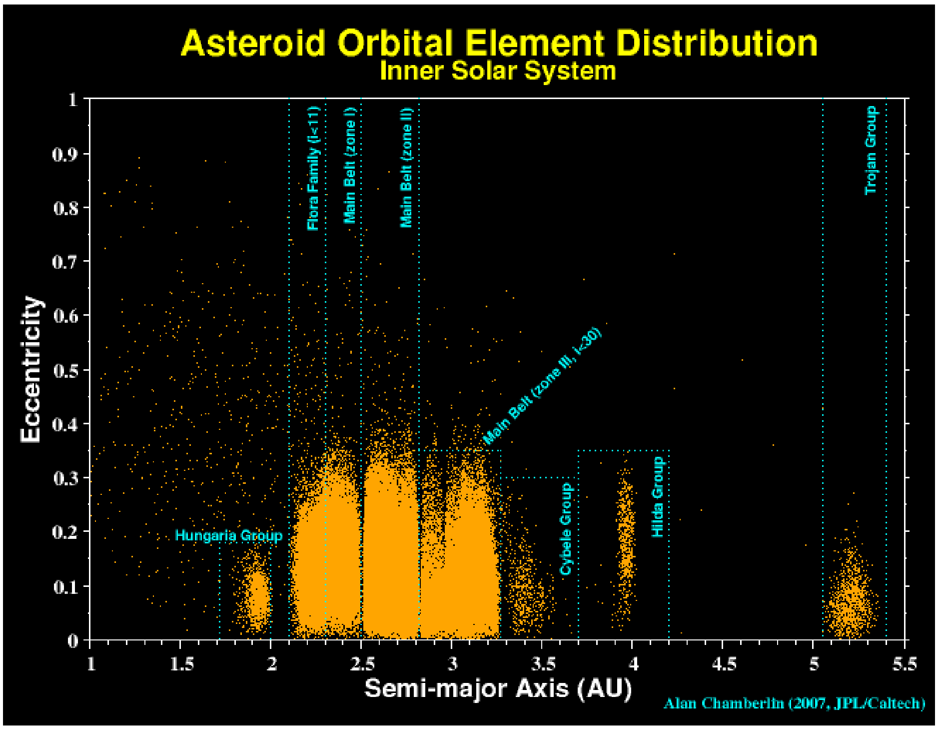

Figure 2.4: The stable and the unstable resonances in the Solar System

Often this interaction forces the objects of the Main Belt in unstable orbits and/or eject them from certain areas. These empty areas are called the *Kirkwood Gaps* (Figure 2.5). They are placed into the Main Belt in 3:1, 5:2, 7:3 and

2:1 resonances. If an asteroid enters a region of resonance with Jupiter, it will eventually be ejected. So the Kirkwood Gaps are continuously refilled with new asteroids from the nearby areas.

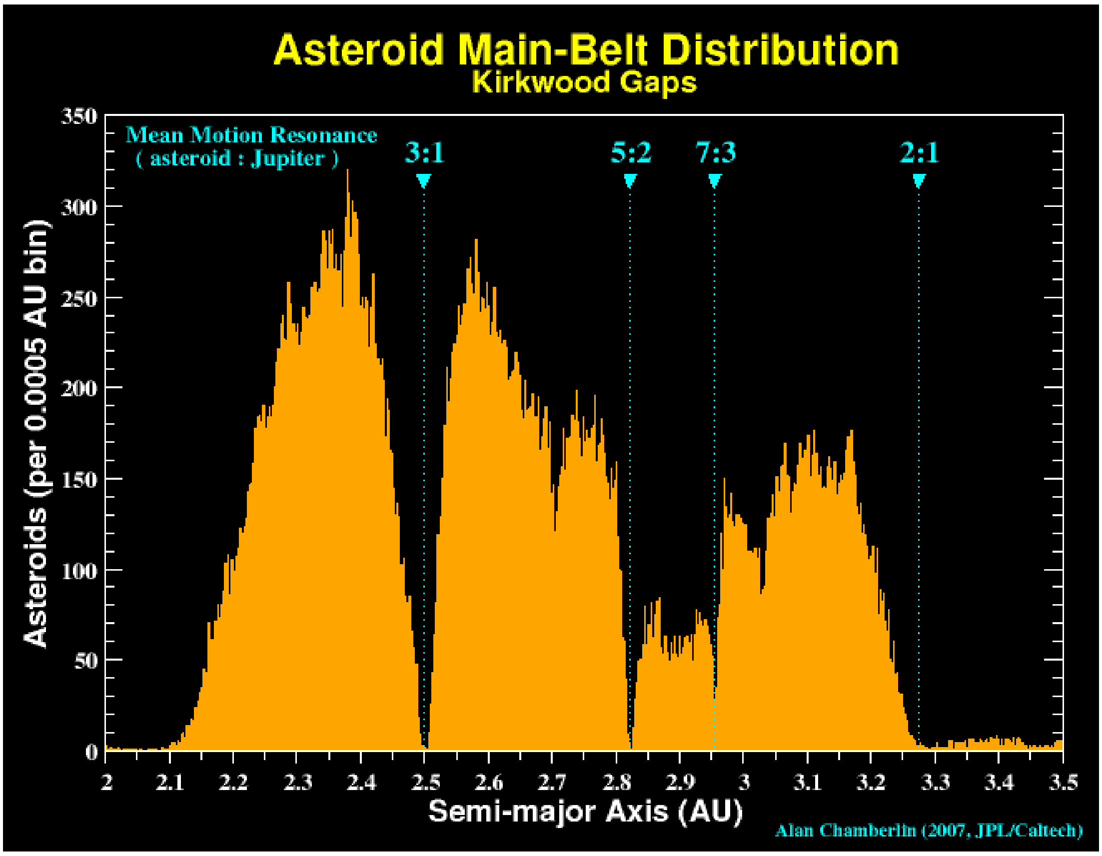

Figure 2.5: The Kirkwood Gaps in 3:1, 5:2, 7:3 and 2:1 resonances.

2.6 The Yarkovsky and YORP effect

Apart from the contribution of collisions and gravitational perturbations another non-gravitational factor, that helps the evolution of the asteroids, is the *Yarkovsky effect*. The phenomenon was discovered by Ivan Yarkovsky at the beginning of the 20^{th} century and explains the force which acts on a rotating small body, caused by anisotropic emission of thermal photons which carry momentum.

As the asteroids are rotating small bodies orbiting the Sun, the "diurnal effect" plays a significant role on them. During the movement of an asteroid on its trajectory it is illuminated by the Sun and as a result its surface is warmer in afternoon and early night than in the late night and early morning. So more heat is radiated from the afternoon side compared in the morning. This radiation emission from the afternoon side leads a prograde body to move towards the opposite direction, away from the Sun, in order to keep its momentum. A retrograde asteroid, following the same law, is going to move inwards (Figure 2.6).

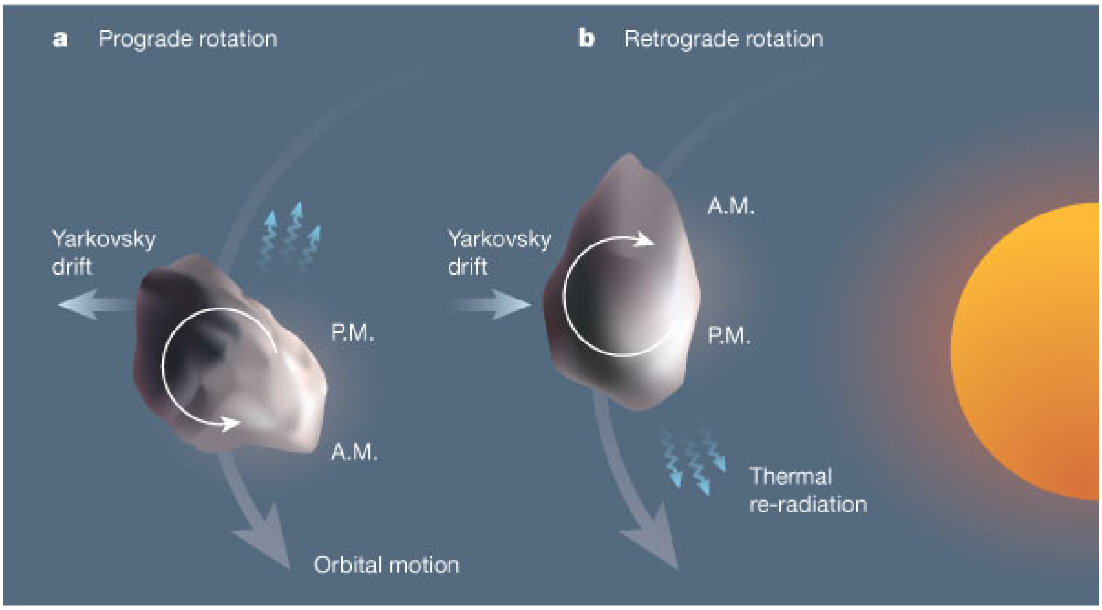

Figure 2.6: The Diurnal Yarkovsky effect on a) a prograde rotating asteroid pushes it outwards and b) a retrograde rotation pushes it inwards.

However, it is hard to measure the Yarkovsky effect. An asteroid's magnitude depends on its shape, albedo, orientation and probable variations over its surface with the wavelength.

Finally asteroids larger than 100 m, but smaller than 40 km, are vulnerable to Yarkovsky effect and change their orbit during the years, while even larger asteroids remain unaffected. This mechanism delivers Main Belt asteroids to chaotic resonance regions and later leads them to Earth-crossing orbits and blend the asteroid families. (6489) Golevka is the first asteroid with a noticeable Yarkovsky effect.

The *Yarkovsky-O'Keefe-Radzievskii-Paddack effect* (YORP) is another variation of the Yarkovsky effect and is responsible for the changes in rotational rate of asteroids and trap them into spin-orbit resonances. The YORP effect can speed up or slow down asteroid rotation depending on surface properties of the small body and its obliquity, ϵ. The asteroid on which this phenomenon was firstly confirmed was the (54509) YORP. After four years of observations, it was calculated that its rotational rate was increasing, and it was not due to close approaches with the Earth [Lowry et al., 2007].

2.7 Planet Crossers

Planet crossers are the asteroids whose orbit cross the orbit of a planet's. As a result there are Mercury-, Venus-, Earth-, Mars-, Jupiter-, Saturn-, Uranus- and Neptune-crossers. There are different categories which depend on their specific orbit.

2.7.1 Types of planetary crossing

First of all there are asteroids, which move on concentric orbits inside or outside the planet's orbit, without crossing it. Another category is the inner and outer grazers which orbit and enter from inside or outside the planet's orbit, without crossing it too. The co-orbital asteroids orbit on the same trajectory with a planet. The last group contains the planet crossers. These objects while orbiting, cross the planet's orbit (Figure 2.7).

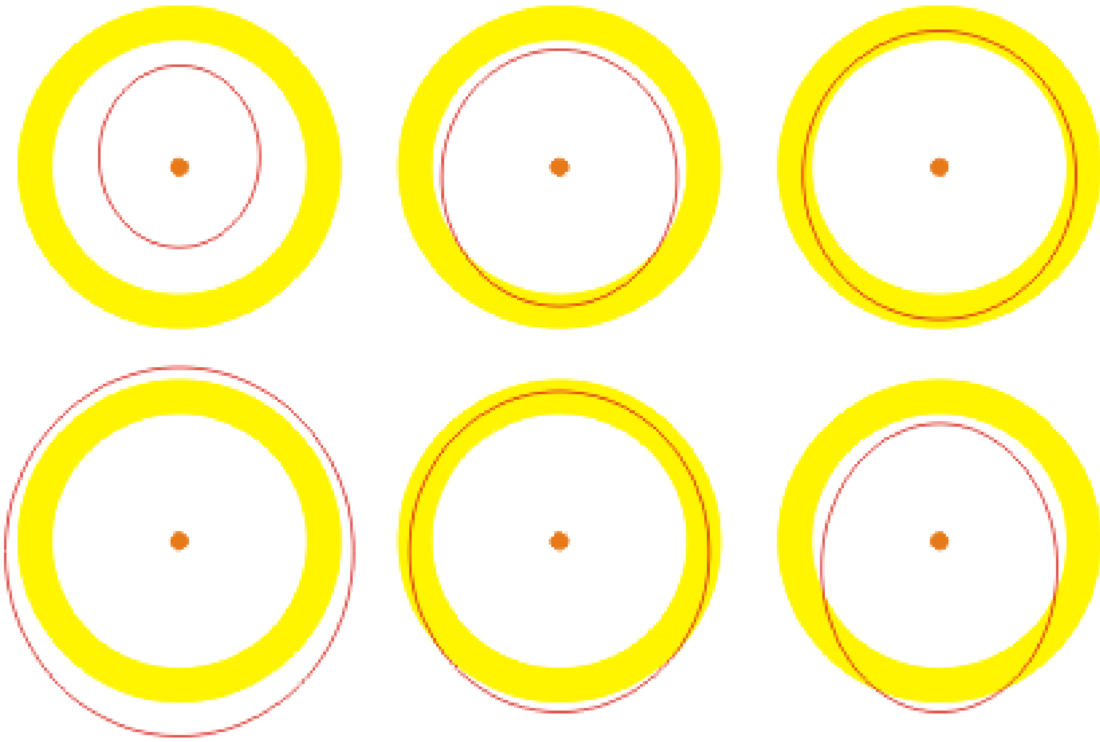

Figure 2.7: The six probable orbits close to a planet.

2.7.2 Near Earth Objects

Near Earth Objects (NEOs) is a group of Solar System bodies with orbits in the Earth's neighbourhood. All NEOs have a perihelion smaller than 1.3 AU and the group contains thousands of *Near Earth Asteroids* (NEAs), *Near Earth Comets* (NECs), meteoroids and artificial solar satellites. NEOs have attracted worldwide interest during the last 30 years because of potential hazardous impacts with Earth. But how do we distinguish them?

2.7.2.1 Near Earth Comets

The basic criteria to certify a comet candidate are their *Jovian Tisserand* parameter, the spectral type and the low albedo (<0.075) [DeMeo and Binzel, 2008].

The Jovian Tisserand parameter gives the strength of the gravitational interaction between Jupiter and a small body, with a_j and a the semi-major axes of

Jupiter and object, respectively :

$$T_j = (a_j/a) + 2[(1-e^2)a/a_j]^{1/2} cos(i) \tag{2.1}$$

Objects with $T_j > 3$ are not strongly affected by Jupiter. These are usually the Main Belt asteroids. On the other hand those with $T_j < 3$ are strongly bonded with Jupiter. Although some Jupiter family asteroids have very eccentric orbits and are perturbed by other planets, the first criterion for identifying a comet candidate is the T_j value (Figure 2.8).

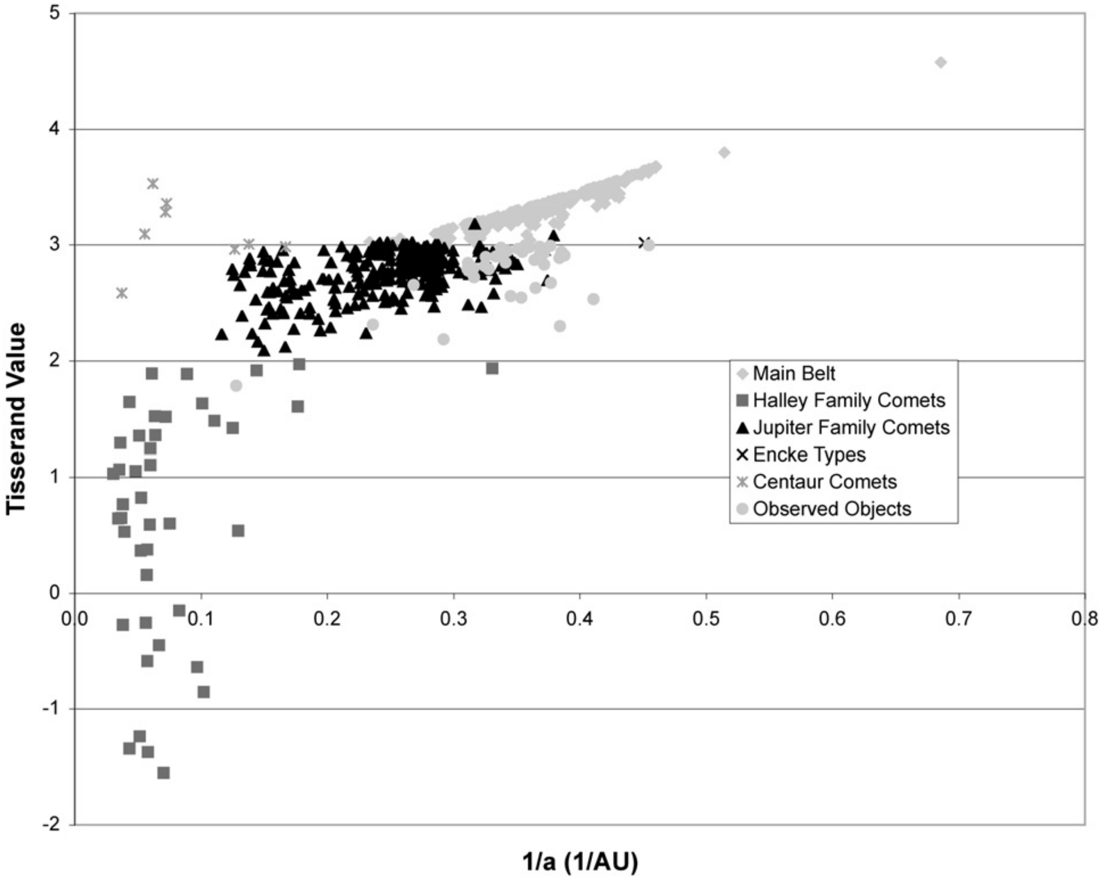

Figure 2.8: The observed objects population separated in dynamical groups.

Another factor is their spectral classification. Even if an object has $T_j < 3$ it will not be considered as a comet unless it belongs to C-, P-, T- ,D-type class.

The typical albedos for comet nuclei have a range between 0.02 and 0.06. For a comet candidate we consider as a maximum value for low albedo objects 0.075.

Until now about 3% of NEOs are listed as active short period NECs, having tails or coma, with q< 1.3 AU and P < 200 yr. Combining the observations along with a dynamical factor for possible origin from the Kuiper belt, a fraction of 8 ± 3% is calculated for NECs population (Figure 2.9).

2.7.2.2 Near Earth Asteroids

NEAs are all the Near Earth Objects with no cometary characteristics, with irregular shape and greater than 50 m in diameter. Respectively, objects with diameter less than 50 m are called meteoroids. The number of asteroids grows as their minimum size decreases. As a result a comparatively large number of asteroids with small sizes have orbits with perihelia closer to the Sun, Earth and Venus.

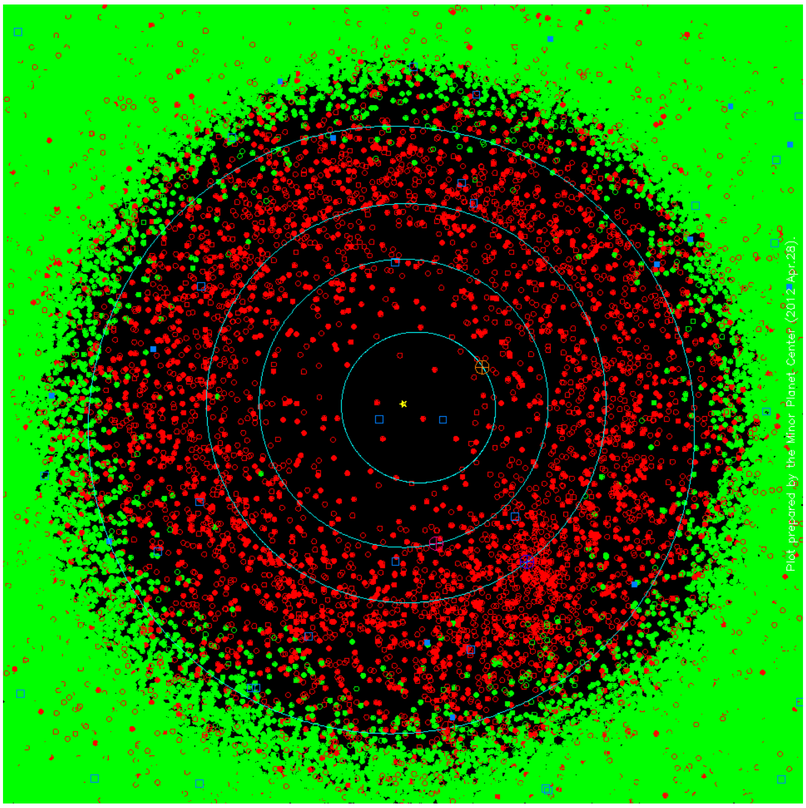

Figure 2.9: NEAs orbits.

Until now, more than 7,000 NEAs have been discovered with a wide range in size, up to several hundreds of km. The largest Near Earth Asteroid is (1036) Ganymed with an estimated diameter 32 km. NEAs end up with these orbits after perturbations with Jupiter. Moreover the Yarkovsky effect is responsible for the continuous import of Main Belt asteroids in near Earth trajectories. In order to characterise an asteroid as near Earth it should orbit within 1.3 AU from the Sun and as a consequence within 0.3 AU from the Earth's orbit.

(887) Alinda was the first Earth-crossing asteroid that was discovered in 1918. Its size is about 5 km in diameter and was found by Wolf at Heidelberg. Although its perihelion distance is 1.15 AU it was not considered as an Earth-crosser asteroid from the beginning. In 1932 E. Delporte in Belgium detected (1221) Amor, a 1 km in diameter asteroid with perihelion distance 1.08 AU. Both of them entered the category of Earth-crossers after the study of Marsden and Williams respectively and their orbits do not overlap Earth's. During the same year at Heidelberg, another small body (1862) Apollo was found with maximum perihelion 1.017 AU which overlaps the orbit of Earth. In 1976 E.F. Helin at Palomar discovered (2062) Aten, which has smaller orbit than Earth and overlaps the second at aphelion[Shoemaker, 1983].

There were three main categories of NEAs based on their osculating elements, shown below (Figure 2.10):

- **The Atens asteroids:** They have semi-major axes < 1 AU with high eccentric orbits. As a consequence their trajectory will not be entirely within the Earth's orbit. Almost all the known Aten asteroids have aphelia greater than 1 AU and the rest that have internal aphelia are called Apohele asteroids or Inner Earth Objects (IEOs).

- **The Apollo asteroids:** They have semi-major axes > 1 AU and perihelia $q < 1.017$ AU. The largest member of this group is (1866) Sisyphus.

- **The Amors asteroids:** Their orbit is beyond the Earth's orbit and they do not cross it. Amors named after (1221) Amor and it is supposed that the Phobos and Deimos are originated from this NEA group. (433) Eros is another member. This group is divided in 4 subgroups Amor I, Amor II, Amor III and Amor IV according to their mean distance from the Sun.

  In order to characterize an asteroid as Amor asteroid, three basic criteria should be confirmed. The first is that they must orbit closer than 0.3 AU,

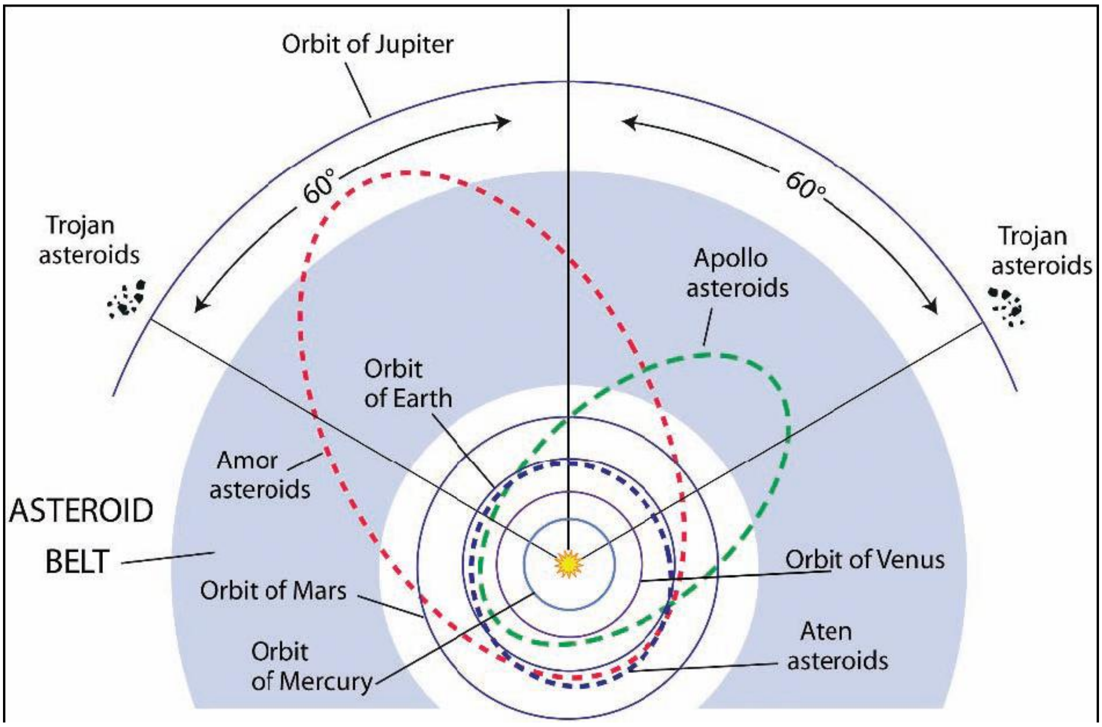

Figure 2.10: NEAs orbits.

which is the minimum distance from Earth in order an object to come really "near" the Earth. Also the trajectory has to be outside the Earth's orbit and not cross its orbit. As a result the Earth's orbit is closer to the Sun at every point of the asteroid's path.

Apart from the above categories there is a more detailed classification, which replaced the previous classification, based on dynamical behaviour and named after the more representative asteroid of every class [Milani et al., 1989]. These are Geographos, Toro, Alinda, Kozai, Oljato and Eros. The six groups are more stable than the previous because some transitions had already been detected and they used to describe their evolution for longer time. In addition the definition of each class depends on long time orbital elements. Actually the time during every asteroid remains in a specific group is tens of thousands of years.

The need for more accurate dynamical classification for Earth crossers and almost Earth crossers was born as these objects move usually on chaotic orbits. This happens because they have large eccentricities, are planet crossers and face strong perturbations by close approaches to planets. All these aspects lead them to chaotic orbits, which means that giving slightly different initial orbital elements end up with a total different orbit. Moreover, this study depends on two basic presuppositions. A large number of asteroids should be studied for a long time and the results should not depend on the details of one orbit. The main parameters are the values and the changes of their orbital elements, the resonances, the number and type of node crossing and the number of close encounters with the planet.

- **Geographos class:** The Geographos asteroids are the Earth-crossers in the most intuitive sense. Their orbits cross the orbit of the Earth. Around the epochs of node crossings, close approaches occur, the closest ones essentially at random with no lower limit of distance from the planet. This means that physical collision can happen, provided the asteroid remains in the class long enough. Moreover, some of the Geographos are also crossing or at least almost crossing Venus, and have close approaches to Venus as well.

  The orbital elements of a Geographos asteroid have a characteristic behaviour, well illustrated by 1620 Geographos, which can be described as piecewise regular. That is, the semi-major axis is almost constant or possibly undergoes small periodic oscillations due to resonances. At node crossings, a number of random impulsive changes including some rarer strong ones alter the semi-major axis. In the long run, this results in a kind of discrete time-step Brownian motion. Nevertheless, in between two successive node crossings the orbit is ostensibly regular: eccentricity and inclination change along secular oscillations and/or trends which are moderately perturbed by the close approaches and changed in a significant way only by the very deep ones.

- **Toro class:** The Toro asteroids are Earth-crossers protected against collisions with the Earth by mean motion resonances with our planet. Their orbits undergo node crossings with the Earth, but during the spans of time in which the geometrical configuration of the orbits is such that close approaches could occur, either they do not occur at all or they are much shallower than one could expect from the distance between the orbits. If they are also Venus-crossing (or almost crossing), close approaches to Venus can occur and sometimes result in such a large change in semi-major axis that the resonance with the Earth is disrupted. Sometimes the resonance with the Earth dissolves by itself, possibly because the critical argument starts librating with an amplitude too large to protect against close approaches, or it circulates. As a result of both mechanisms, this class is the least stable. Almost no asteroid remains a Toro for more than 200,000 years, and many exchanges with the Geographos class occur.

The orbital elements show variations of α with the intermediate periods (a few hundred years) typical of the mean motion resonances. The amplitude of this change is not very large. Within the resonance band, regular oscillations are sometimes interrupted by comparatively rapid changes of the average value. This behaviour can be understood as a change in the critical argument which is librating, as it has been shown in cases of chaotic resonance phenomena. Eccentricity and inclination change in a regular fashion, undergoing secular oscillations and/or trends with superimposed small oscillations with the intermediate periods.

- **Kozai class:** The Kozai asteroids do not have close approaches with the Earth or they have only shallow ones in spite of the fact that the perihelion distance drops below q = 1 AU every time the eccentricity is close to its maximum value. The mechanism which is responsible for this is not related to mean motion resonances, but rather to secular perturbations. No node crossing occurs, for most objects in this class, not even almost crossings, because whenever the eccentricity is close to its maximum the argument of perihelion ω is close to either 90^o or 270^o. So the perihelion of the asteroid is either well above or well below the Earth's orbital plane. We find ω libration or e-ω coupling. When ω librates it never gets close to 0^o or 180^o; when ω circulates, the large oscillation in eccentricity is at its minimum whenever ω is close to 0^o or 180^o so that the perihelion distance is larger than 1AU. This mechanism has been known for quite some time as a protection for asteroids close to Jupiter, such as (1373) Cincinnati and for other real and fictitious objects outside the 2:1 resonance with Jupiter.

  The evolution of the orbital elements of the Kozai asteroids is very regular, the semi-major axis changes very little, and the variations appear as either oscillations or impulsive changes correlated with node crossings with Mars. Some Kozai asteroids are at the same time protected with respect to the Earth by the secular perturbations mechanism and with respect to Mars by a mean motion resonance. Not surprisingly, this is the most stable of all the classes, with only one transition recorded in our sample. Eccentricity and inclination are large and have very large regular oscillations. Some objects in the Kozai class are almost Earth-crossing, but no approach closer than 0.05 AU occurs.

- **Alinda class:** The Alinda asteroids are in mean motion resonance with Jupiter. The resonance must be of low enough order, and the asteroid deep enough into it, for the resonant state to last for a long time (e.g. more than one period of the perihelion) while protecting it from close approaches to Jupiter even when the aphelion is quite high (4 AU or more recall that a close approach to Jupiter is defined as an approach at less than 1 AU , which is the typical limiting value for the closest approach of a main belt asteroid to Jupiter). Another important feature of the Alinda asteroids is that the short periodic perturbations on the perihelion are so strong that most of the Alinda are supercrossers. For an Alinda, the fact of being Earth-crosser at some time is not relevant to predict the long term behaviour of the close approaches to the Earth. The orbital elements can change so much and so quickly that an Alinda can become Earth crossing, and often Venus crossing, many times over the time span of the data.

  As a result of the resonant perturbations, the semi-major axis oscillates with quite a large amplitude around the resonant value.

- **Eros class:** The Eros asteroids in our sample are those which do not cross the orbit of the Earth because their perihelion is always higher than 1 AU. Most of them are almost-crossers with the Earth and have shallow approaches, typically at distances not lower than 0.03 AU. The definition is completed by two negative requirements: an Eros type orbit is neither in a deep resonance with Jupiter, otherwise it is an Alinda, if the resonance lasts more than a period of ω, nor Jupiter-approaching.

The eccentricity of the Eros asteroids undergoes significant changes. The obvious features of the secular evolution of an Eros-type orbit is that there are oscillations with the argument $2\,\omega$, but also longer term oscillations and trends.

- **Oljato class:** The Oljato asteroids have orbits which show large-scale chaotic effects. These asteroids are not Jupiter-crossing, but they have high eccentricity. As a result, they are Venus-crossers and at the same time have an aphelion not too far from Jupiter (above 4 AU in most cases). Moreover, the eccentricity undergoes large secular changes, so that it can peak at values above 0.8. The inclination is low, or at least oscillates with low minima. Also because of this, the number of close approaches to all the inner planets is large. The Oljato normally have either no close approach to Jupiter or very shallow ones (e.g. at =0.9 AU). However, deeper encounters can occur and result in transitions to either a fully cometary orbit or to an Alinda class orbit.

  The Oljato asteroids are also continuously perturbed by close approaches. While it is easy to describe large changes in α - including jumps in and out of resonances as chaotic, it is a challenging task to separate the effects of long range Jovian perturbations from the effects of short distance interactions with the other planets.

  It is important to stress that a high eccentricity is not enough for an object to be listed in the Oljato class. There are asteroids which undoubtedly belong to the Geographos class like (1580) Betulia, (2102) Tantalus, and (1973) N A , whose eccentricity shows large, regular variations reaching 0.8 or more. They belong to the Geographos class because the regular variations in eccentricity are due to the high inclination by which they never get close to Jupiter, not even when the aphelion is above 4 AU.

  An asteroid must have shallow encounters to Jupiter in order to belong to the Oljato class. Because of the large mass of Jupiter many asteroids which have encounters outside the 1AU boundary that we have chosen for our close approaches data base are perturbed enough to be included in the Oljato class. Oljato-type orbits are also different from fully cometary orbits, which are Jupiter-crossing and undergo very close approaches.

2.7.3 Types of resonances

Asteroids become planet crossers by increasing their eccentricity after resonances. There are two main resonances. The powerful resonances include the v_6 secular resonance and the mean motion resonances in 3:1, 5:2 and 2:1 with Jupiter at 2.5, 2.8 and 3.2 AU respectively.

2.7.3.1 v_6 resonance

An asteroid falls in this secular resonance when its perihelion longitude is equal to the sixth secular frequency of a planet, especially Saturn's. These asteroids are placed into the inner border of the Main Belt, which is divided in two regions, the powerful and the border region. The asteroids from the powerful area, due to the resonance, increase their eccentricities and become Earth and Venus crossers or collide with the Sun. The median time which required for a minor planet to become Earth crosser is 0.5My and the lifetime of bodies in v_6 resonance is 2My. The 80% of them collide with the Sun, while the 12% are ejected in hyperbolic orbits. The mean time for an asteroid to spend in the NEO region is 6.5My and the collision probability is 0.01. The objects in the border region are not affected so strongly by the v_6 resonance, but they are still able to become Mars-crossers. In order to enter an asteroid the NEO region it must be affected by close encounters with Mars. The total time needed increases as the distance from the resonance increases too.

2.7.3.2 3:1 resonance

Inside the region of the 3:1 mean motion resonance there are two subareas. The central region is where the the asteroids have regular oscillations and periodically cross the orbit of Mars. The second larger border region is where the evolution of eccentricities is chaotic and these objects become Earth-crossers and Sun-grazers. Because of the close encounters with Mars, objects from the central region can travel towards to the border region and then pushed to NEOs region. From the asteroids which are into the resonance the time to become Earth-crossers is 1 My with a lifetime of 2 My. Also the 70% of them result into the Sun and the 28%

follow hyperbolic orbits. The probability for a Near Earth Asteroid to make an impact on Earth is 0.002.

2.7.3.3 5:2 resonance

The same mechanism that affects the asteroids of the border area in the 3:1 resonance, also affects all the asteroids in the 5:2. Because this resonance is in 2.8 AU, closer to the Jupiter than the previous, the majority of asteroids are ejected and only the 8% of them collide with the Sun. The probability to collide with the Earth is 0.00025.

2.7.3.4 2:1 resonance

This resonance is very stable and no mechanism is able to destabilize the asteroids in the centrer. However, the edges of the region are unstable, but several millions of years are required to make them Earth-crossers. Their lifetime is only 0.1My and they are ejected due to Jupiter's perturbations very soon. The mean probability to collide with the Earth is only 0.00005.

2.7.3.5 Diffusive resonances-Chaotic diffusion of asteroids

Apart from the main mean motion resonances of Jupiter-asteroid, there are other areas of Jupiter-Saturn-asteroid resonances or Mars-asteroid resonances. Because of these kind of resonances the main belt is mostly chaotic. As a result of this chaoticity the semi major axes are bound into these resonances and lead to slow change of proper inclinations and eccentricities. Asteroids from the inner belt which are captured in resonances tend to be Mars-crossers and asteroids from the outer belt tend to be Jupiter crossers during several millions to billions years.

The rate that asteroids escape and become Mars-crossers is hight, due to v_6 and mean motion resonances with Mars. As a consequence, the population of Mars-crossers is large too. Mars-crossers are the bodies which orbit out of the 1.3 AU and cut the orbit of Mars and their number is four times larger then the NEOs. In order a Mars-crosser to be an Earth-crosser it changes its semi-major axes because of the close encounters with the planet until it enters a resonance that will lead it to a semi-major axis smaller than 1.3 AU. Finally there are not many Mars-crossers with a semi-major axis >2.8 AU as their lifetimes decreases while they move to Jupiter-crossing limit.

2.7.4 Potentially Hazardous Asteroids

About 90% of the potential Earth-impacting projectiles are near-Earth asteroids or short-period comets. The other 10% are intermediate or long-period comets. Impacts by Earth-approaching asteroids and comets pose a significant hazard to life and property. Although the annual probability of the Earth being struck by a large asteroid or comet is extremely small, the consequences of such a collision are so catastrophic that it is prudent to assess the nature of the threat and prepare to deal with it.

Generally *Potentially Hazardous Objects* (PHO) are called the asteroids and comets that make very close approaches to Earth and their size is large enough to cause severe damage on Earth after an impact. The *minimum orbit intersection distance* (MOID) is a way to measure the collisional risk between two objects. The MOID value is different for each planet in the Solar System. For example the Earth's MOID is 0.05 AU and Jupiter's 1 AU. So, as the bodies are getting larger, the MOID value is increasing too. In combination with the orbit the size matters equally, as larger asteroids are able to cause more catastrophic consequences.

Figure 2.11: The global map of impacts.

The greatest risk from cosmic impacts is associated with objects large enough to perturb the Earth's climate on a global scale by injecting large quantities of dust into the stratosphere. Such an event could depress temperatures around the globe, leading to massive loss of food crops and possible breakdown of society. Such global catastrophes are qualitatively different from other more common hazards that we face, because of their potential effect on the entire planet and its population. Various studies have suggested that the minimum mass impacting body to produce such global consequences is several tens of billions of tons, resulting in a groundburst explosion with energy as a million megatons of TNT. The corresponding threshold diameter for Earth-crossing asteroids or comets is between 1 and 2 km . Smaller objects, tens of meters in diameter can cause severe local damage but pose no global threat. The regions of known impacts are shown in Figures 2.11-2.12.

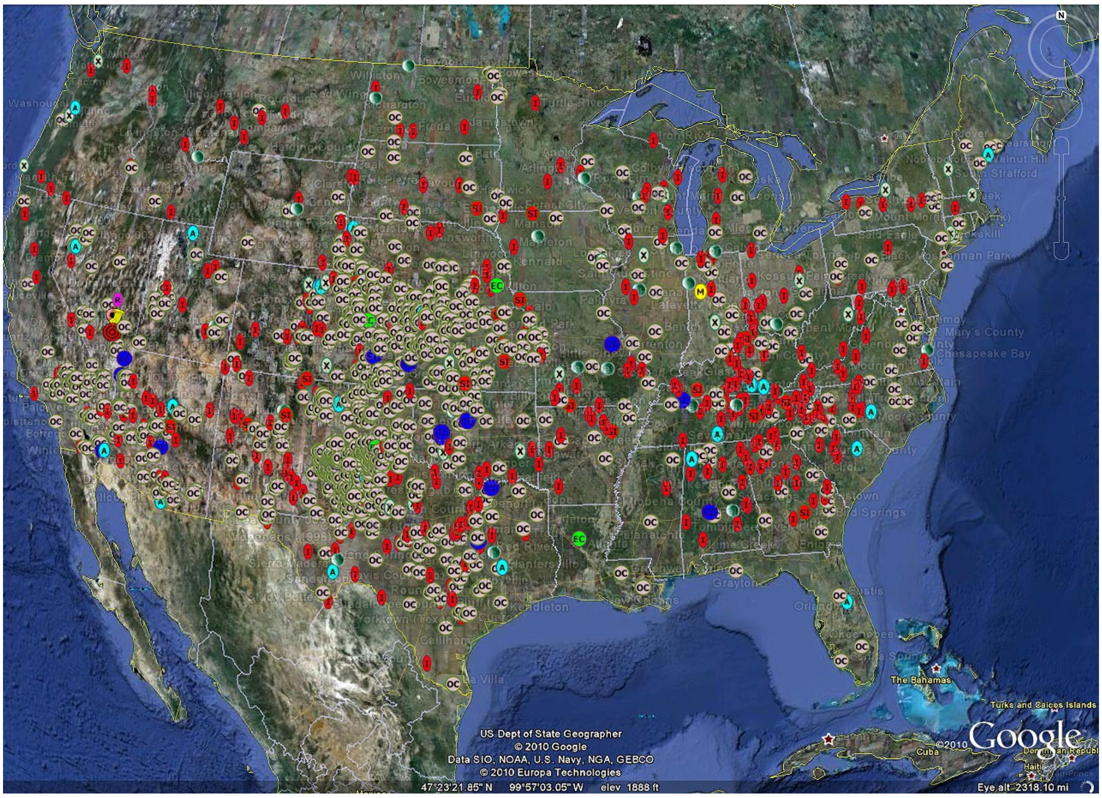

Figure 2.12: The red dots show iron meteorites, the white and green show ordinary chondrites and the blue show carbonaceous chondrites.

Significant attention by the scientific community to the hazard began in 1980 when Luis Alvarez and others proposed that such an impact, and the resulting global fall of dust, resulted in the mass extinctions of lifeforms on Earth, ending the age of dinosaurs [Alvarez et al., 1980]. The objective of a NEO survey is to find these objects during their periodic approaches to the Earth, to calculate their long-term orbital trajectories, and to identify any that may impact the Earth over the next several centuries. The chance that a NEO will be discovered less than a few years before impact is small.

2.7.4.1 Size vs Risk.

Small impacting objects that produce ordinary meteors dissipate their energy in the upper atmosphere and have no direct effect on the ground below. Only when the incoming projectile is larger than 10m in diameter it begins to be hazardous to humans. The hazard can be conveniently divided into three categories that depend on the size or kinetic energy of the body:

- Impacting body generally is disrupted before it reaches the surface, so most of its kinetic energy is dissipated in the atmosphere, resulting in chiefly local effects.
- Impacting body reaches ground sufficiently intact to make a crater, effects are still local, although nitric oxide and dust can be carried large distances, and there will be a tsunami if the impact is in the ocean.
- Large crater-forming impact generates sufficient globally dispersed dust to produce a significant, short-term change in climate, in addition to devastating blast effects in the region of impact.

The threshold size of an impacting body for each category depends on its density, strength, and velocity as well as on the nature of the target. In Figures 2.15-2.18 are some remarkable craters, remnants from impacts.

10 to 100 m diameter impactors

Bodies near the lower limit of this range intercept Earth every decade. Bodies about 100 m in diameter make larger strikes, on average, several times per millennium. The kinetic energy of a 10 m projectile travelling with a typical atmospheric entry velocity of 20 km/s is about 100 kilotons TNT equivalent, equal to several Hiroshima-size bombs (Figure 2.13). The kinetic energy of a 100 m diameter body is equivalent to the explosive energy of about 100 megatons, comparable to the yield of the very largest thermonuclear devices.

For the 10 m projectiles, only rare iron or stony-iron projectiles reach the ground with a sufficient fraction of their entry velocity to produce craters, as happened in the Sikhote-Alin region of Siberia in 1947. Stony bodies are crushed and fragmented during atmospheric deceleration, and the resulting fragments are quickly slowed to free-fall velocity, while the kinetic energy is transferred through an atmospheric shock wave. Part of the shock wave energy is released in a burst of light and heat (called a meteoritic fireball) and part is transported in a mechanical wave. Generally, these 100 kiloton eruptions occur high enough in the atmosphere so that no damage occurs on the ground, although the fireball can attract attention from distances of 600 km or more and the shockwave can be heard and even felt on the ground.

With increasing size, asteroidal projectiles reach progressively lower levels in the atmosphere before disruption, and the energy transferred through the shockwave is correspondingly greater. There is a threshold where both the radiated energy from the shock and the pressure in the shockwave can produce damage. A historical example is the Tunguska event of 1908, when a body perhaps 60m in diameter was disrupted in the atmosphere at an altitude of about 8 km (Figure 2.14). The energy released was about 12 megatons, as estimated from airwaves recorded on meteorological barographs in England, or perhaps 20 megatons as estimated from the radius of destruction. Even though the impact event was powerful enough to brighten the skies over London, thousands of kilometres away, no impact crater has ever been found. Siberian forest trees were mostly knocked to the ground out to distances of about 20 km from the end point of the fireball trajectory, and some were snapped off or knocked over at distances as great as 40 km.

Circumstantial evidence suggests that fires were ignited up to 15 km from the endpoint by the intense burst of radiant energy. The combined effects were similar to those expected from a nuclear detonation at a similar altitude, except,

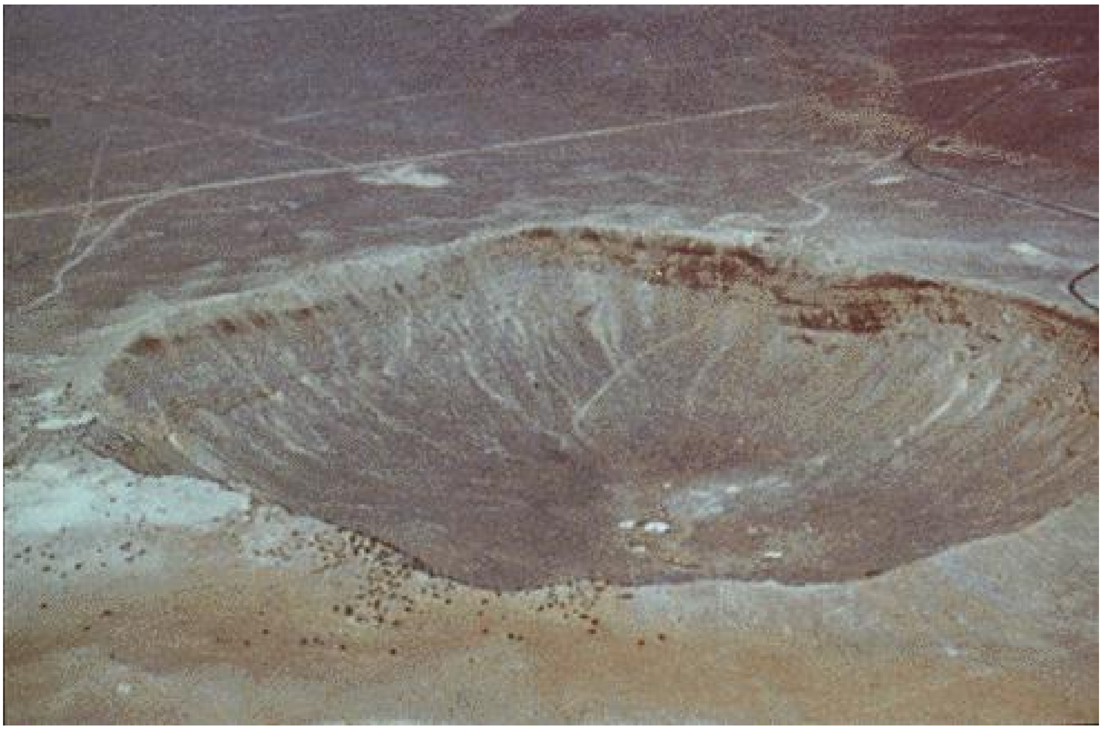

Figure 2.13: The Arizona crater was the first to be identified as an impact crater on Earth. A small asteroid of about 24.5 m impacted between 20,000 and 50,000 years ago. The size of this impact crater is 1.2 km around and 170 m deep.

of course, that there were no accompanying bursts of neutrons or gamma rays nor any lingering radioactivity. If a Tunguska-like event happen over a densely populated area today, the resulting airburst would be like that of a 10-20 megaton bomb: buildings would be flattened over an area 20 km in radius, and exposed flammable materials would be ignited near the centre of the devastated region.

An associated hazard from such a Tunguska-like phenomenon is the possibility that it might be misinterpreted as the explosion of an actual nuclear weapon, particularly if it were to occur in a region of the world where tensions were already high.

100 m to 1 km diameter impactors

Incoming asteroids of stony or metallic composition that are larger than 100m in diameter may reach the ground intact and produce a crater. The threshold size depends on the density of the impactor and its speed and angle of entry into the atmosphere. Evidence from the geologic record of impact craters as well as

Figure 2.14: The Tungusta impact area.

theory suggests that, in the average case, stony objects greater than 150 m in diameter form craters. They strike the Earth about once per 5000 years and, if impacting on land, produce craters about 3 km in diameter. A continuous blanket of material ejected from such craters covers an area about 10 km in diameter. The zone of destruction extends well beyond this area, where buildings would be damaged or flattened by the atmospheric shock, and along particular directions by flying debris. The total area of destruction is not, however, necessarily greater than in the case of atmospheric disruption of somewhat smaller objects, because much of the energy of the impactor is absorbed by the ground during crater formation. Thus the effects of small crater-forming events are still chiefly local.

Toward the upper limit of this size range, the megaton equivalent energy would so vastly exceed what has been studied in nuclear war scenarios that it is difficult to be certain of the effects. Extrapolation from smaller yields suggests that the "local" zones of damage from the impact of a 1 km object could envelop whole states or countries, with fatalities of tens of millions in a densely populated region. There would also begin to be noticeable global consequences, including alterations in atmospheric chemistry and cooling due to atmospheric dust, perhaps analogous to the "year without a summer" in 1817, following the explosion of the volcano Tambora.

Comets are composed in large part of water ice and other volatiles and therefore are more easily fragmented than rocky or metallic asteroids. In the size range from 100 m to 1km, a comet probably cannot survive passage through the atmosphere, although it may generate atmospheric bursts sufficient to produce local destruction.

1 km to 5 km diameter impactors

At these larger sizes, a threshold is finally reached at which the impact has serious global consequences, although much work remains to be done to fully understand the physical and chemical effects of material injected into the atmosphere. In general, the crater produced by these impacts has 10 to 15 times the diameter of the projectile; i.e., 10-15 km diameter for a 1 km asteroid. Such craters are formed on the continents about once per 300,000 years. At impactor sizes greater than 1km, the primary hazard derives from the global veil of dust injected into the stratosphere. The severity of the global effects of large impacts increases with the size of the impactor and the resulting quantity of injected dust. At some size, an impact would lead to massive world-wide crop failures and might threaten the survival of civilization. At still larger sizes, even the survival of the human species would be put at risk.

What happens when an object several kilometres in diameter strikes the Earth at a speed of tens of kilometres per second? Primarily there is a massive explosion, sufficient to fragment and partially vaporize both the projectile and the target area. Meteoric phenomena associated with high speed ejecta could subject plants and animals to scorching heat for about half an hour, and a global firestorm might them ensue. Dust thrown up from a very large crater would lead to total darkness over the whole Earth, which might persist for several months. Temperatures could drop as much as tens of degrees C. Nitric acid, produced from the burning of atmospheric nitrogen in the impact fireball, would acidify lakes, soils, streams, and perhaps the surface layer of the oceans. Months later, after the atmosphere had cleared, water vapour and carbon dioxide released to the stratosphere would produce an enhanced greenhouse effect, possibly raising global temperatures by as much as ten degrees C above the pre-existing ambient temperatures. This global warming might last for decades, as there are several positive feedbacks; warming of the surface increases the humidity of the troposphere thereby increasing the greenhouse effect, and warming of the ocean surface releases carbon dioxide which also increases the greenhouse effect. Both the initial months of darkness and cold, and then the following years of enhanced temperatures, would severely stress the environment and would lead to drastic population reductions of both terrestrial and marine life.

2.7.4.2 The threshold size for a global catastrophe

The threshold size of impactor that would produce one or all of the effects discussed above is not accurately known. The geochemical and palaeontological record has demonstrated that one impact (or perhaps several closely spaced impacts) 65My ago of a 10 km NEO resulted in total extinction of about half the living species of animals and plants. This so-called K-T impact may have exceeded 100 megatons in explosive energy. Such mass extinctions of species have recurred several times in the past few hundred million years; it has been suggested, although not yet proven, that impacts are responsible for most such extinction events. We know from astronomical and geological evidence that impacts of objects with diameters of 5 km or greater occur about once every 10 to 30My.

Death by starvation of much of the world's population could result from a global catastrophe far less horrendous than those cataclysmic impacts that would suddenly render a significant fraction of species actually extinct, but we know only very poorly what size impact would cause such mortality. The uncertain results could be expressed either as a wide range of possible consequences for a particular size (or energy) of impactor or as a range of impactor sizes that might produce a certain scale of global catastrophe. We take the second approach and express the uncertainty as a range of threshold impactor sizes that would yield a global catastrophe of the following proportions:

- It would destroy most of the world's food crops for a year, and /or
- It would result in the deaths of more than a quarter of the world's population, and/or

- It would have effects on the global climate similar to those calculated for "nuclear winter", and/or
- It would threaten the stability and future of modern civilization.

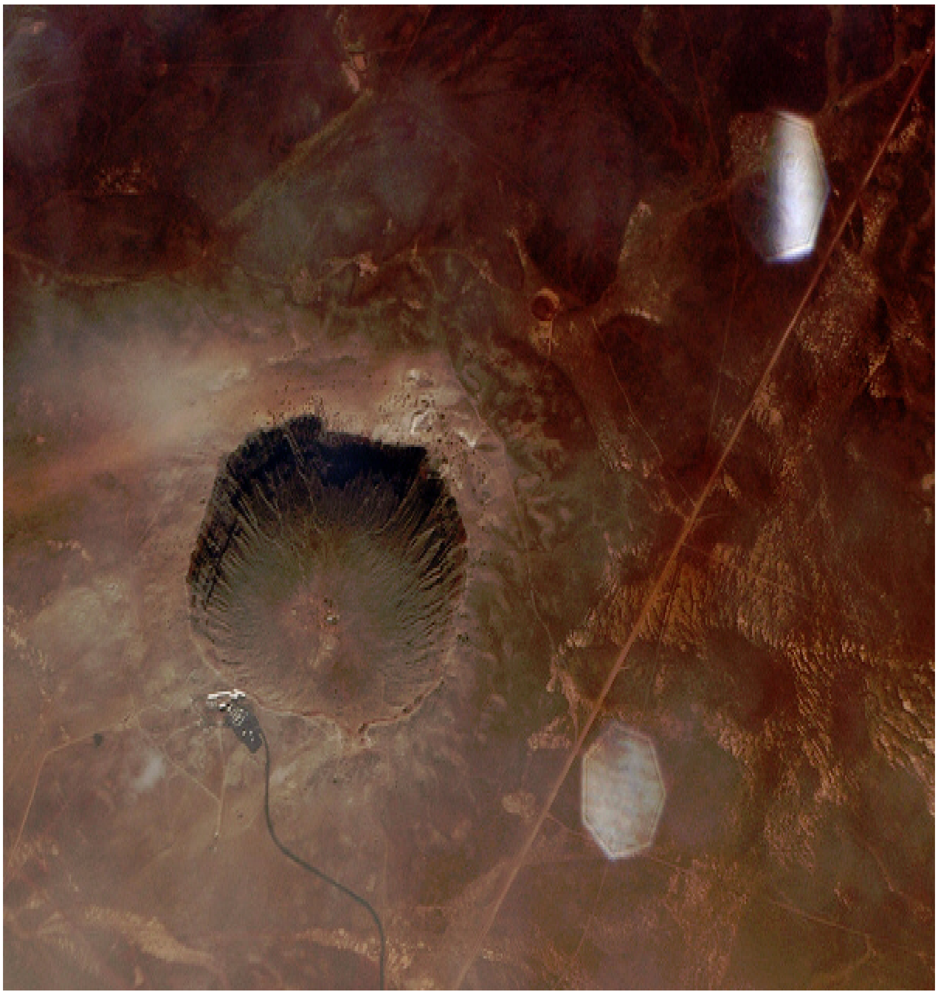

Figure 2.15: Barringer (Winslow) crater in Arizona is one of the smaller examples with a diameter of 1.2 km and depth of 570 ft. The impact occurred 49,000 years ago.

A catastrophe having one, or all, of these traits would be a horrifying thing unprecedented in history, with potential implications for generations to come.

We are talking about a catastrophe far larger than the effects of the great World Wars, it would result from an impact explosion certainly larger than if 100 of the biggest Hydrogen bombs ever tested were detonated at once. On the other hand, we are talking about an explosion far smaller (less than 1% of the energy) the the impact 65My ago. Such a catastrophe that would threaten modern civilization, not an apocalypse that would threaten the survival of the human species.

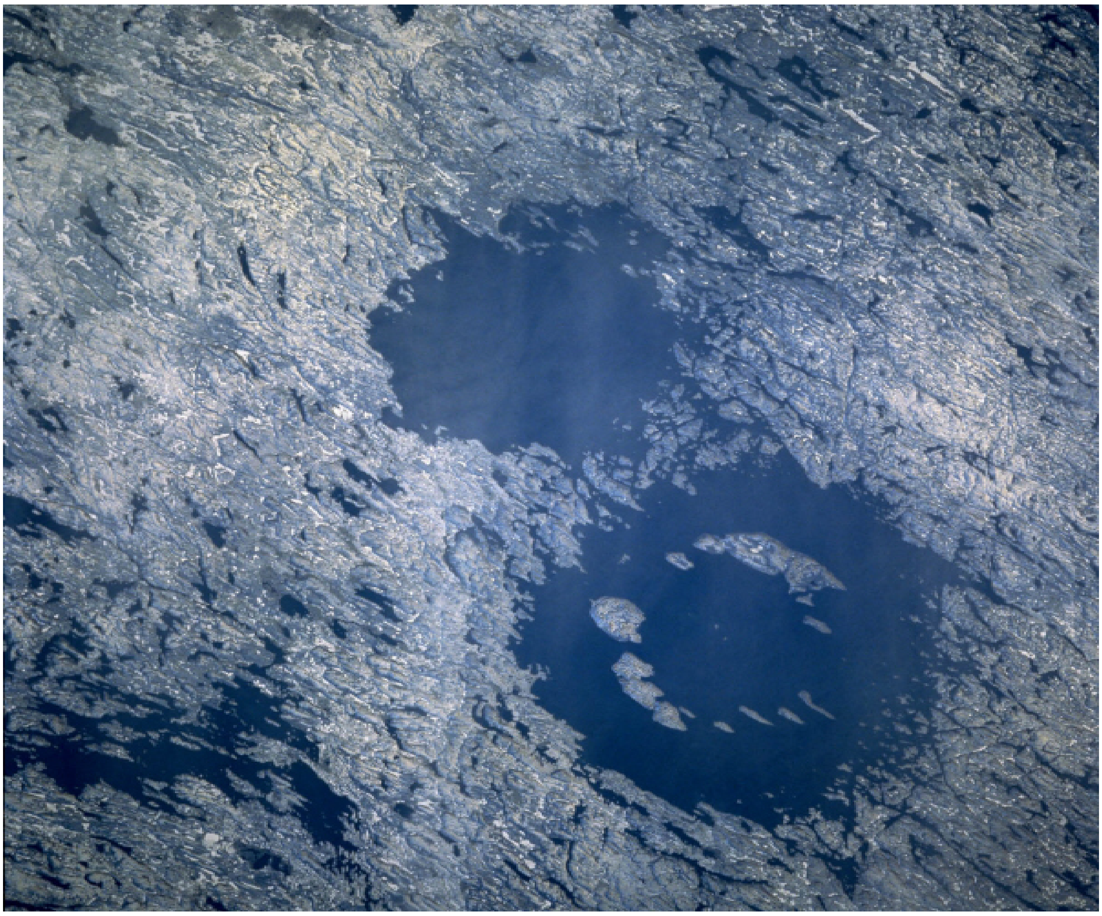

Figure 2.16: These twin circular lakes were formed simultaneously by the impact of an asteroidal pair which slammed into the planet approximately 290My ago. The lakes are located near Hudson Bay within the Canadian Shield. The larger western structure contains a ring of islands with a diameter of about 10 km that surrounds the centre of the impact zone. They constitute a central uplifted area and are covered with impact melts. The central peak of the smaller Clearwater Lake East is submerged. The lakes are named after their exceedingly clear water. The surrounding terrain shows widespread scarring from glaciation. The multitude of linear and irregular shaped lakes are the result of gouging or scouring action caused by the continental ice sheets that once moved across this area.

What is the range of impactor sizes that might lead to this magnitude of global catastrophe? At the July 1991 Near-Earth Asteroid Conference in San Jaun Capistrano, California, the most frequently discussed estimate of the threshold impactor diameter for globally catastrophic effects was about 2 km. An estimate of the threshold size was derived for this Workshop in September 1991 by Brian

Toon, of NASA Ames Research Center. Of the various environmental effects of a large impact, Toon believes that the greatest harm would be done by the sub-micrometer dust launched into the stratosphere. The very fine dust has a long residence time, and global climate modelling studies imply significant drops in global temperature that would threaten agriculture worldwide.

Figure 2.17: Manicouagan Crater in northern Canada is one of the oldest impact craters known. Formed about 200My ago, the present day terrain supports a 70 km diameter hydroelectric reservoir in the tell-tale form of an annular lake. The crater itself has been worn away by the passing of glaciers and other erosional processes. Still, the hard rock at the impact site has preserved much of the complex impact structure and so allows scientists a leading case to help understand large impact features on Earth and other Solar System bodies. Also visible above is the vertical fin of the Space Shuttle Columbia from which the picture was taken in 1983.

The quantity of sub-micrometer dust required for climate effects equivalent to those calculated for nuclear winter is estimated at about 10,000 Teragrams (Tg) (1 Tg = 1012 g). For a 30 km/s impact, this translate to a threshold impacting body diameter of between 1 and 1.5 km in diameter.

The threshold for an impact that causes widespread global mortality and threatens civilization almost certainly lies between about 0.5 and 5 km diameter, perhaps near 2 km. Impacts of objects this large occur from one to several times per million years.

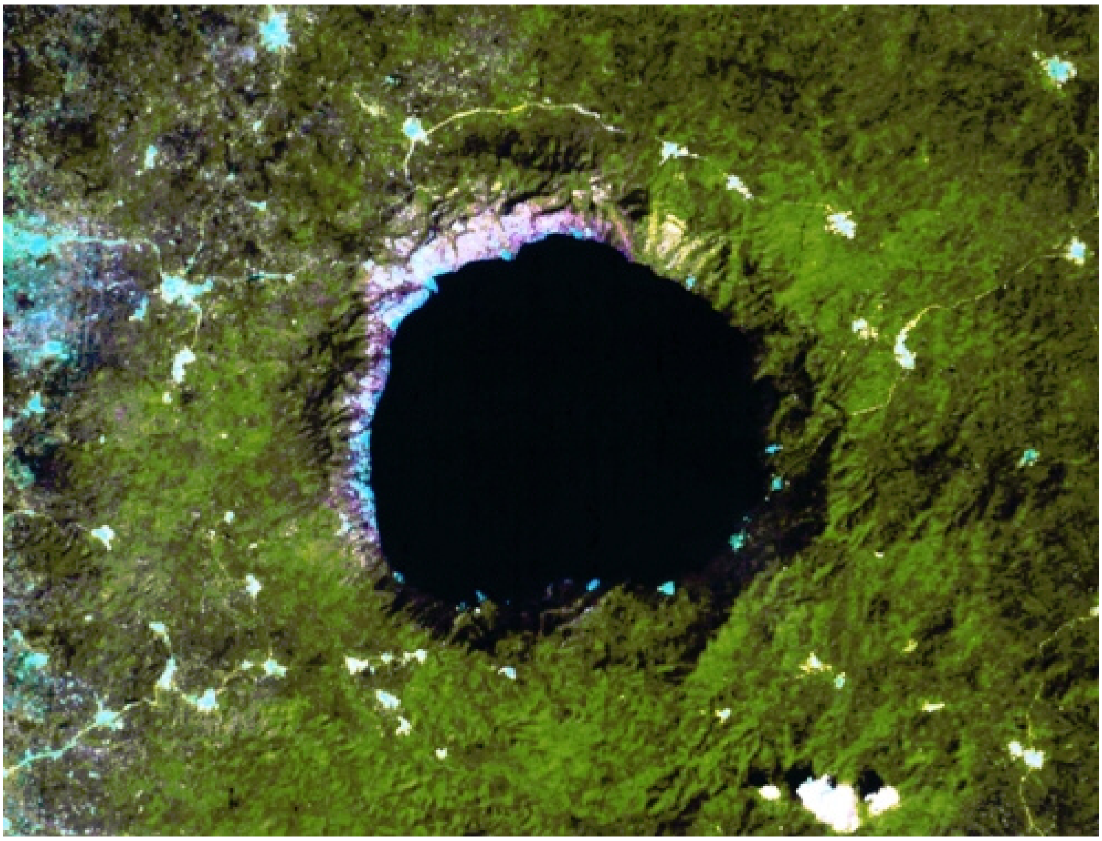

Figure 2.18: Bosomtwe Crater, Lake Bosomtwe, Ghana - the actual impact crater which hosts Lake Bosomtwe is 10.5 km in diameter, the lake itself is presently 7 km. The impact took place 1My ago. The crater has been eroded due to overflow from the lake.

Chapter 3

Studying an asteroid

3.1 Asteroid Families

3.1.1 Asteroid orbits

The calculation of an asteroid's orbit is one of the oldest inversion problems in astronomy.

A different method can be used to identify asteroid families that formed recently. Instead of using the proper orbital elements, this new method relies directly on five osculating orbital elements: semi-major axis a, eccentricity e, inclination i, perihelion longitude ϖ, and nodal longitude Ω. The very young families that formed in the last $\sim$ 1Myr show up as clusters in 5D space, because fragments produced by a breakup have similar starting orbits and because they typically take $>$ 1My before they can become dispersed by planetary perturbations and radiation forces. The clustering of fragments in mean anomaly M is not expected due to the effects of Keplerian shear.

Six Keplerian elements are needed for this purpose. These are the a, e, i, Ω, ω and M which mean respectively the semi-major axis, eccentricity, inclination, longitude of the ascending nodes, argument of perihelion and mean anomaly. The first two elements describe the size and shape of the ellipse. The semi-major axis particularly is the distance between the two bodies and not the distance to the centre of mass. The inclination which is measured at the ascending node and the longitude of the ascending node give the orientation of the orbital plane of the asteroid. Finally the argument of the periapsis gives the orientation of the eclipse and mean anomaly defines the position of the asteroid on the trajectory at a specific time. Especially the mean anomaly is an angle that varies linearly with time and does not refer to a real geometric angle. However the true anomaly represents the real geometric angle on the trajectory's plane and is a value between the periapsis and the current position of the asteroid (Figure 3.1).

In n-body problem we take into account gravitational perturbations due to planets and other objects together with non-gravitational and relativistic effects which create the real orbit . In this case all six Keplerian parameters change over time.

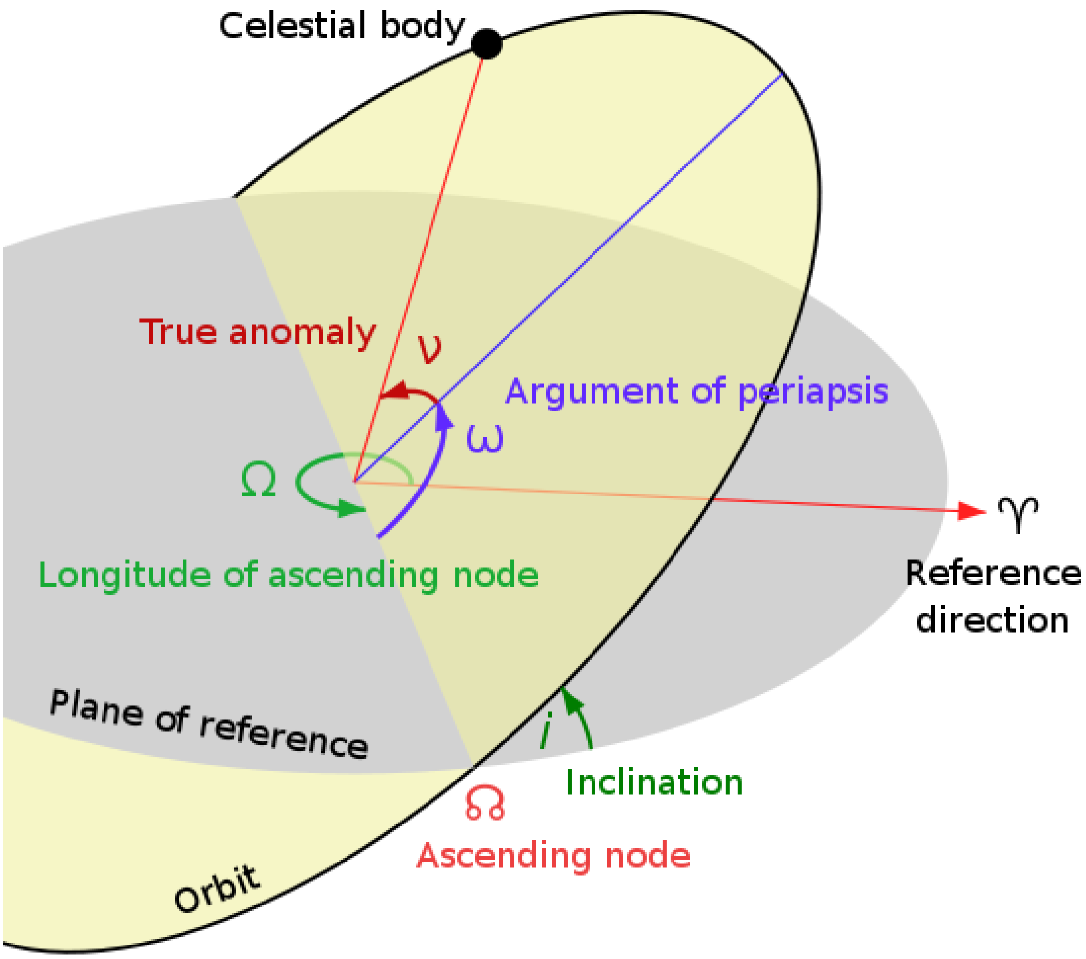

Figure 3.1: The definitions of the six orbital elements which characterise the orbit of an asteroid.

In a two-bodies problem, asteroid-Sun, these values are stable except M, which changes by time. These are called osculating elements which characterize an osculating orbit. We suppose that the asteroid orbits without perturbations around the Sun and so its orbital elements are able to be calculated using the object's position in the sky and velocity relative to the Sun. Generally a perturbed trajectory can be considered as a group of points each of which is contributed by a curve.

The standard method to identify an asteroid family is to search for concentrations of orbits in 3D space of proper elements which can be derived from the osculating elements at a specific epoch: proper semimajor axis a_p , proper eccentricity e_p and proper inclination i_p. These elements, being more constant over time than the osculating orbital elements, provide a dynamical criterion that a group of asteroids has a common origin.

They change their values in a quasi-periodic and predictable way because of major planets and other small bodies perturbations. These changes happen in a large time scale so the osculating do not differ much from the proper elements. On the contrary, in the 99% of the main belt asteroids, part from the asteroids in Kirkwood gaps, these differences are less than 0.02 AU in semi-major axis, 0.1 in eccentricity and 2^o for inclination.

The idea of the proper elements is based on the linear theory of secular perturbations . This theory does not take on account short periodic perturbations and introduces a constant semi-major axis, the proper semi-major axes a_p. Another way to extract the proper elements is to numerically integrate the the full equations of motion. According to this method we should take averages of the a, e, i of times longer than the periods of circulation of the angular variables. Unfortunately this method gives proper elements with low reliability.

The activity for determination the asteroid proper elements was very intense the previous decades. Now the proper elements are able to be computed for every asteroid with accurate osculating elements. This determination of the proper elements led to the development of a more reliable classification in families and of complete theories of of asteroid motion.

3.1.2 The "battle" of families

The first attempt for a classification on asteroid population was done by Kiyiotsugu Hirayama [Hirayama, 1918]. He used the proper elements in order to group the known asteroids. From his results he ended up with the idea that those groups was not a matter of chance but the relevant asteroids have a common origin. His hypothesis describe that the asteroids that belong in a group are actually fragments of a parent body. The Hirayama families are five: *Eos, Themis, Koronis, Flora, Maria.*

After Hirayama, many papers were published on this subjects from several authors. Each one used a different database for the proper elements, so the number of the families varies according to the procedure each author followed. The range was from 15 to 117 families (Table 3.1). Another reason for the existence of this huge range is the calibration of their identification method that used the previous studies. Because of the disagreement about the real number of asteroid families only the first four were taken seriously into consideration.

The last two decades the situation has improved because of the identification procedures which became more objective. Also the databases have more accurate proper elements and so researchers are able to examine larger sample of asteroids.

If we accept that the asteroids, members of the same family, had similar osculating elements just after the formation of the family we should also realize that these elements have been changed. The orbital elements face variations due to planetary perturbations. The orbital evolution of the asteroids is not totally unpredictable over long timescales. If it was, then we would not be able to predict, using the osculating elements from different objects at the same epoch, the common origin. At some point the long-term orbital characterization can be described by proper elements. These consist an average of osculating elements for large timescales. As a result the osculating elements vary in a family as a function of time but the proper elements do not. So the orbital similarities can be analysed with the proper and not the osculating elements.

Although the import of the proper elements was significant for the progress of the determination of asteroid families, it did not solve the problem of the different family identification related to a different database. The aim was to find a metric in the space for the proper elements, to measure the distance between two orbits. There are two techniques for classification. The Hierarchical Clustering Method (HCM)[Zappala et al., 1990] and the Wavelet Analysis Method (WAM)[Bendjoya et al., 1991].

Family name	Named after	a	e	i
Eos	221 Eos	2.99 - 3.03	0.01 - 0.13	8 - 12
Eunomia	15 Eunomia	2.53 - 2.72	0.08 - 0.22	11.1 - 15.8
Flora	8 Flora	2.15 - 2.35	0.03 - 0.23	1.5 - 8.0
Hygeia	10 Hygeia	3.06 - 3.24	0.09 - 0.19	3.5 - 6.8
Koronis	158 Koronis	2.83 - 2.91	0 - 0.11	0 - 3.5
Maria	170 Maria	2.5 - 2.706		12 - 17
Nysa	44 Nysa	2.41 - 2.5	0.12 - 0.21	1.5 - 4.3
Themis	24 Themis	3.08 - 3.24	0.09 - 0.22	0 - 3
Vesta	4 Vesta	2.26 - 2.48	0.03 - 0.16	5.0 - 8.3
Adeona	145 Adeona			
Astrid	1128 Astrid			
Bower	1639 Bower			
Brasilia	293 Brasilia			
Gefion	1272 Gefion	2.74 - 2.82	0.08 - 0.18	7.4 - 10.5
Chloris	410 Chloris			
Dora	668 Dora			
Erigone	163 Erigone			
Hansa	480 Hansa	2.66	0.06	22.0
Hilda	153 Hilda	3.7 - 4.2	>0.07	<20
Karin	832 Karin			
Lydia	110 Lydia			
Massalia	20 Massalia	2.37 - 2.45	0.12 - 0.21	0.4 - 2.4
Meliboea	137 Meliboea			
Merxia	808 Merxia			
Misa	569 Misa			

Neamea	845 Neamea			
Nemesis	128 Nemesis			
Rafita	1644 Rafita			
Veritas	490 Veritas			
Theobalda	778 Theobalda	3.16 - 3.19	0.24 - 0.27	14 - 15

Table 3.1: Some of the most important Main Belt asteroid families along with the respective ranges of the orbital elements.

3.2 Asteroid Spectral Types

The majority of the Main Belt asteroids are small in size and have no different internal matter compared with their surface. However, this does not happen with the large bodies. When the family identification started, spectroscopic observations were done in order to confirm the reliability of groupings. Spectroscopic identifications were focused on the characterization of the mineralogical compositions of different families. Also the spectroscopic observations were looking for thermal differentiation of the parent body and possible space-weathering process.

The first colour measurements were shown up on 1929 by Bobrovkikoff. However that spectra were not numerous or precise. After some decades, when UBV photometry was used to study the asteroids, two groups of objects were found with differences in their reflectance properties. Almost at the same period Zellner recognized a distribution in albedos and also suggested the to main categories, the dark carbonaceous and the brighter stony types.

The first taxonomy of asteroids was produced by Chapman in 1975 and was based on a system of letters. The letter C was used for the carbonaceous objects, S for stony and U for the rest. Other who improved the classification system were Bowell et al in 1978 and Tholen and Barucci in 1989.

Tholen Classification

The first widely used spectral type classification was done by D. Tholen [Tholen, 1984]. The classification was a logical extension of the previous systems and was done using the *Eight-Colour Asteroid Survey* (ECAS) and information obtained from the seven independent colour indices (Table 3.2). Moreover albedo measurements helped to define some of the class boundaries.

This taxonomy included 14 types of asteroids, the first two of which were the most populated classes, C and S. In addition there were six more distinct classes A, B, D, F, G and T. For E, M and P types there were no clear spectra but they were distinguished by albedo. When albedo information was not available too, the remaining asteroids were jumped into the X-class. Finally the Q, V and R-types were created because of three unusual asteroids, 1862 Apollo, 4 Vesta and 349 Dembowska respectively. Although other attempts were made in order to improve the Tholen taxonomy, no one succeed to overcome it for many years.

Group	Type	Reference Asteroid	Description
C-Carbonaceous	B F G C	2 Pallas 704 Interamnia 1 Ceres 10 Hygeia	 the majority of C-group
S-Silicaceous		15 Eunomia, 3 Juno	
X-Several types	M E P	16 Psyche 44 Nysa, 55 Pandora 259 Aletheia, 190 Ismene	metallic objects higher albedo than M lower albedo than M
	A D T Q R V	446 Aeternitas 624 Hector 96 Aegle 1862 Apollo 349 Dembowska 4 Vesta	

Table 3.2: Tholen Taxonomy

SMASS Classification

The SMASS classification is based on the *Small Main-Belt Asteroids Spectroscopic Survey* of 1447 asteroids (Table 3.3). The new survey had higher resolution than ECAS and a variety of narrow spectral features was extracted. Even though albedo was used in the first taxonomic categorization of asteroids and plays a role for distinguishing some of the classes within the Tholen taxonomy, albedo is not utilized in the development of this taxonomy. The primary reason for this is one of practicality as there is currently a lack of albedo information for the majority of the asteroids sampled in SMASSII [Bus and Binzel, 2002].

The new taxonomy system improved the previous one. The three major groups S-, C- and X-type asteroids remain with their initial definitions. According to specific spectral features, 26 classes were defined. Beyond the common types a new L-class is introduced along with classes with intermediate characteristics. These are the Cb, Cg, Cgh, Ch, Ld, Sa, Sk, Sl, Sq, Sr, Xc, Xe and Xk. The main desire was to stay close to Tholen's taxonomy. The analysis of Bus and Binzel produced three spectral components. The first component is a spectral slope which is defined by fitting a line to each spectrum according to the equation:

$$r_i = 1.0 + \gamma(\lambda_i - 0.55) \tag{3.1}$$

where r_i is the relative reflectance at each channel, λ_i is the wavelength of the channel in microns and γ is the slope of the line.

3.3 Albedo

Albedo refers to the ratio of the reflecting radiation over incident radiation of a body. Generally the albedo depends on the directional distribution of the incident radiation, except from the Lambertian surfaces. The Lambertian surfaces scatter radiation in all directions and that is the reason why their albedo does not depend on the incoming radiation. Asteroids do not have a Lambert disk, as they are airless objects.

Two types of albedos are used in astronomy. The V-band geometric albedo and the Bond Albedo. Their values are different as the first measures brightness when the light source is directly behind the observer (Earth) and the second measures the total proportion of the electromagnetic energy reflected.

The geometric albedo is a ratio of the actual asteroid brightness at a zero phase angle, looking straight at the direction of illumination. For an Earth observer this happens when the asteroid is at opposition. The correlation between the geometric albedo (p), the absolute magnitude (H) and the object's diameter (D) is:

$$p = \left(\frac{1329 \cdot 10^{-H/5}}{D}\right)^2 \tag{3.2}$$

Main group	Subtype	Reference Asteroid	Description
C-Carbonaceous	B		Tholen B and F types
	C		the majority of C-type
	Cg, Ch, Cgh		Tholen G-type
	Cb		transition objects between C and B types
S-Silicaceous	A		
	Q		
	R		
	K	181 Eucharis, 221 Eros	
	L	83 Beatrix	
	S		the majority of S-type
	Sa, Sq, Sr, Sk, Sl		transition objects between plain S and the other types
X-mostly metallic	X		the majority of X-type/ Tholen M, E, P-type
	Xe, Xc, Xk		transition types between plain X and E, C, M-types
	T		
	D		
	Ld		more extreme spectral features than L-type
	O	3628 Boznemcova	
	V		

Table 3.3: SMASSII Taxonomy

The geometric albedo is quite difficult to be determined as their reflectance is stronger for a small range of phase angles around zero.

The Bond albedo takes into account all wavelengths at all phase angles and was originally defined for spherical bodies. It is related to the geometric albedo (A):

$$A = pq \tag{3.3}$$

where q is the phase integral and is given as an equation of scattered flux I(a).

The angle a is the angle between the source of radiation and the observing direction with range 0 to 180^o.

3.4 Determination of the Mass

The determination of an asteroid's mass is a difficult task. If an asteroid's mass is known determining the volume its equivalent to determine its density. The main difficulty in determining asteroid masses is their extremely small size.

A way to determine the mass of an asteroid is by observing a gravitational effect on a second body like a natural satellite or a body like another asteroid or a spacecraft, that creates perturbations on the test body (Figure 3.2). Firstly the perturbation of the test body can be estimated using the two-body ballistic particle model:

$$tan\theta/2 = \frac{G(m+M)}{v^2 b} \tag{3.4}$$

where θ is the angle of deflection in the centre of the mass frame of reference, v is the relative velocity of the encounter and b the impact parameter.

We should take into account that most asteroids orbit near the ecliptic and so a coplanar encounter will change in a first approximation only the semi-major axis or eccentricity. Also the perturbation is weak and as a result the change in orbital elements is small. With this method the masses of Mathilde, Eros, Ceres, Pallas, Vesta, Hygiea were found.

Another possibility is an asteroid to have a companion, a natural satellite. The first example was 243 Ida with its satellite Dactyl, where Ida's mass was determined considering a stable orbit for Dactyl. Adaptive optics enabled the detection of these natural satellites as they can resolve very faint objects from the main body. The contrast is sharpened and the resolution is increased to 0.1 arcsec [Close et al., 1999]. After that the previous method is used in order to calculate the mass.

According to the Doppler method at the beginning of the process the signal goes out as a nice waveform. It's reflected from the parts of the asteroid that are closest to the radio dish first, but while those first reflections are happening, the radio wave is still propagating toward more distant parts of the asteroid. So when the radio dish detects the return signal, the sharp signal has been spread out in time.

The first reflection comes from the nearest parts of the object. The last reflections come from the most distant parts of the object that you can see. Take the amount of time that separates the first and last reflections, multiply it by the speed of light, and you get the distance between those two points. Then double that, assuming the body is quasi-spherical and has a hidden hemisphere behind the hemisphere we can see. This will not be a particularly accurate estimate.

One thing we cannot do is figure out which reflections were coming from which parts of the asteroid. All we know is how strong the return signal was with respect to time.

As an asteroid rotates, some parts of it are moving toward us, while other parts are moving away. As the broadcast radio wavefronts hit the part of the asteroid that is moving toward us, the asteroid smacks into each wavefront faster than it would if it was not rotating. The speed of the wavefronts does not change, because the speed of light is constant, so the wavefronts end up being packed closer together. This is a Doppler shift. The asteroid has taken the broadcast wavelength and reflected it at a shorter wavelength from the parts of the asteroid that are rotating toward us. On the other side of the asteroid, which is rotating away, the opposite thing happens, each arriving wavefront smacks into the asteroid a little later than it would if the asteroid was not rotating, so the reflected waves are spread farther apart.

The asteroid is not only rotating, it is also moving at some high speed with respect to Earth. So the whole return signal is already going to be Doppler shifted in one direction or the other depending on whether the asteroid is coming at us or going away from us. The Doppler shift due to the asteroid's rotation is a small increment of shift on top of the shift due to the asteroid's motion.

At the radio dish, there is a detector that can split the incoming reflected waves into its different wavelengths.The radio dish records the time and strength of the return signal at many different wavelengths. The faster the object is rotating, the more Doppler-shifted the return signals are; fast rotators spread out more across the wavelength axis. Objects that are not rotating at all collapse into a blip at the central wavelength.

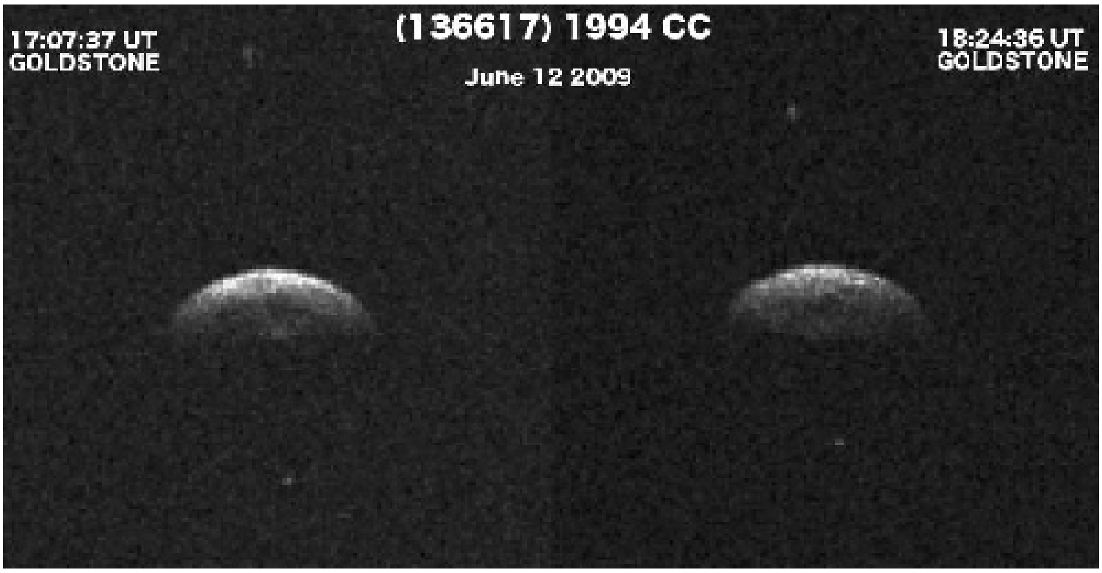

Figure 3.2: The triple asteroid system (136617) 1994 CC, which consists of a central object approximately 700 m in diameter and two smaller moons, each about 50 m, that orbit the central body. The two images, obtained on June 12, 2009, show how the positions of the two small moons changed during the 77 min that elapsed between images. The images have a resolution of 19 meters/pixel.

3.5 Determination of the Size

Apart from the previous mentioned techniques like adaptive optics or perturbations there are other two ways to determine the size of an asteroid. These are the occultations and the direct imaging.

Observing stellar occultations by asteroids there are made accurate determinations of the length of the chord observed. During the process of the method individual chord lengths are determined by timing the length of the occultation at a known place within the path on Earth. The asteroids rate is known from the ephemeris and so the timing is able to be converted to length. It is required to have multiple observations of the chords from different places in order to extract the shape during a single occultation.

The main disadvantages of the method are the limitation of the observers and the frequency of the phenomenon. There must be considered that the largest part of the Earth's surface is covered by water and as a result it is impossible to have the whole path on land and simultaneously to have observers spread in it. Moreover from a single event only a two-dimensional projection of the object can be made.

The direct imaging is the most recent attempt to estimate the asteroid sizes. As the years go by new more efficient and with better resolution telescopes space or ground-based are built. The best example is the GAIA mission with 20 milliarcsec resolution (Figure 3.3). According to that telescope's capabilities a 50 km asteroid in 1.5 AU will be 2 px in the frame. However, with GAIA the uncertainty of the shape will be about 40-50%.

The GAIA mission will be able to determine the basic physical properties of large numbers of objects. In particular, GAIA will directly measure sizes of about 1,000 objects, will derive spin properties and overall shapes of about 10,000 objects, and will also produce a new taxonomic classification of tens of thousands asteroids. A justification of the above mentioned predictions is given, based on a large body of simulations carried out so far. Coupled with the direct determination of the masses for about 100 objects, GAIA size measurements are expected to produce accurate measurements of average densities for about 100 objects belonging to a large variety of taxonomic classes. Moreover, GAIA will produce a much better knowledge of the inventory and size and spin distributions of the whole population, of the distribution of taxonomic classes as a function of heliocentric distance, and of the dynamical and physical properties of dynamical families [Cellino et al., 2007].

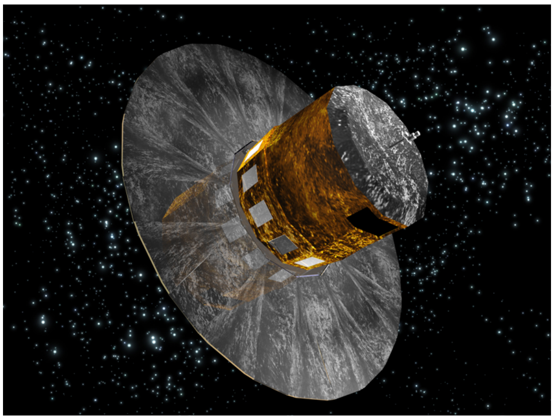

Figure 3.3: GAIA mission

3.6 Density and Composition

From the analysis of the surface properties such as reflectance spectra or albedo, it is possible to make inferences on composition. These observables however tell us about surface composition only, which may or may not be reflective of the bulk composition of the body. The largest asteroids (mass above 10^{20} kg) are apparently compact bodies without any macroporosity. This contrasts strongly with all the other less massive small bodies that have 20% or more macroporosity. The fraction of voids increases dramatically for icy bodies like comets and TNOs. Finally, primitive C-type asteroids tends to have larger macroporosity than the basaltic S-type.

Macroporosity, if present to a large extend, may have strong consequences on certain physical properties such as gravity field, thermal diffusivity, seismic velocity and on collisional lifetimes. Macroporosity can also help in understanding the collisional history: intact bodies are expected to have low-to-no macroporosity, while heavily impacted objects may have large cracks.

Direct measurement of the bulk density (ρ) involves the independent measures of the mass (M) and volume (V): $\rho = \mathrm{M/V}$. Indirect density calculation method is used for small bodies with diameters of a few to tens of kilometres where the other methods to estimate their mass cannot be used. The gravitational influence of these very small bodies is too tiny to be measured. Even in the case of binary systems, their angular extent is generally too small to be imaged with current technology. The only exception are the small binary NEAs that can be imaged with radar during close approaches with Earth. Yet, a large fraction of the currently known binaries are small-sized systems discovered by studying their light-curves.

We can summarize some correlations between the asteroid spectral types (Figures 3.4-3.5):

- Asteroids in the S-class are more dense than those in the C-class.
- Asteroids in the C-class seem to have larger macroporosity than those in the S-class.
- The density of asteroids from both the S-complex and the C-complex seems

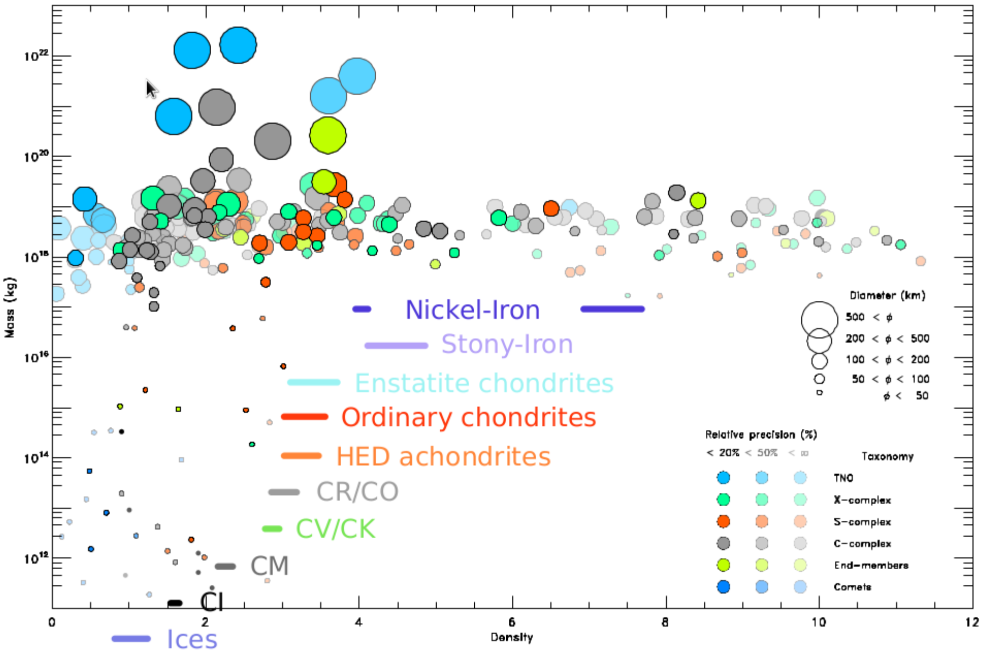

Figure 3.4: [Carry, 2012]

to increase with the mass, apparently resulting from a decreasing macroporosity.

- In both C and S-class, NEAs seem to have a lower density than MBAs, following the trend between mass and density observed for MBAs.
- At comparable sizes, B-types appear significantly denser ($\rho\sim2.4$)than the other types of the C-complex that gather around $\rho\sim1.4$.
- The density of the X-class asteroids covers a large range, from the most dense Xc-types with $\rho\sim4.9$ to X-types with $\rho\sim1.8$.

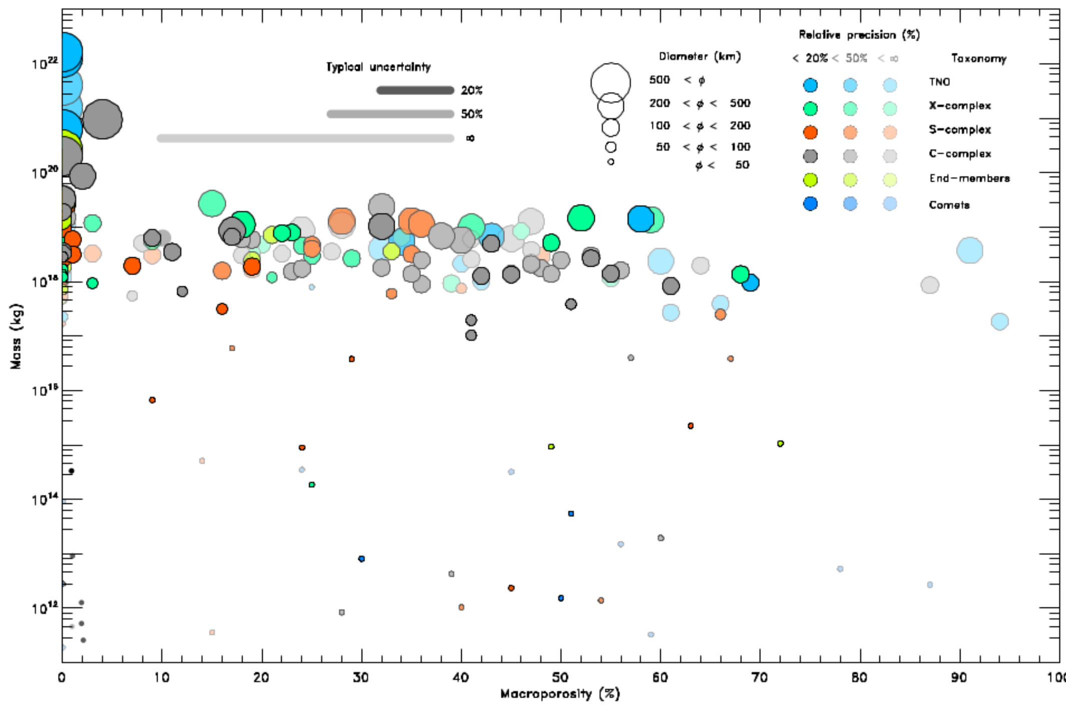

Figure 3.5: [Carry, 2012]

3.7 The Rotation of the asteroids

The fundamental characteristic of asteroid rotation is the rotational angular momentum:

$$\vec{L} = \hat{I}\vec{\omega} \tag{3.5}$$

where the angular momentum vector $\vec{L}$ and the inertia tensor $\hat{I}$ are changed because of collisions and other processes during asteroid evolution. Generally, the spin vector $\vec{\omega}$ is not constant because the moment of inertia varies about the instantaneous spin axis which direction and size changes over time, usually on the order of its rotational period.

With groundbased observations it is not possible to measure the angular momentum. Instead the spin vector can be observed. Using the above equation and with an estimation of the moment of inertia from the shape and size, the angular momentum will be calculated. The spin vector can be determined with several methods, but the most frequently used is the light-curve observations.

The distribution of the asteroids rotation period varies due to their size.

- Asteroids larger than D=40 km follow a Maxwellian. This low border was estimated because the range within exist the larger deviations from the Maxwellian distribution is 30-40 km. Also if a distribution is close to a Maxwellian this means that the system is collisionally quiet. This result indicates that either they are original main belt bodies or the major remnants of collisions.

- The rotation periods of small asteroids 0.15 km<D< 10 km do not follow a Maxwellian and appear to have two maxima at slow and fast rotations. Moreover there is a cut off at spins faster than 12 periods per day. Some of them are inner planet-crossers binaries with a really fast rotating primary component. They consist also fragments of larger bodies that gained angular momentum after collisions but their spins and shapes were affected by other non-collisional factors.

- In the intermediate size range 10 km<D<40 km the populations of large and small asteroids overlap. Within this range a steep increase of the mean spin rate occurs. Also some members of this category belong to the dynamical families. Some of the families have specific rotation distributions which are related to specific formation conditions of the families.

- The very small asteroids with D<0.15 km are coherent fragments of larger ones. This assumption was made because they rotate so fast that if they were composed from different bodies they could not be hold together by self gravitation. Most asteroids with absolute magnitude H< 22 rotate with periods of less than 2 h. The observed periods are so fast that these bodies cannot be held together. Sometimes these fragments are called "monoliths". However, in the fastest rotators the tensile strength which exist is extremely less than the typical tensile strength of a consolidate rock.

3.7.1 Binaries and Pairs

The most abundant binary population is that of close binary systems among near-Earth, Mars-crossing and main belt asteroids that have a primary diameter of about 10km or smaller. They have a total angular momentum very close to, but not generally exceeding, the critical limit for a single body in a gravity regime. This suggests that they formed from parent bodies spinning at the critical rate (at the gravity spin limit for asteroids in the size range) by some sort of fission or mass shedding. The YORP effect is a candidate to be the dominant source of spin-up to instability. Gravitational interactions during close approaches to the terrestrial planets cannot be a primary mechanism of formation of the binaries, but it may affect properties of the NEA part of the binary population.

Asteroid pairs are called objects which show similarities in their orbits (Figure 3.6). There is a distance d in the 5D space (a, e, i,ω, Ω) that is defined as:

$$\left(\frac{d}{na}\right)^2 = k_a\left(\frac{\delta a}{a}\right)^2 + k_e(\delta e)^2 + k_i(\delta sini)^2 + k_\Omega(\delta\Omega)^2 + k_\omega(\delta\omega)^2 \tag{3.6}$$

where n is the mean motion and the δa, δe, $\delta\omega$, $\delta\Omega$ and δsini are the separation vectors of neighbour bodies.

The asteroid pairs have an unknown origin and there is a lot of discussion about the mechanism which produce these pairs.

- According to the first possibility the pairs may have been produced by catastrophic collisions. These objects were ejected in almost identical trajectories following stable orbits. However there are some arguments against this mechanism.

- A large fraction of small asteroids may be spun up by YORP beyond the cohesion strength threshold. If the identified pairs are indeed produced by the YORP-induced fission, we would expect that most of them should have, at least initially, nearly identical orbital inclinations. This is because the most common terminal spin states of the YORP-induced evolution have = 0^o or 180^o . Therefore, the fragments released by centrifugal force from the parent body should stay in the same orbital plane and have similar i values.

- A large number of binaries has been identified among the main-belt and near-Earth asteroids. The binaries with km-sized components may be created and destabilized by radiation effects. Moreover, a large number of binary systems is produced by catastrophic collisions with many of them

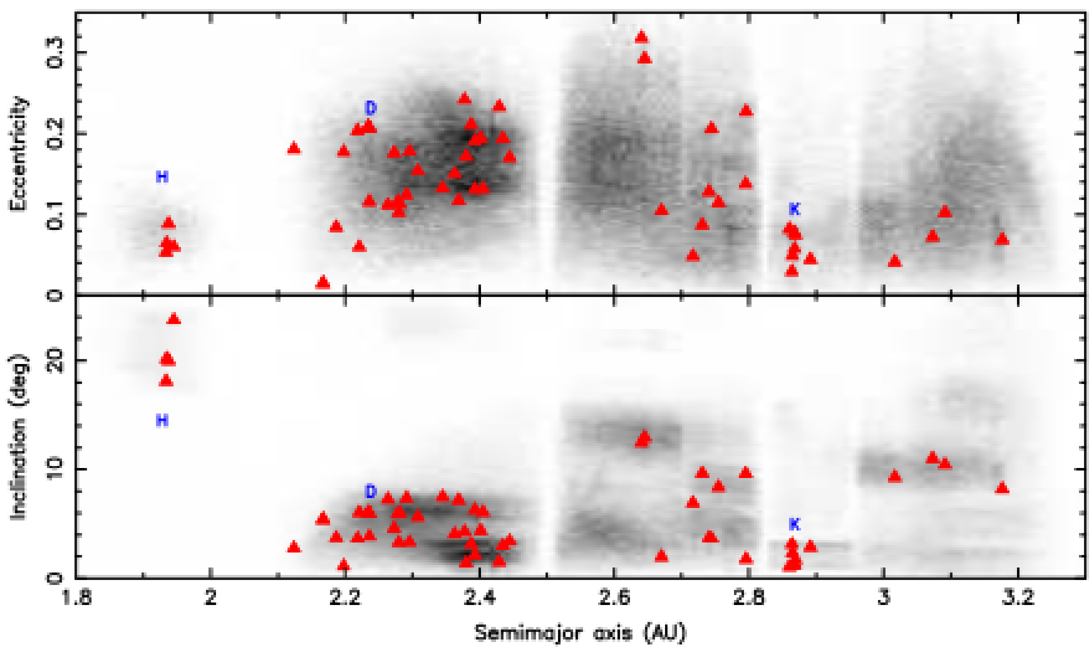

Figure 3.6: The orbital distribution of identified pairs across the Main Belt and Hungaria regions[Vokrouhlický and Nesvorný, 2008]

eventually dissolving due to dynamical instabilities. Therefore, the identified pairs may be binary systems that have become unbound. Also, the mass ratio, μ, of paired objects broadly matches that of the NEA binaries, which are thought to have formed by the YORP fission or disruptive collisions. Therefore, dissolved NEA-like binaries by radiation effects or inherent dynamical instabilities are identified as a possible formation mechanism of asteroid pairs.

3.7.2 Studying the light-curve

The knowledge of basic physical characteristics of asteroids as a function of the spin rate, the spin axis orientation, the shape, the size, the mass, the spectral type is important for understanding the history and the current state of the asteroid population. Apart from a few asteroids directly imaged by spacecraft, our knowledge about asteroid physical properties is based on remote sensing techniques. And from all these techniques, time-resolved photometry is by far the most important source of information because it is in principle available for all known asteroids.

The asteroids as they orbit around the Sun reflect the sunlight and due to their small size and long distance from the Earth, mostly appear star-like to optical ground-based telescopes. Thus, in the visible wavelengths, we observe the total amount of sunlight reflected from the surface of the asteroid at each epoch of observation. As we understand their apparent magnitude is changing during the orbit because the angle of the Sun, the asteroid and the Earth is changing too. The intensity of the reflected radiation depends on the phase angle, the angle between the Earth and the Sun, as seen from the asteroid, due to the scattering properties of the surface material and shadowing effects on the surface, more light is reflected at small phase angles than at larger ones. So, the smallest apparent magnitude is gained when the asteroid is in opposition with the Sun. At that point we are able to see the maximum illuminated area.Especially, near opposition (zero phase angle), the intensity increases rapidly and this phenomenon is called the opposition effect.

Apart from the orbit the asteroids spin around themselves and every time show a different area of their surface.The rotational phase of the asteroid, as well, affects the amount of observed radiation at a certain epoch; since asteroids are irregular, the part of its surface area which is both visible and illuminated, changes as it rotates. Thus, the total amount of reflected sunlight, seen by the observer, varies, unless we have a pole-on view to the asteroid. A sequence of brightness measurements taken during a revolution is called a light-curve. If an asteroid was a perfect sphere then the reflected light would be the same every moment and the light-curve a flat line. However the shapes are irregular and as result the reflected light is different through the time and the produced light-curve follows in most cases a sinusoidal curve with alterations related to the surface's anomalies.

The more densely sampled the light-curve points are, the more detailed information is obtained about the shape and albedo of the target. The restrictions of ground-based optical observations come mostly from the long exposure times needed to achieve an adequate signal-to-noise ratio. With slowly moving MBAs, this is usually no problem, and they represent the majority of the observed asteroid population. NEAs, on the other hand, often move fast in the field-of-view of the telescope, making long exposure times difficult. MBAs move slowly, and remain visible for long periods of time, giving flexibility to the timing of the observations. They are also relatively bright, and does not often require the use of large professional telescopes, from which it is thus very hard to obtain observing time for MBAs.

They are observable only at most a few months during each apparition and apparitions can be years apart. Thus, to obtain photometric data from a wide range of observing geometries required, e.g., for spin-axis and shape estimation, long-term or especially intensive observing programs are usually needed.

The discussion of the shape production began over a century ago when Henry Norris Russell mentioned in his paper that it s very important to determine the shape of an asteroid using its light-curve. But what can we learn from a light-curve?

The first is the orientation of the spin axis of the asteroid and its exact rotation rate. In fact, this is really the most important information over the shape of the asteroid. The spin axis is given as the ecliptic coordinates, longitude and latitude, of the direction in which the north pole of the spin axis (+Z) is pointing. If the latitude is 0^o, then the equatorial plane of the asteroid is coincident with the plane of the ecliptic. If the orbit of the asteroid also has a very small inclination to the ecliptic, then we not see much change in the shape of light-curve except for those caused by the variations at large phase angles when shadows on the asteroid become longer and change shape. If the latitude is near 90^o, then at some apparitions, we will see the asteroid nearly pole-on. This allows for even more dramatic changes in the shape and amplitude of the light-curve at different apparitions. The definition of the spin axis is important because we are able to study the YORP effect, which consist the primary force behind the formation of of binary asteroids and the excess of fast and slow rotators.

In order to extract a shape, there are some standard data requirements.

- Light-curves of sufficiently different geometries are required.
- Light-curves within the data set should cover a range of phase angles, including some at phase angles of 10^o and, for an even better solution, 20^o.

- The range of geometries and phase angle coverage is more important than the density of the data set, though excessively sparse light-curves may be a hindrance.
- Removing nearly redundant curves (in date) or bad (too sparse, high noise) can help remove biases and is more expedient than trying to apply weighting to individual curves.

The light-curve inversion method developed by Kaasalainen & Torppa (2001) and Kaasalainen et al. (2001) is a powerful tool for deriving asteroid shapes and spins from their light-curves observed over several apparitions. Models obtained by light-curve inversion are interesting as such, but their main importance is that, by using the light-curve inversion, we can reveal new physical phenomena. For example, it was used when the alignment of spins of the Koronis family members was revealed or when the YORP effect was detected . In general, the analysis of spin states and shapes of asteroids has been always related to the inversion of disk-integrated light-curves. Light-curve inversion has become a standard tool for revealing asteroids nature from photometry. Moreover, light-curves can be combined with other data. For example, adaptive optics images can provide us with non-convex details and thermal infrared observations can determine the correct absolute size of the object, its thermal inertia, and albedo. The reliability of models derived from photometry has been proven by comparison with the real shapes revealed by spacecraft and by laboratory experiments. A significant aspect of the inversion is the choice of the scattering law. All the visible light detected from the asteroids is scattered sunlight. To be able to find out what kind of an object produces a certain light-curve we need to compute the model brightness. The amount of radiation reflected from a surface is the differential brightness integrated over the visible and illuminated part of the surface

$$L_m = F_{\odot} \int \int_{A_+} S da \tag{3.7}$$

where F is the flux density of the incident light, da is the area of a surface element and S is the scattering function at the surface element. A_+ refers to the part of the surface that is both visible and illuminated. The corresponding equation for a discretized polyhedron surface is

$$L_m = F_\odot \sum_i S_i a_i \tag{3.8}$$

where the index i refers to the sum over all the visible and illuminated facets. For most of the asteroids, with the exception of the largest ones, the albedo is usually assumed to be uniform across the surface in global scale. The choice of the scattering law, however, is not straightforward. Currently, there is no universally accepted scattering law that would explain all the features in the variation of the observed brightness of asteroids.

There are scattering laws with no direct physical meaning of the parameters. Such empirical functions are generally of the form

$$S = S(\mu, \mu_o, \omega, a), \tag{3.9}$$

where $\mu = En$ and $\mu_o = E_o n$, E and E_o being the unit vectors pointing to the observer and to the Sun, as seen from the asteroid, n the unit surface normal, ω is the albedo and the phase angle. The most simple expression for the scattering, with zero parameters, is geometric scattering, according to which the reflected brightness depends only on the area projected towards the observer, i.e., $S = \mu$. Geometric scattering is applicable at the zero-phase-angle observing geometry, and it is often applied in methods that assume small-phase-angle observations. One example of a one-parameter scattering law is the combination of the Lommel-Seeliger and Lambert laws

$$S(\mu, \mu_o) = \frac{\mu\mu_o}{\mu + \mu_o} + c\mu\mu_o \tag{3.10}$$

where the first term is the Lommel-Seeliger part and the second term the Lambert part. Lambertian law is often applied in the case of bright surfaces, whereas the Lommel-Seeliger law is more suitable for low-albedo objects. Considering asteroids, a combination of the two laws, with the Lambertian weight depending on the assumed albedo of the object, has proven to be suitable for reproducing the desired light-curve features. Especially, at small phase angles the maxima and minima of the light-curves generated with different scattering laws deviate from each other only by a few percent.

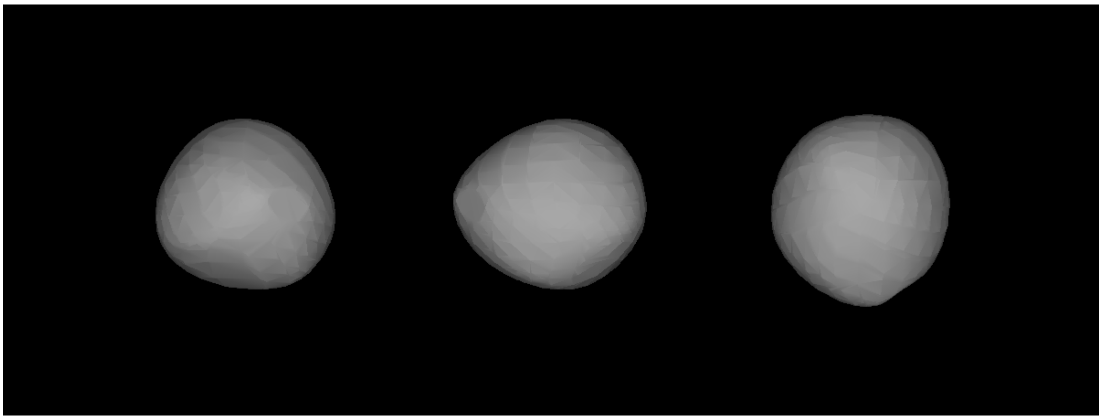

Figure 3.7: 2 Pallas with rotation period P=7.81323h and spin axis at λ=35 β=-12

In order to collect all the characteristics of the most possible asteroids a database was created. The Database of Asteroid Models from Inversion Techniques (DAMIT) provides access to all published asteroid models derived by the light-curve and other inversion methods [Durech et al., 2010]. For each asteroid in the database, the basic physical parameters are given: the shape model, the spin axis orientation and the rotation period. DAMIT also contains information about the light-scattering model used in the inversion.

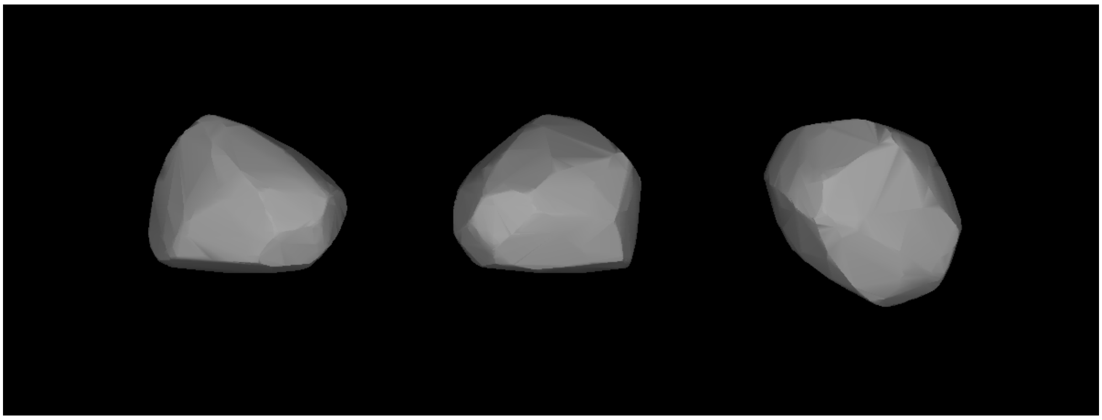

Figure 3.8: 5 Astraea with rotation period P=16.80061h and spin axis at λ=126 β=42

Until now DAMIT hosts about 329 of 202 asteroids. There can be more models for one asteroid, usually because of a limited geometry. Asteroid shape models are represented by polyhedrons with triangular surface facets. There is a file of the x, y, z Cartesian coordinates of the polyhedron. Vertices of the corresponding triangle are listed as seen from outside the body in the counter clockwise sense. Because it is impossible to infer size information from photometry alone, most of the models are scale-free and are arbitrarily scaled to have a unit volume. The model always rotates around its z axis, which is usually close, but not exactly identical, to the maximum principal axis of the inertia tensor, assuming a uniform density distribution. The orientation of the spin axis is expressed in ecliptic coordinates (λ, β).

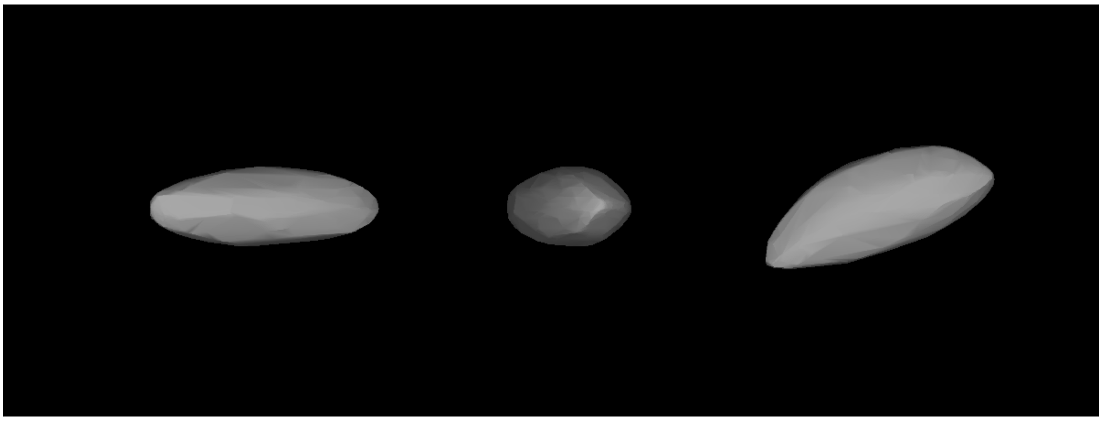

Figure 3.9: 1620 Geographos with rotation period P = 5.223336 h and spin axis at λ = 58 β = -49

The vast majority of DAMIT asteroid shape models are convex. Each shape model is visualized and shown from three directions. There are two views from the asteroids equator and one from its pole (Figures 3.7-3.13). The three views correspond to the views from the positive x, y, z axes, respectively. Disk-integrated light-curves contain very little information about shape non-convexities. To reveal non-convex features from light-curves, observations at very high phase angles are necessary. Moreover, non-convex solutions lack the stability and uniqueness properties of the convex solutions. Reliable non-convex shape models can be derived only when light-curves are combined with high-resolution data as adaptive optics images.

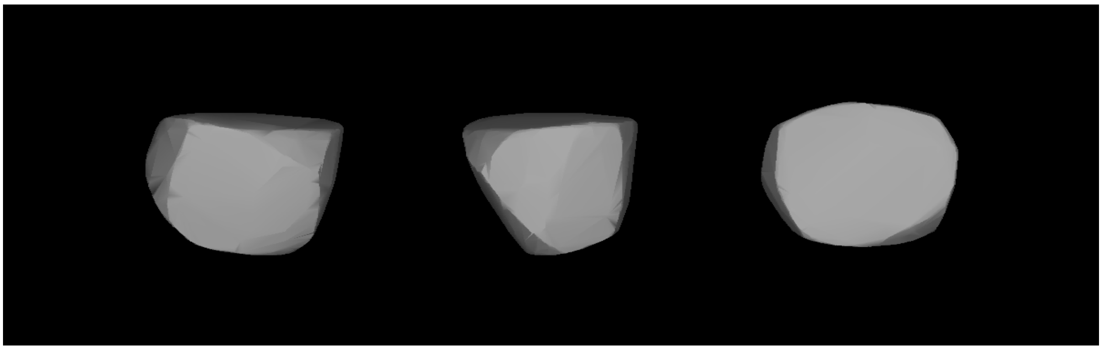

Figure 3.10: 68 Leto with rotation period P = 14.84547 h and spin axis at λ = 103 β = 43

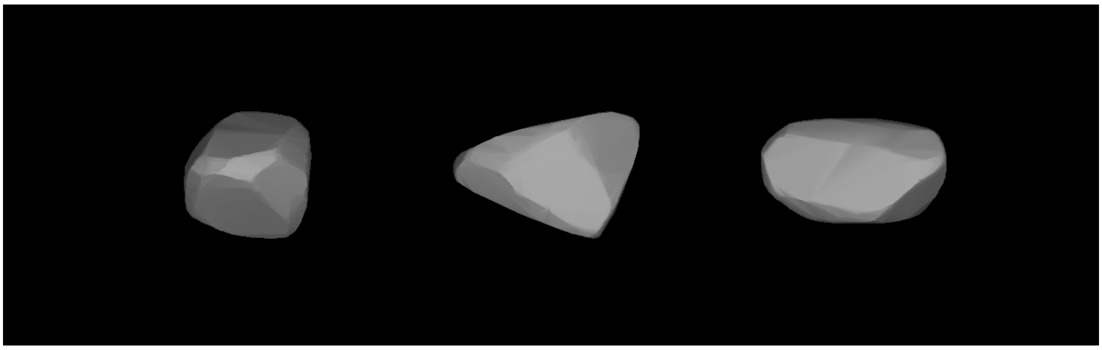

Figure 3.11: 601 Nerthus with rotation period P = 13.5899 h and spin axis at λ = 173 β = 44

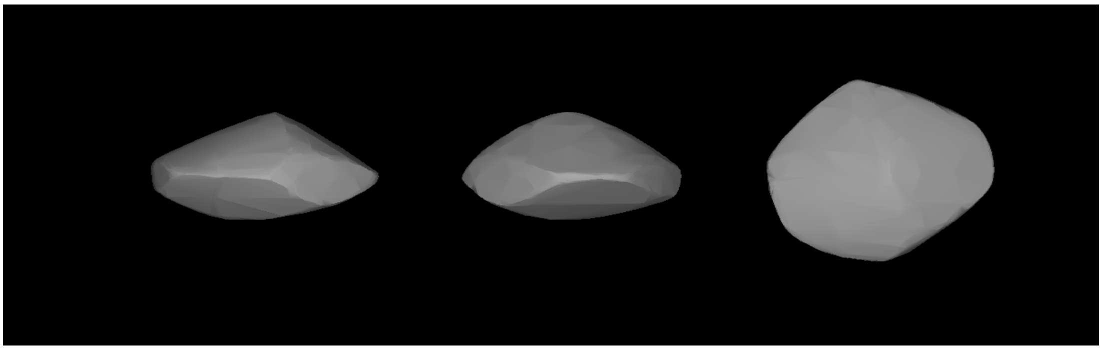

Figure 3.12: 683 Lanzia with rotation period P = 8.62926 h and spin axis at λ = 245 β = 42

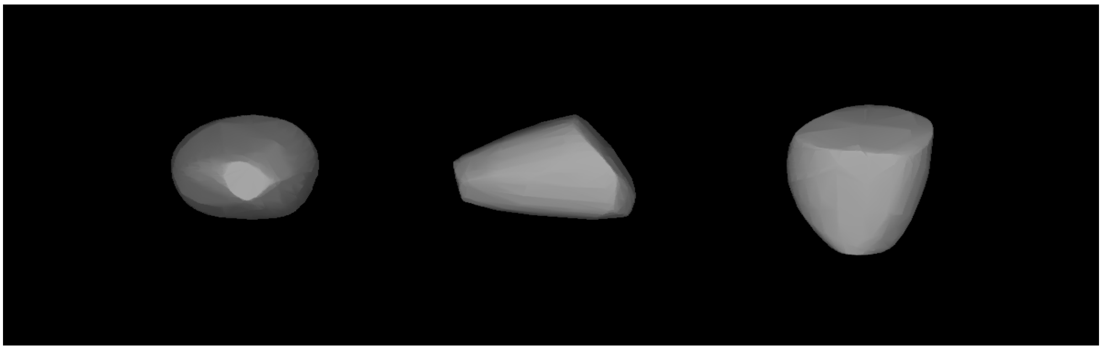

Figure 3.13: 41 Daphne with rotation period P = 5.98798 h and spin axis at λ = 198 β = -32

Chapter 4

Observing an asteroid

4.1 The Observatories

In order to observe an asteroid some aspects should be taken into account. The most important is the instrumentation and especially the CCD camera. The pixel size also plays a significant role. For example, for a given seeing if pixels are much smaller than the seeing value then the image will be oversampled and the efficiency of the system drops as the light of the star is spread over a much larger number of pixels. This increases the noise and decreases the signal-to-noise ratio (SNR). On the other hand if the pixels are too large, there is an undersampled image. In this case, we are not getting a good statistical profile of the star and so the accuracy of both astrometry and photometry suffer. Seeing also affects the observations.

The observations for this project were undertaken at two different locations: at the Holomon Astronomical Station and at Skinakas Observatory.

4.1.1 Holomon Astronomical Station

Holomon Astronomical Station (Figure 4.1) was established eight years ago and was an initiative of Prof. John Seiradakis of the Observatory of Thessaloniki, Department of Physics. It is located inside the Aristotle University's Forestry Department's Campus at Mt. Holomon Chalkidiki, at an altitude of 900 m. The place was a kind offer from the Aristotle University's Forest Director, Mr. G.

Panourgias. Its geographical coordinates are: 23 30 19.6 E and 40 25 58.4 N. The aim was to fulfil the educational needs of its students. During all these years, the Director provides as accommodation and all the facilities that we need.

Area restrictions

Figure 4.1: The logo of the Holomon Astronomical Station, indicating its location in the Chalkidiki peninsula

The main disadvantage of the location is the nearby forest. Often, humidity severely affects the observations. Additionally, the trees cover a significant portion of the western sky. Toward the East observations cannot be initiated until the target rises above at least 25^o, because of road lights. As a consequence of all these, observations have to be terminated relatively early in the night because of the trees obscuring the western sky or due to high humidity. Even if the atmosphere looks clear, humidity or low fog can appear at any time. As a result the telescope can catch frost and it should be cleaned immediately. In order to overcome this problem a circular device wrapping the tube was constructed. This device has 50 small resistances connected in parallel. When plugged in, the heat which is created helps to destroy the frost or even prevents its appearance.

In order to determine the weather conditions at Mt. Holomon and the turbulence of the atmosphere we continuously make additional seeing and meteorological measurements (Figure 4.2). It is well known that atmospheric turbulence seriously limits the resolution of earth-bound telescopes.

Although a star appears as an unresolved point source outside the atmosphere, for example when observed by the Hubble Space Telescope, the same star would appear as an extended disk, the so-called "seeing disk", when observed from a telescope on the Earths surface. This effect often makes images taken from the ground less sharp. Astronomical sites with excellent seeing conditions are therefore extremely important for high resolution optical observations. Seeing measurements, using a two-aperture Differential Image Motion Monitor, the

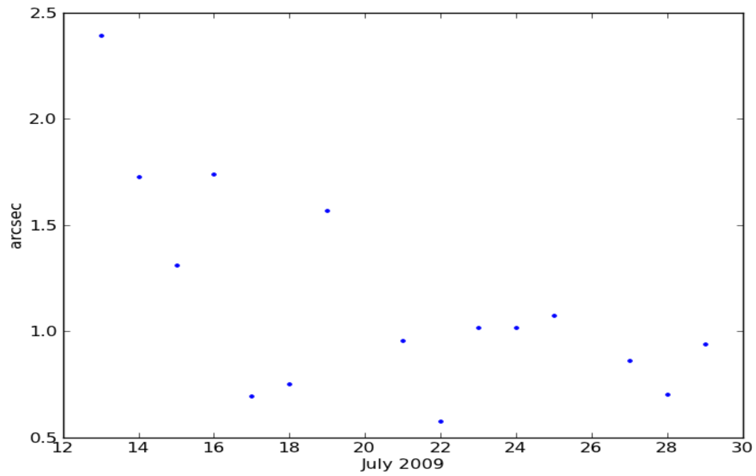

Figure 4.2: Seeing measurements

DIMM method, have been carried out since 2003 (Nestoras J.S., 2006). After 44 hours of observations on July 2009, a mean value of 1.15 arcsec has been obtained, which is a good value and enable us to avoid having an ovesampled or undersampled image. Since March 2010 a weather station was installed near the Astronomical Station, monitoring every hour temperature, humidity, dew-point, precipitation, wind speed and wind direction (Figure 4.3).

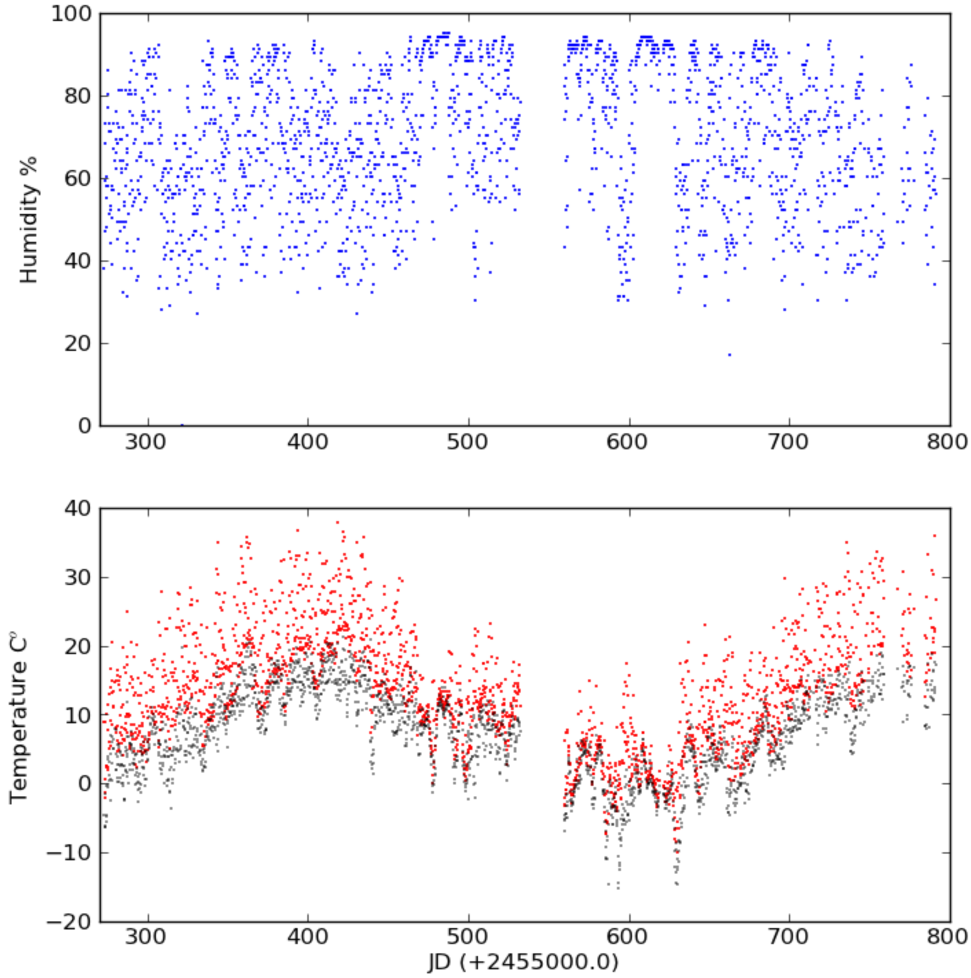

Figure 4.3: Weather data

Equipment used

All successful observations were made with a Schmidt-Cassegrain 11in telescope (Figure 4.4) (Table 4.1). The CCD cameras were an ATIK 4000 and an ATIK 11000 (Table 4.2). The mount was a Skywatcher EQ6 Skyscan Pro. Camera and mount operations are controlled via the Maxim DL software. Below are the characteristics of the instrumentation.

Figure 4.4: The 11" Smidt-Cassegrain

Telescope
Optical Design: Schmidt-Cassegrain
Aperture: 279.4 mm (11in)
Focal Length(F): 2800 mm (110.24in)
Focal Ratio(f/): 10.02

Table 4.1: Telescope specifications

	ATIK 4000	ATIK 11000
Pixels/Pixel size:	2048x2048/7.4x7.4 μ	4008x2672/9x9 μ
Quantum Efficiency:	55%	50%
RMS:	11e-	13e-
Dark Current:	0.01 e-/sec	0.03 e-/sec

Table 4.2: Cameras specifications

4.1.2 Skinakas Observatory

Figure 4.5: Skinakas Observatory

Skinakas Observatory belongs to the University of Crete and is located on Mt. Ida at 1750 m in the region of Herakleion, Crete with geographical coordinates 24 53 57 E and 35 12 43 N (Figure 4.5). After submitting the relative proposal we were given 4 nights of observations. We met no difficulties related either to the weather conditions or to the equipment. The fact that it is not affected from light pollution and has very good astronomical seeing place the Skinakas Observatory the best operational observatory in Greece.

Equipment used

The telescope that was used is the 1.3 m Ritchey-Chretien with an ANDOR DZ436 camera along with an R-Bessel filter (Figure 4.6) (Tables 4.3-4.4). Below are the characteristics of the instrumentation. It is obvious that in both cases the fields of view (FOV) are large enough for asteroid observations and finally we will be able to find plenty of suitable comparison stars of similar brightness.

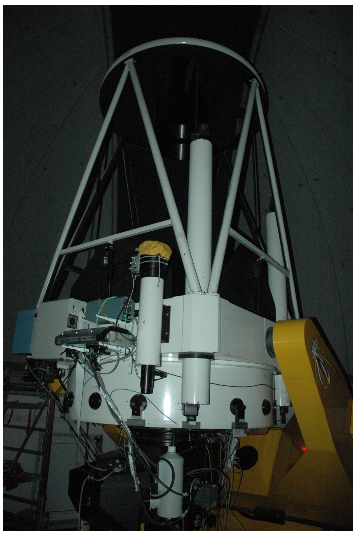

Figure 4.6: The 1.3m Ritchey-Chretien

Telescope
Optical Design: Ritchey-Chretien
Aperture: 1290 mm
Focal Length(F): 9857 mm
Focal Ratio(f/): 7.64

Table 4.3: Telescope specifications

ANDOR DZ436
Pixels/Pixel size: 2048x2048 /13.5x13.5 μ
Quantum Efficiency: 95%
RMS: 4e-
Dark Current: 1 e-/px/sec
FOV: 9.5x9.5 arcmin

Table 4.4: Cameras specifications

4.2 Target Selection

Before deciding which targets to observe we have to determine which targets can be observed. A suitable filter should also be determined. Filtered observations are certainly preferred, especially if there is a collaboration with other observers or observing an asteroid over a long period of time, for several weeks or months. When standard magnitude bands as Johnson and Cousins are used, all the observations can be directly matched to those who also reduce their observations to the same bands.

If the intention is to simply determine the period and amplitude of the lightcurve during a given month, then unfiltered observations are acceptable. Unfiltered observations can be combined with data based on a standard system. It is sometimes difficult but it can be done. The disadvantage of filtered observations is that they reduce the amount of light reaching the detector. Sometimes filtered observations are advantageous. If, for example, we observe with a filter the rms of the light-curve may be smaller, because we have smaller rms in the narrow band of wavelengths.

Generally the SNR is the statistical term that defines the ratio between the useful signal (photons from the target) versus the total signal received (the photons from the star, sky background, inherent noise in the chip, etc). The basic formula can be stated a

$$S/N = netobjectcounts/sqrt(netobjectcounts + skybackgroundcounts) \quad (4.1)$$

The larger this number, the more signal (photons) from only the target. A good value is 100, which means that the noise is about 1% of the total signal. Translated to magnitudes, a SNR of 100 means that your measurements are of about 0.01 mag (stellar magnitude) precision.

But what about asteroid observations? When the amplitude of the light-curve is 0.1 m or less, we can see that a value of 100 becomes fairly important, as we do not want the "scatter" to be a significant portion of the light-curve and loose the signal inside the noise. On the other hand, if the amplitude is larger, e.g., 0.2 m - 0.5 m, we can afford a slightly noisier signal if it means the difference between getting data or not. Practical experience has shown that there are still good results when the SNR drops to 50 and even a little below (implying a precision of about 0.02 m).

There is an experimental way to determine the proper range of apparent magnitudes that can be observed. We take into account the equipment and the brightness of the sky. In this Thesis we used frames from the same telescope of the exoplanet HAT-p19b. We did data reduction and photometry in order to extract the instrumental magnitudes of the field stars and their σ. After that we downloaded, using the *Aladin software*, the catalogue of the same field stars but with their true apparent magnitudes. The match of the stars was done and the correlation between the magnitudes (Figure 4.7). Using least square in the magnitudes plot, the formula between the instrumental and true apparent magnitudes was calculated. From this procedure we finally found every magnitude with which σ value is connected. From this diagram now it is possible to determine the highest magnitude limit with good precision (Figure 4.8).

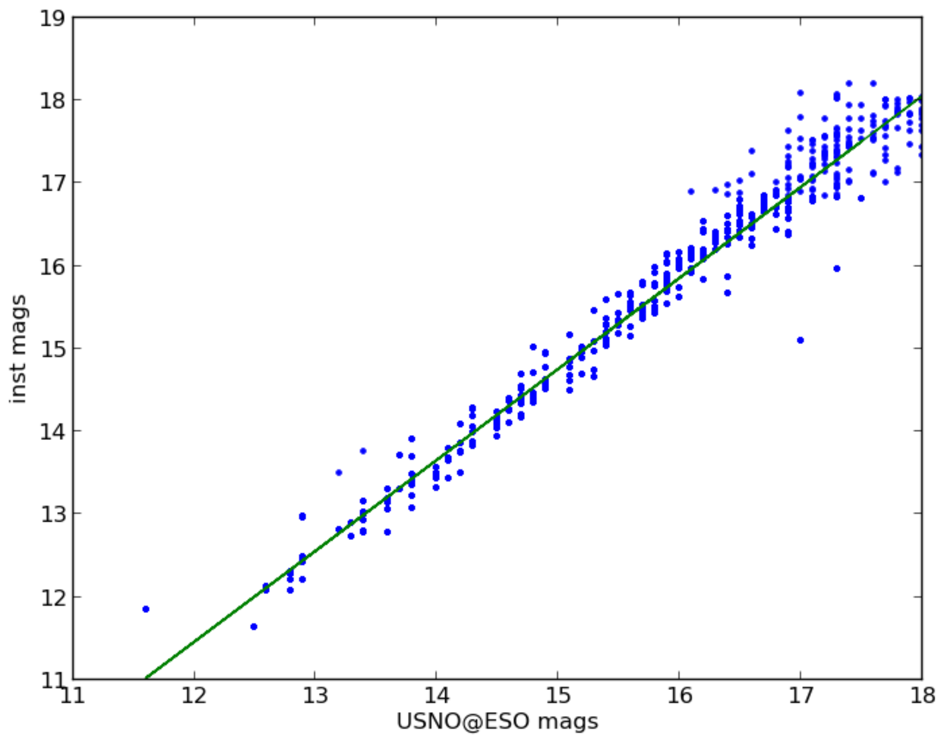

Figure 4.7: Catalogue magnitudes vs instrumental magnitudes

Another factor which was taken into account was their position in the sky because of the location limitations and the total observing time we had in the end. Finally asteroids' rate was the last restriction. An asteroid, as a moving target, has a rate which is changing very quickly. Very fast moving and faint targets cannot be observed in a proper way.

The reason is that if we need to achieve a good SNR we have to increase the exposure time. On the other hand there is a danger to have the asteroid with trails on the frame. So it is more wise for such small telescopes to select relatively bright objects with a slow motion. Because of this reason NEAs are not good targets. As it has been mentioned previously, for the first time it would be appropriate to observe an asteroid when it is in opposition. At that time it has the brightest apparent magnitude.

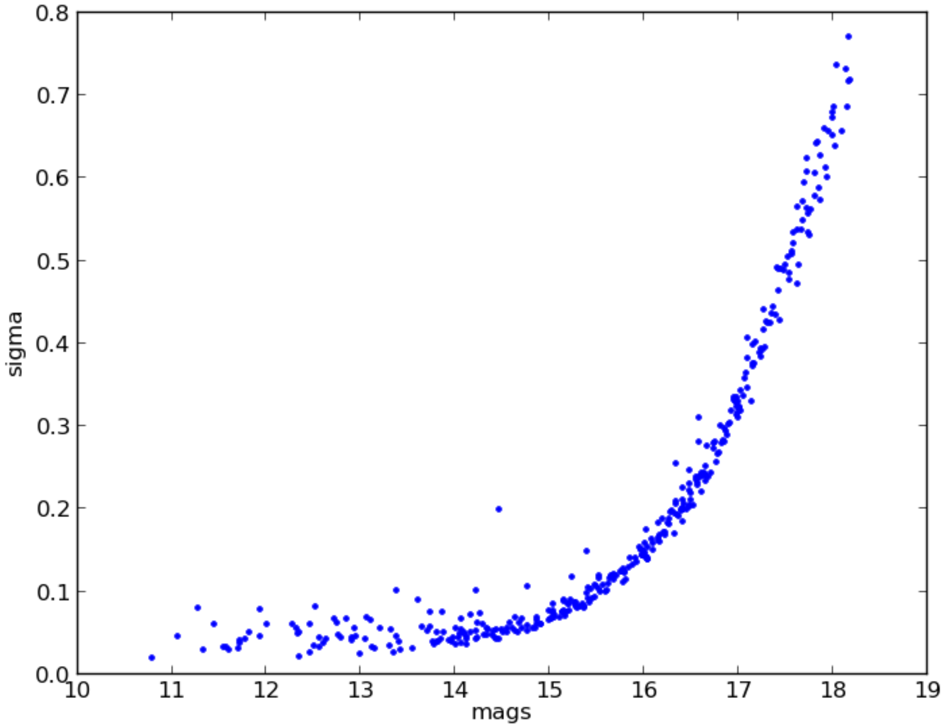

Figure 4.8: The targets were selected according to their precision using this diagram

Below are presented the six main targets along with their orbital elements and a view of their trajectories (Figures 4.9-4.14).

(266) Aline

Aline was discovered on 17-May-1887 and belongs to the Gefion family.

e: 0.1575
a: 2.8028 AU
i: 13.4011 deg
M: 77.3485 deg
period: 1713.9620 d
q: 2.3611 AU
Q: 3.2445 AU
absolute magnitude (H): 8.80 mag
diameter: 109.09 km
geometric albedo: 0.0448

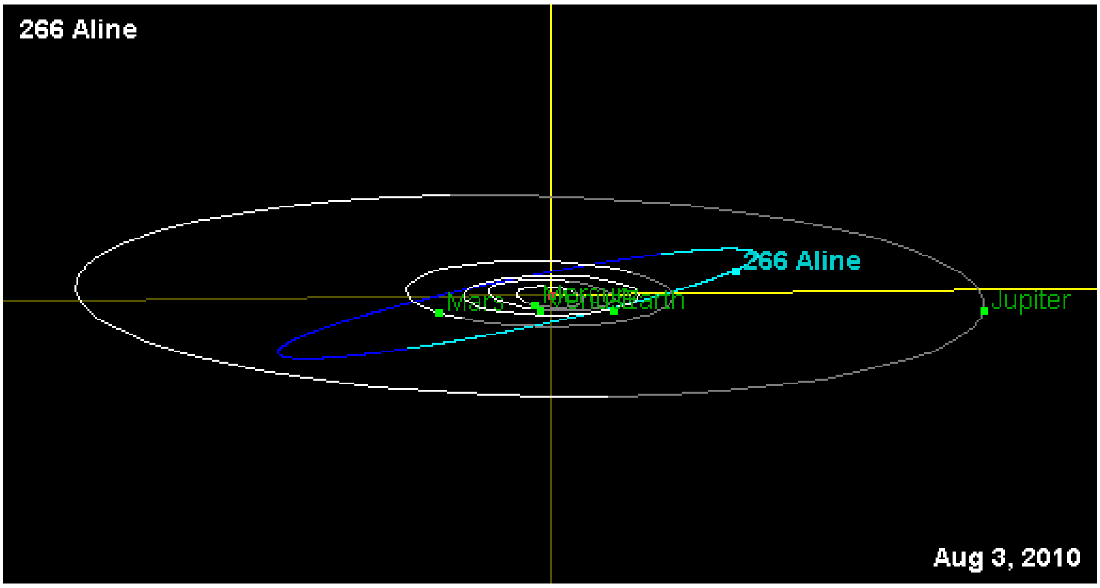

Figure 4.9: The trajectory of (266) Aline

(426) Hippo

Hippo was discovered in 25-Aug-1897 and we cannot tell exactly in which family it belongs because of its inclination.

e: 0.1031
a: 2.8893 AU
i: 19.4754 deg
M: 287.2502 deg
period: 1793.8761 d
q: 2.5913 AU
Q: 3.1873 AU
absolute magnitude (H): 8.42 mag
diameter: 127.1 km
geometric albedo: 0.0469

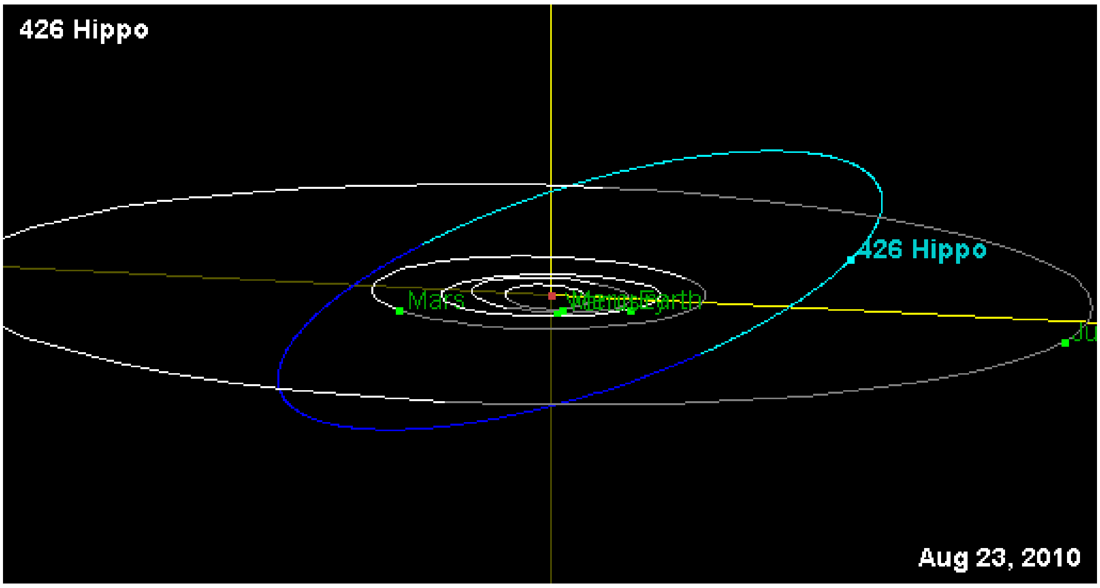

Figure 4.10: The trajectory of (426) Hippo

(478) Tergeste

Tergeste was discovered in 21-Sep-1901 and we do not know its family.

e: 0.0862
a: 3.0202 AU
i: 13.1858 deg
M: 295.9061 deg
period: 1917.2132 d
q: 2.7597 AU
Q: 3.2808 AU
absolute magnitude (H): 7.98 mag
diameter: 79.46 km
geometric albedo: 0.1798

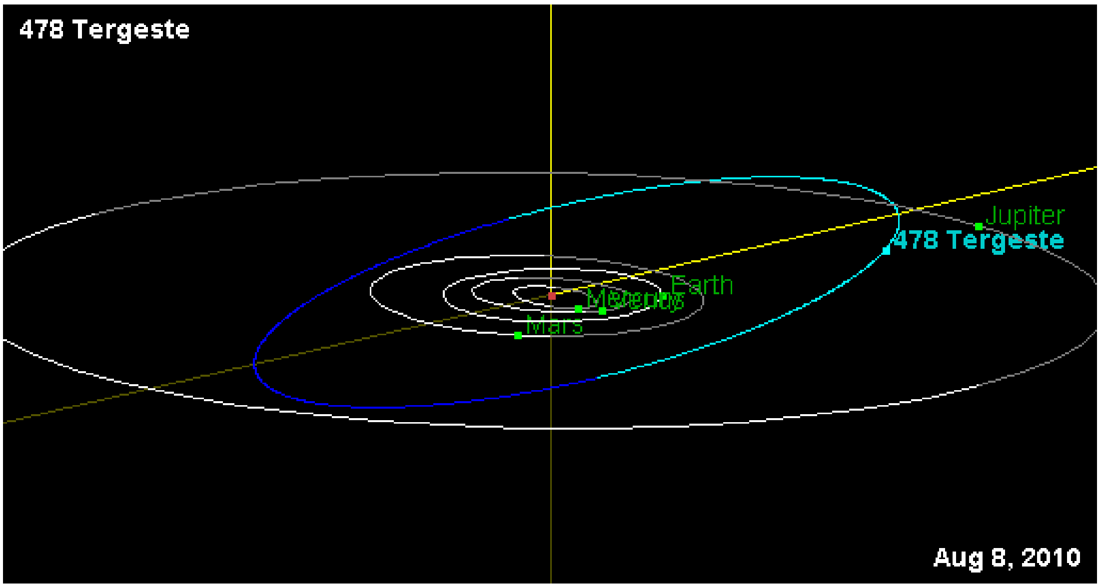

Figure 4.11: The trajectory of (478) Tergeste

(664) Judith

Judith probably belongs to Themis family and was discovered in 24-Jun-1908.

e: 0.2209
a: 3.2190 AU
i: 8.5626 deg
M: 115.6123 deg
period: 2109.5454 d
q: 2.5077 AU
Q: 3.9303 AU
absolute magnitude (H): 9.97 mag
diameter: 72.68 km
geometric albedo: 0.0344

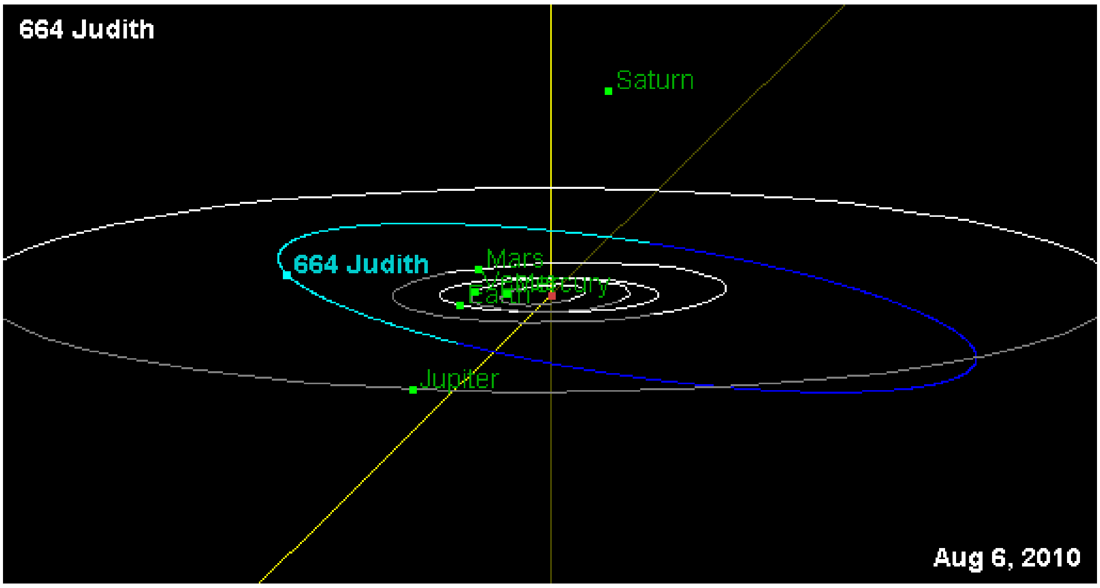

Figure 4.12: The trajectory of (664) Judith

(16959) 1998 QE17

(16959) does not belong to any known family and was discovered in 17-Aug-1998.

e: 0.3077
a: 2.6240 AU
i: 10.6302 deg
M: 16.3654 deg
period: 1552.6107 d
q: 1.8166 AU
Q: 3.4315 AU
absolute magnitude (H): 13.0 mag
diameter: ?km
geometric albedo: ?

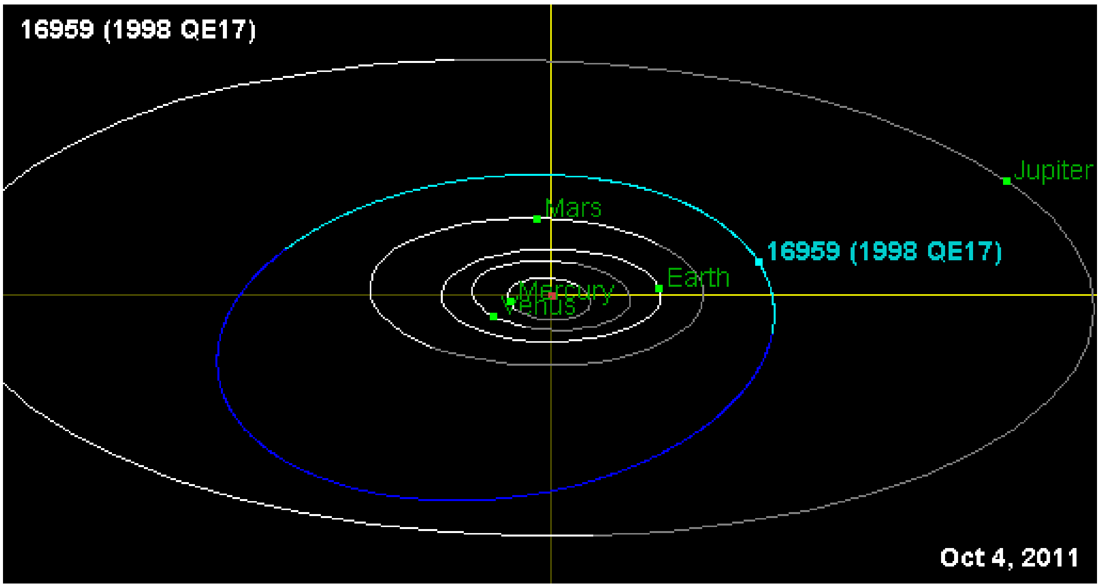

Figure 4.13: The trajectory of (16959) 1998QE17

(32910) 1994 TE15

(32910) 1994TE15 is a Mars-crosser asteroid and does not belong to any known family. It is probable a background asteroid. It was discovered in 13-Oct-1994.

e: 0.2543
a: 2.1821 AU
i: 4.796 deg
M: 158.3663 deg
period: 1177.4196 d
q: 1.6270 AU
Q: 2.7372 AU
absolute magnitude (H): 14.5 mag
diameter: ?km
geometric albedo: ?

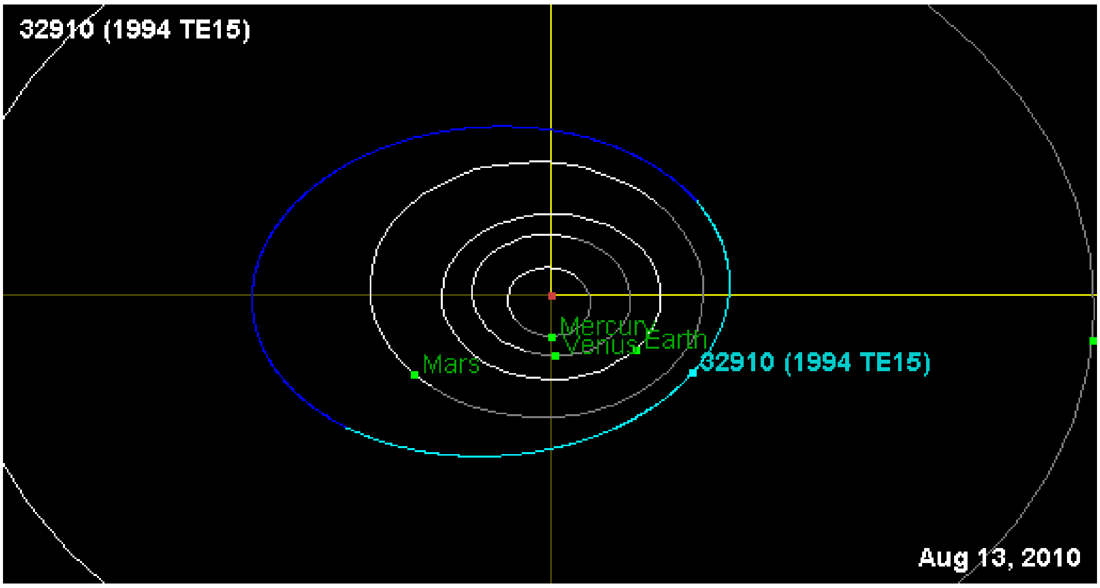

Figure 4.14: The trajectory of (32910) 1994TE15

Apart from these targets some others were initially selected to be observed but due to bad weather conditions and wrong telescope selection during the first months we did not obtain valuable results. These asteroids were: (150) Nuwa, (194) Prokne, (202) Chryseis, (850) Altona, (567) Eleutheria and (2381) Landi.

4.3 Data reduction and Photometry

All the required reduction frames were undertaken during observations. Data reduction and Photometry were done with *MPO CANOPUS* from *Minor Planet and Divide Observatory*. This software is particularly suited to moving targets.

The main problem which this software solves is the problem of the moving target. As the asteroid orbits the Sun, it changes its position every moment with a specific rate. So we need a precise astrometry to be done and to find a way to follow the target considering its rate. This program after the astrometry calculates the exact trajectory of the asteroid according to its rate taken from the ephemeris.

After the trajectory is pointed onto the first reference frame we are able to exclude areas of light that may interfere with the asteroids photometry. These areas can be other stars or galaxies.

With MPO CANOPUS we do differential photometry. Because the target changes its position in the sky every night we have to change comparison stars for photometry. The fist success is to find nearby the asteroid 2 to 5 comparison stars of the same apparent magnitude. If this does not happen we are going to have some small difficulties at the last step where we create the Composite Light-Curve (CLC) of the object.

Moreover the photometry is done using photometric apertures (Aperture Photometry). The program allows to set the apertures of the target and comparison stars at different stages of the procedure and they depend on how many pixels our objects have on the frame. We should be careful on this step because the asteroid due to its spin and irregular shape changes its magnitude during the night. Sometimes, if the amplitude of the light-curve is unknown we do not know by how much. As a result we select a slightly bigger aperture than that we see at the time of the choice.

4.4 Results

Here we present the results of all observations. There are raw data from every single night and where it is possible the final composite light-curve is given. (266) Aline and (664) Judith were observed from Holomon Astronomical Station using the 11” Schmidt-Cassegrain telescope and ATIK 4000. Later on, the Observatory of Thessaloniki bought a brand new CCD camera, ATIK 11000. This CCD with R filter was used for asteroid (16959) 1998QE17. We used the facilities of Skinakas Observatory for asteroid (32910) 1994TE15 which had, until then, unknown light-curve and rotation period. The ephemerides for every asteroid were obtained from Minor Planet Center (Tables 4.5-4.10).

4.4.1 (266) Aline

	El.	Ph.	V	rate(arcsec/min)
03-08-2010	148.0	12.2	12.6	0.41
05-08-2010	149.5	11.7	12.6	0.43
07-08-2010	151.0	11.2	12.5	0.45
09-08-2010	152.3	10.7	12.5	0.46

Table 4.5: (266) Ephemeris

Aline was observed for four night (Figures 4.15-4.18) and its rotation period was found to be P = 13.05 ± 0.07 h with an approximate amplitude A = 0.08 mag (Figure 4.19). The period is very close to the one, 13.01 h, reported by Pilcher and Benishek (2011).

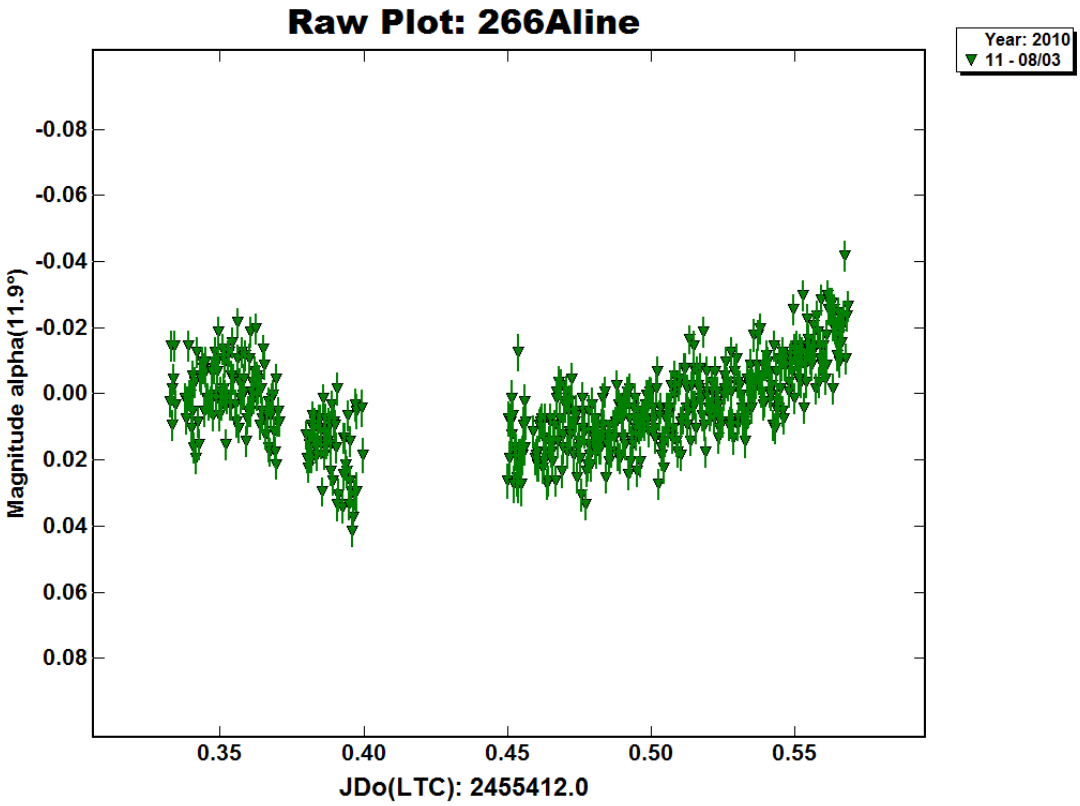

Figure 4.15: Raw data of 03-08-2010

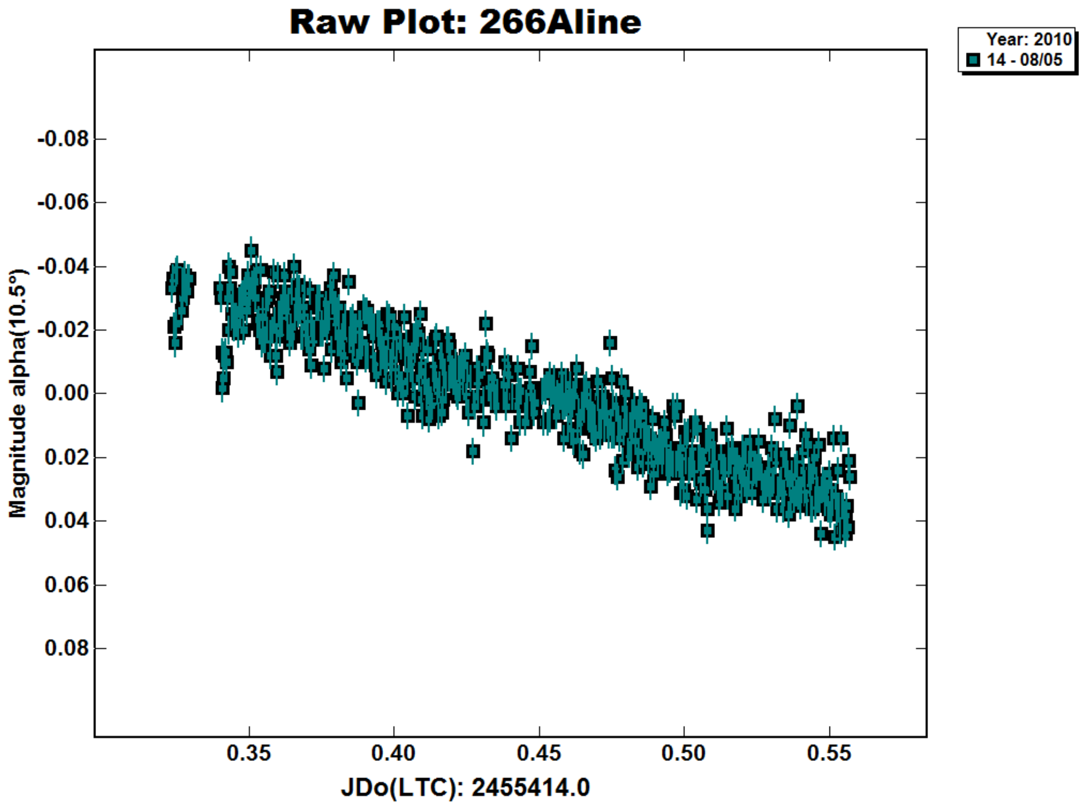

Figure 4.16: Raw data of 05-08-2010

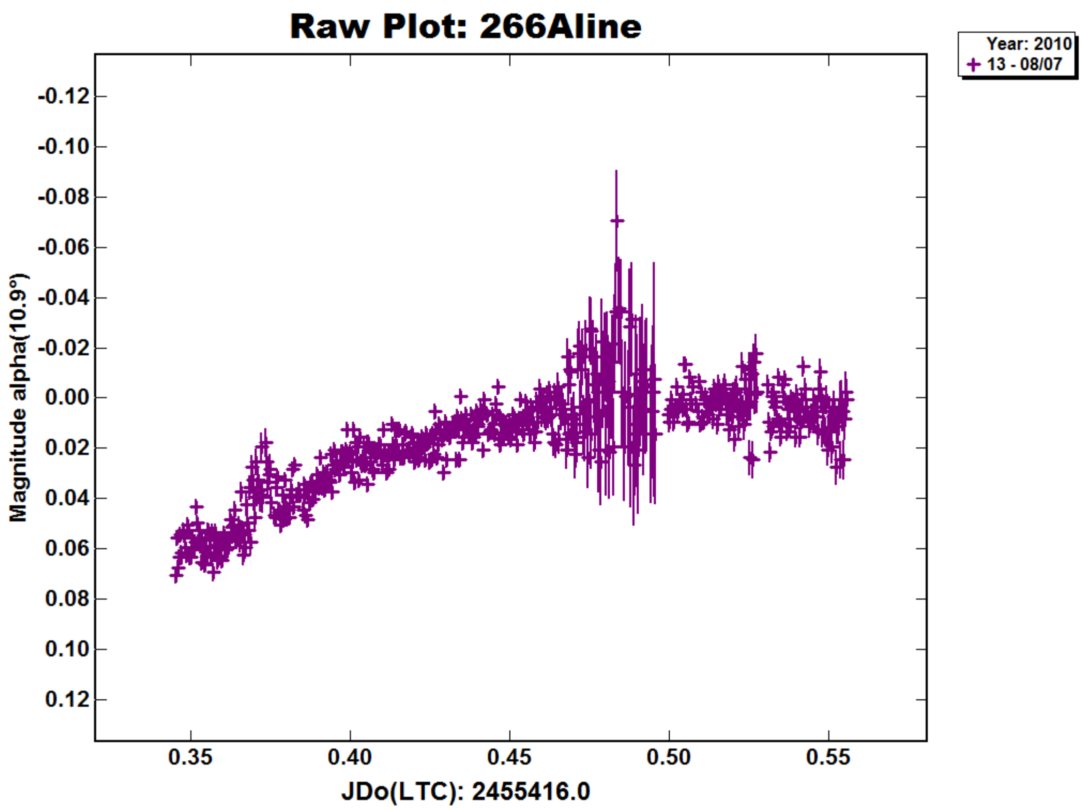

Figure 4.17: Raw data of 07-08-2010

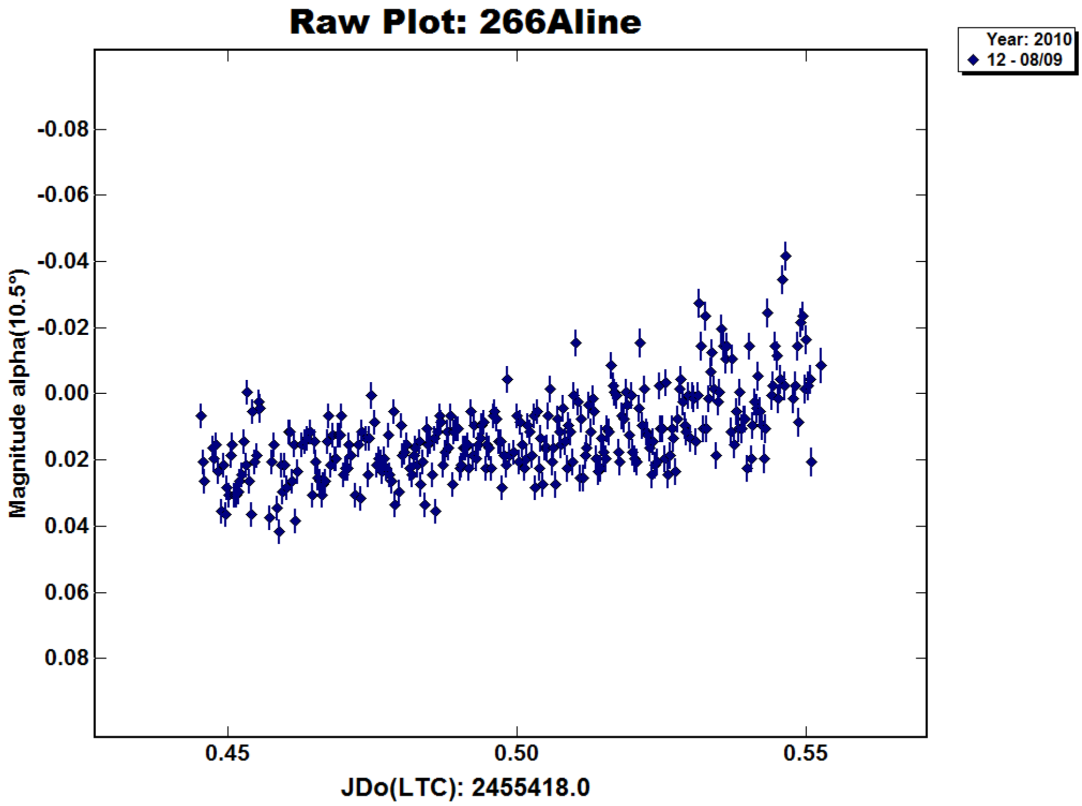

Figure 4.18: Raw data of 09-08-2010

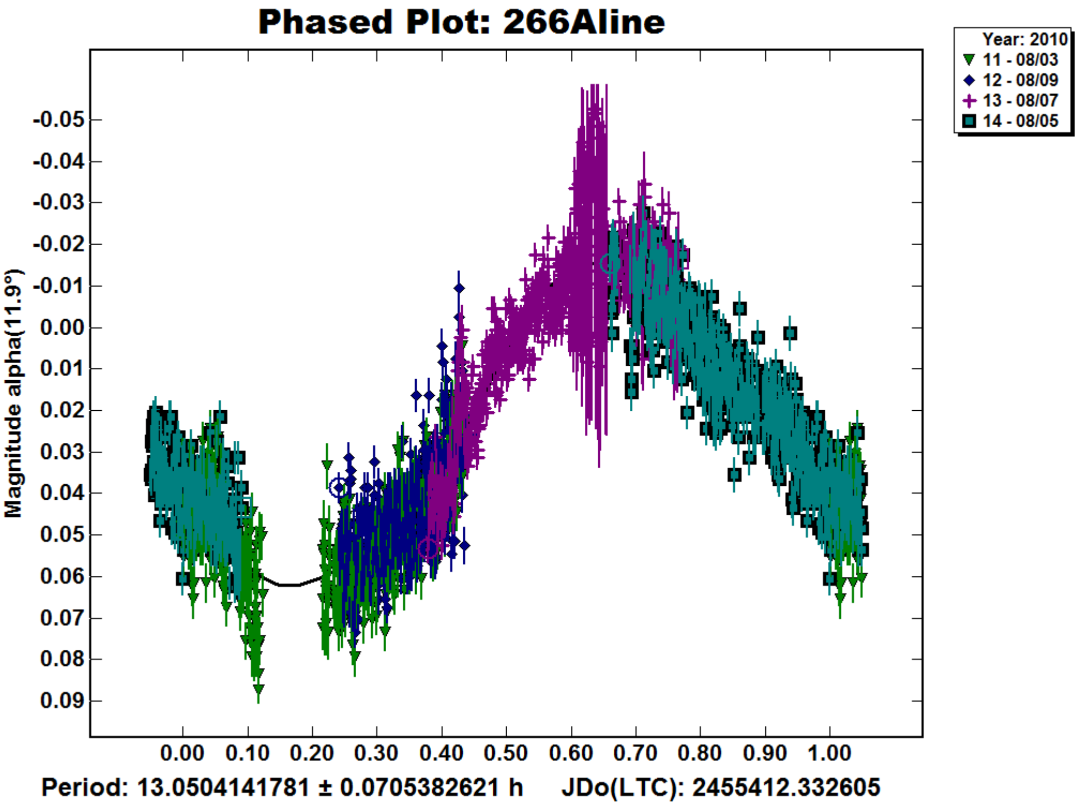

Figure 4.19: The Composite Light-Curve of (266) Aline

4.4.2 (426) Hippo

	El.	Ph.	V	rate(arcsec/min)
23-08-2010	151.6	8.7	13.3	0.51

Table 4.6: (426) Ephemeris

Hippo is a main belt asteroid with large rotation period, 34.3 h, as it has been determined so far from previous observations. Because of high humidity it was not possible to obtain a good part of its light-curve (Figure 4.20).

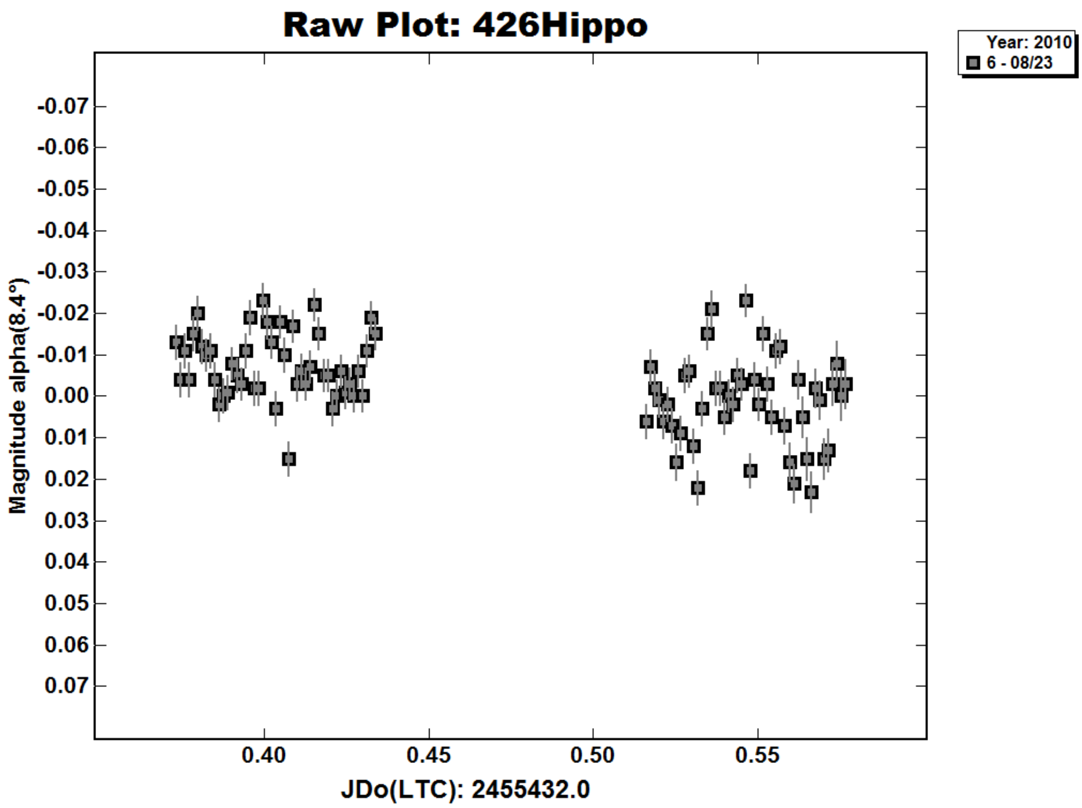

Figure 4.20: Raw data of 23-08-2010. Due to humidity the signal is lost into the noise.

4.4.3 (478) Tergeste

	El.	Ph.	V	rate(arcsec/min)
08-08-2010	150.5	8.8	13.0	0.39
09-08-2010	149.6	9.0	13.0	0.39
10-08-2010	148.7	9.3	13.0	0.38
11-08-2010	147.8	9.5	13.1	0.37

Table 4.7: (478) Ephemeris

Tergeste was observed during clear nights (Figures 4.21-4.24) and although it is a relatively bright asteroid we were not able to combine our data well enough in order to extract a part of its phase plot. However, we present a trial in Figure 4.25. According to previous observations its rotation period is 16.104 h.

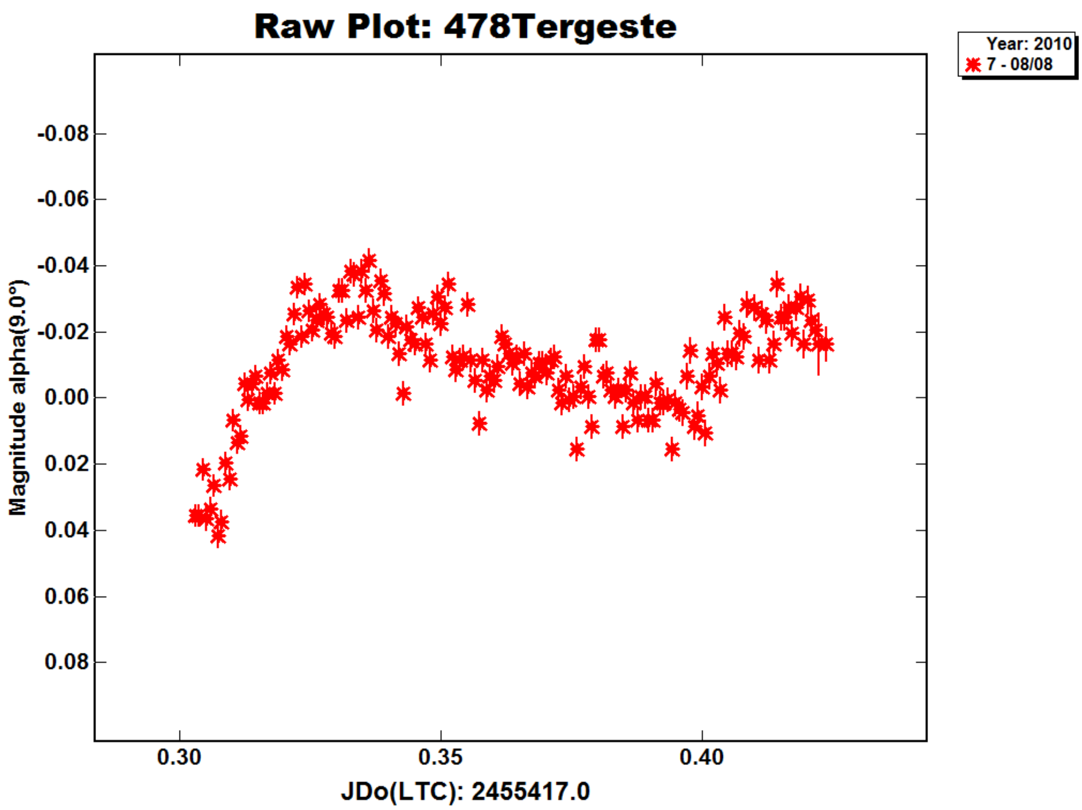

Figure 4.21: Raw data of 08-08-2010

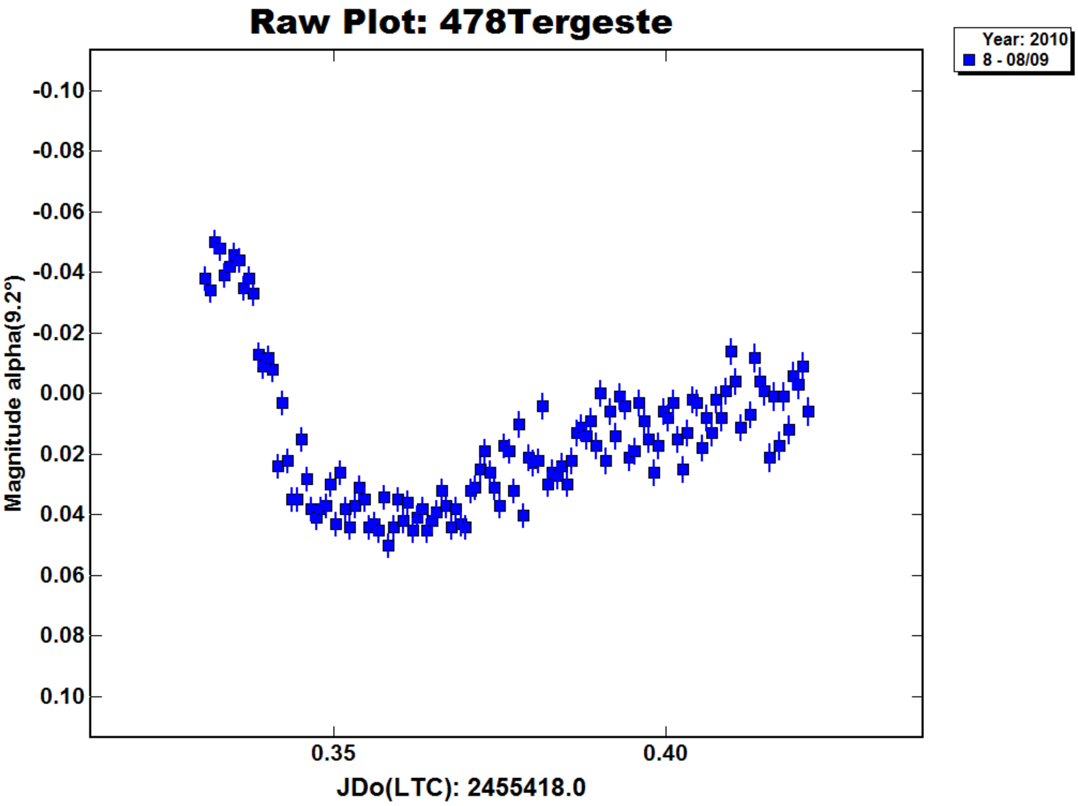

Figure 4.22: Raw data of 09-08-2010

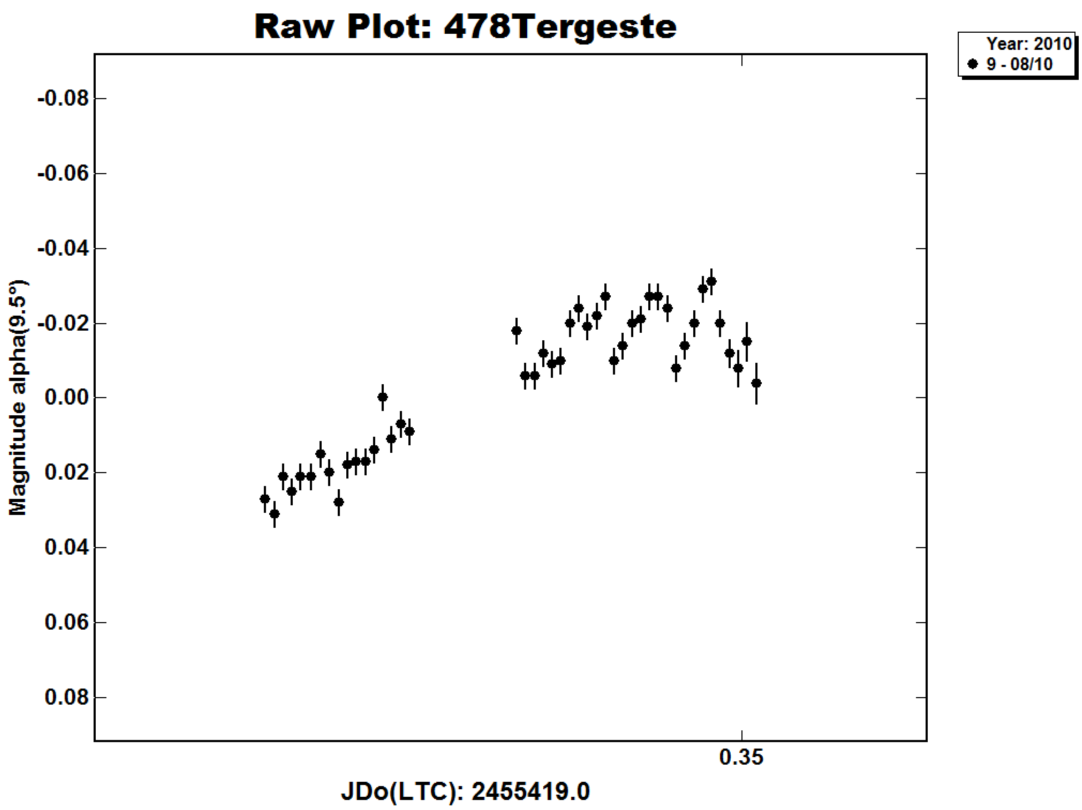

Figure 4.23: Raw data of 10-08-2010

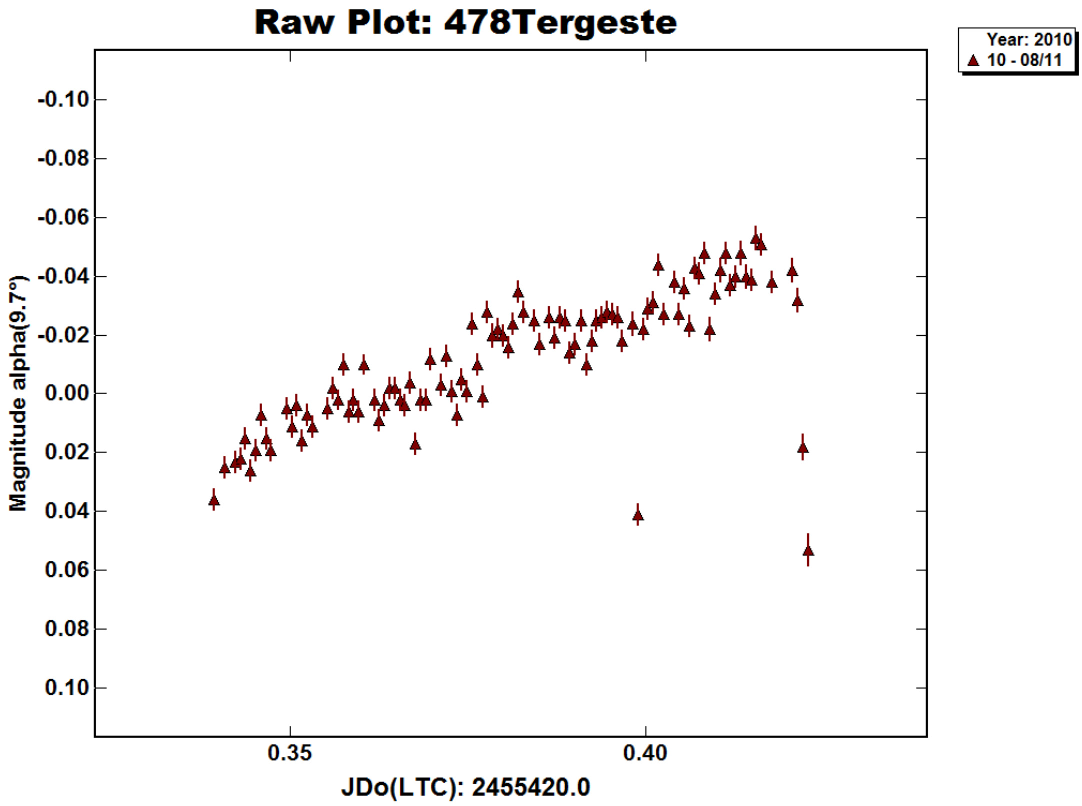

Figure 4.24: Raw data of 11-08-2010

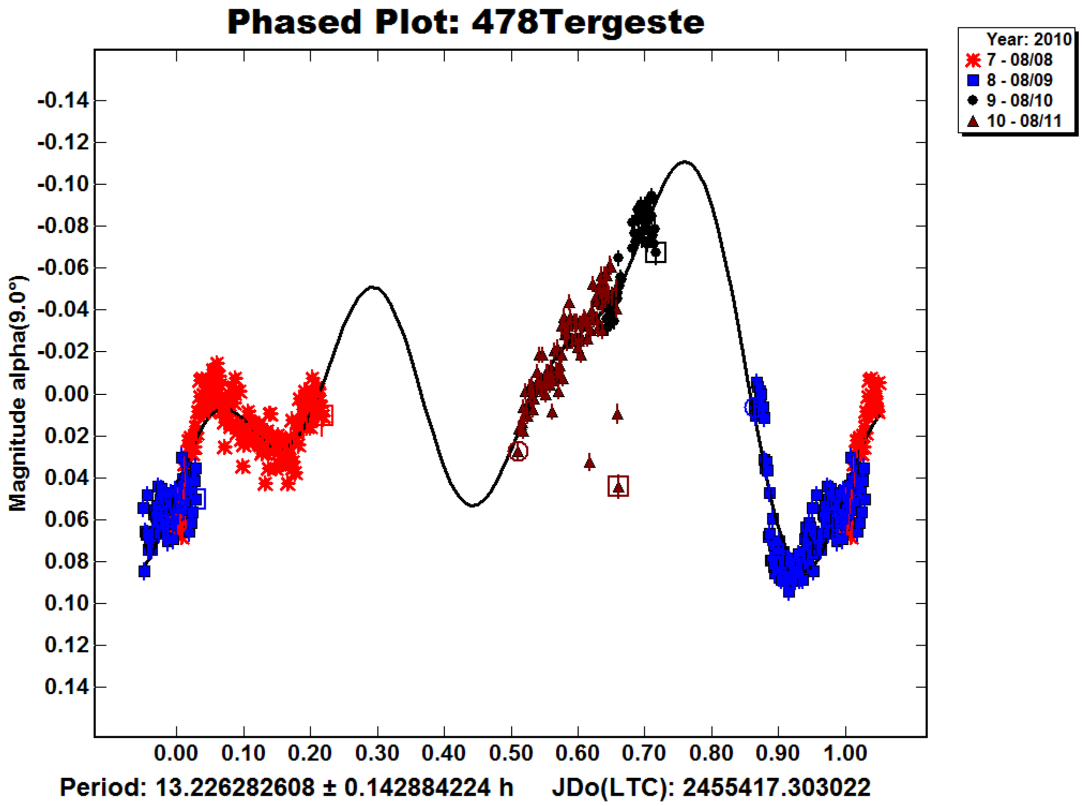

Figure 4.25: A try to make the CLC. The phased plot does not match to previous light-curves.

4.4.4 (664) Judith

	El.	Ph.	V	rate(arcsec/min)
02-08-2010	154.6	9.8	13.7	0.39

Table 4.8: (664) Ephemeris

Unfortunately, we were not able to obtain enough data to determine the period as we got only a part of it (Figure 4.26). The rotation period was found 10.6829 h.

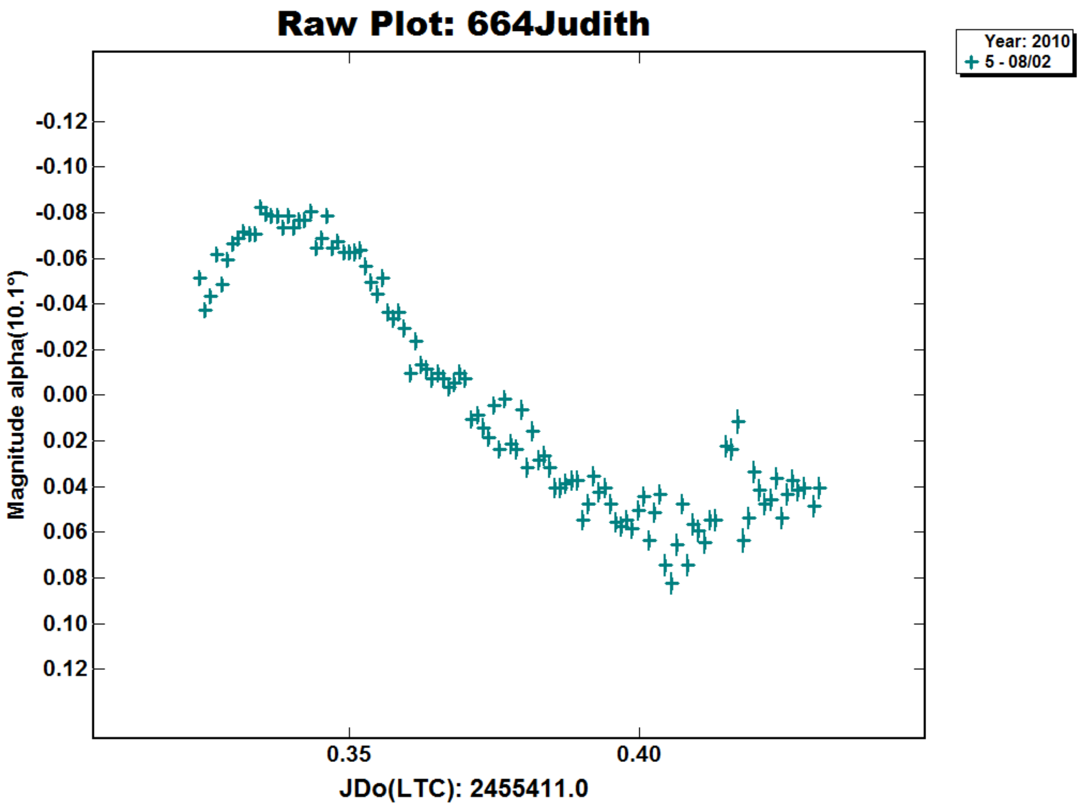

Figure 4.26: Raw data of 02-08-2010

4.4.5 (16959) 1998QE17

	El.	Ph.	V	rate(arcsec/min)
02-10-2011	168.6	5.9	14.8	0.66
04-10-2011	168.3	6.0	14.7	0.65
05-10-2011	167.1	6.2	14.7	0.65

Table 4.9: (16959) Ephemeris

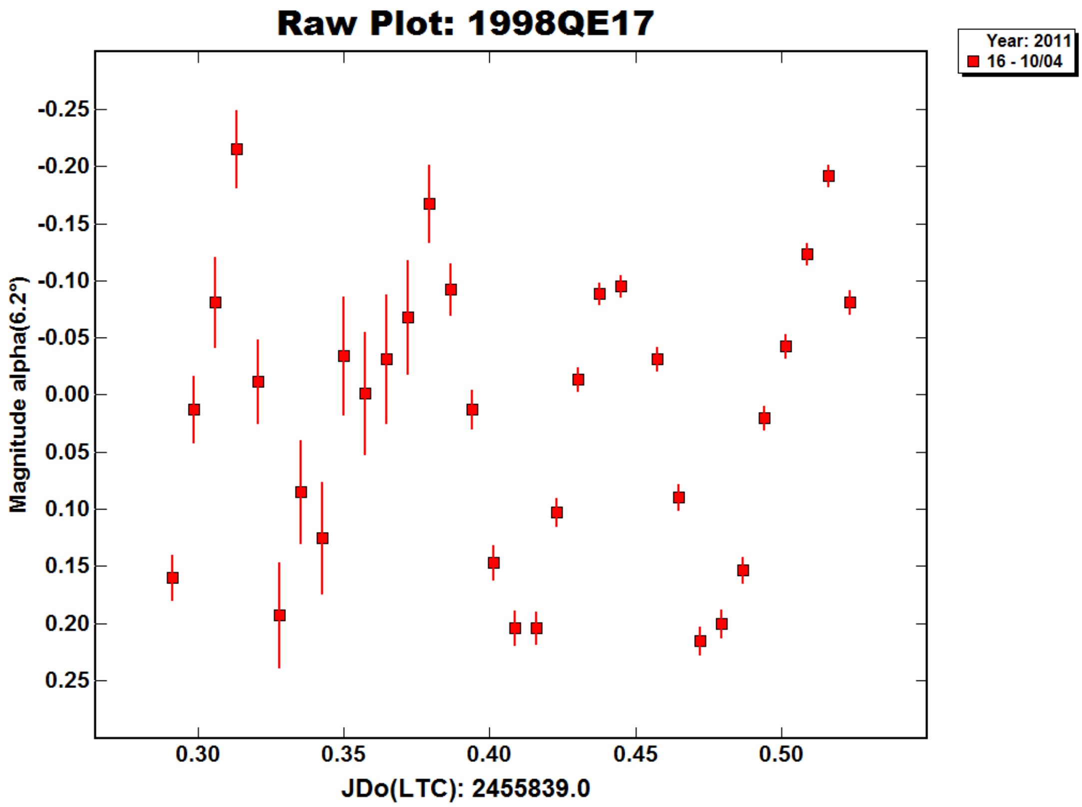

Figure 4.27: Raw data of 04-10-2011

We had three nights of observations (Figures 4.27-4.28). We extracted the light-curve and calculated its period, P = 3.227 ± 0.085 h, and amplitude, A = 0.45 mag (Figure 4.29). Considering previous observations the rotation period was double: 6.4 h. We believe that in those data was fitted in a wrong mode. Our result agrees with the simultaneous observations, 3.226 ± 0.001 h, [Ferrero, 2012].

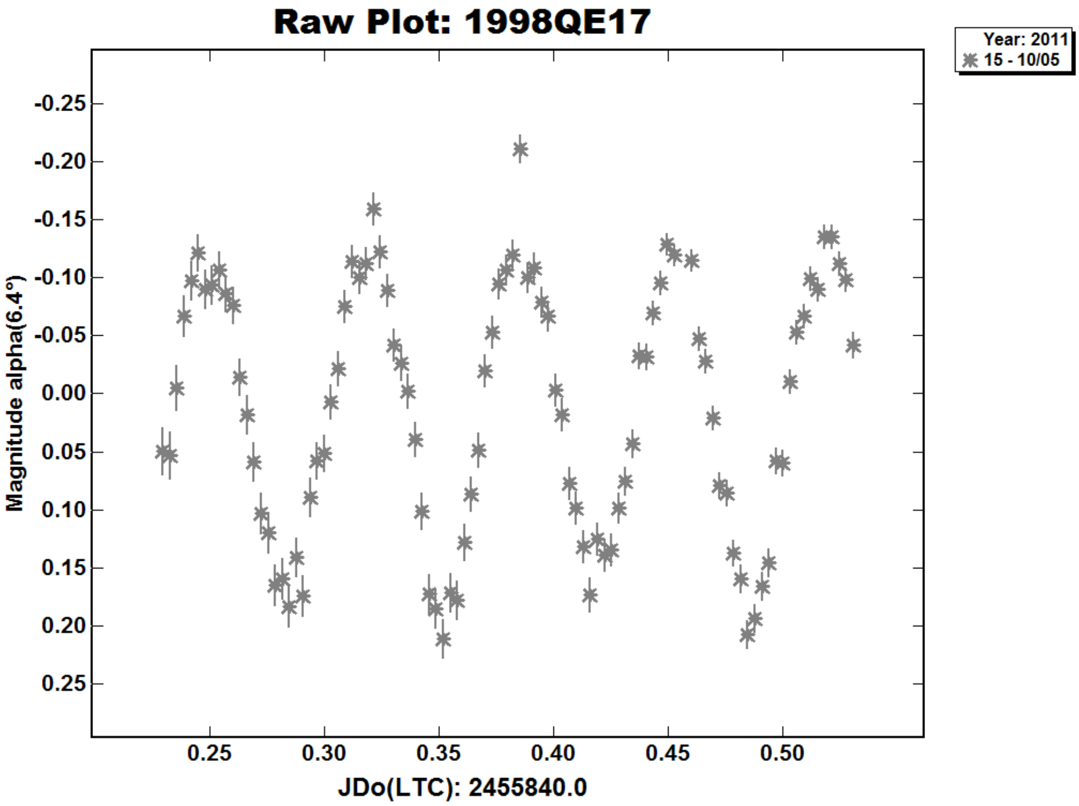

Figure 4.28: Raw data of 05-10-2011

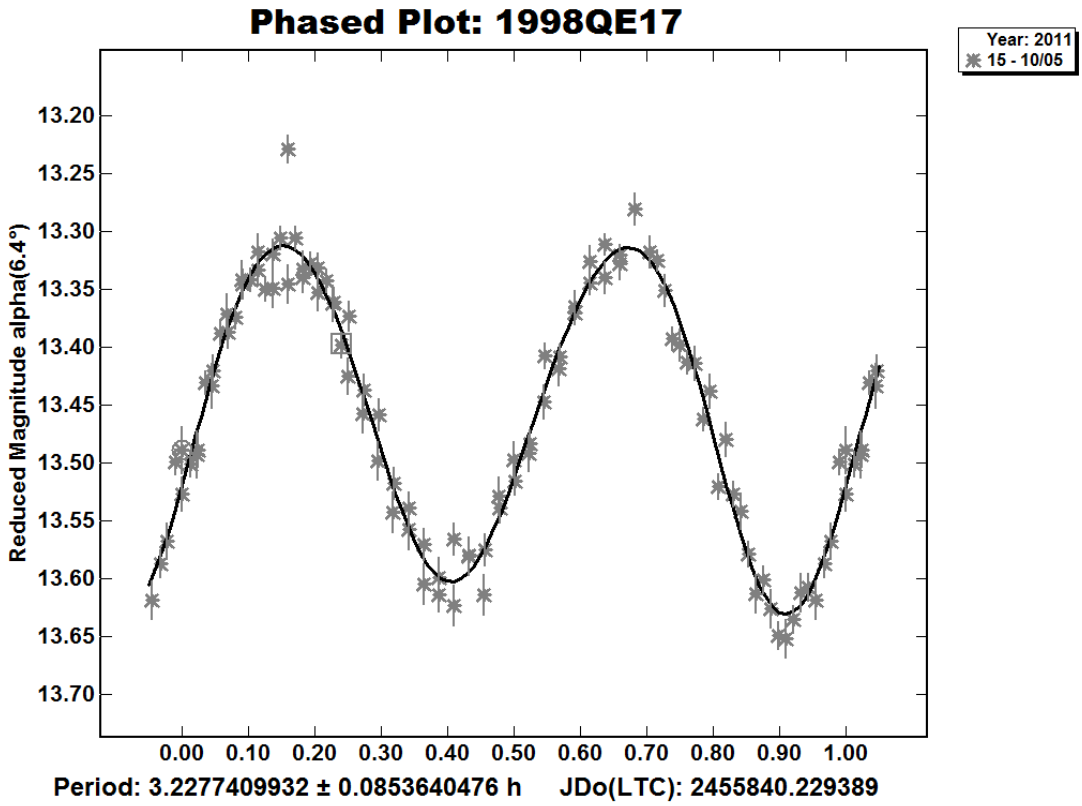

Figure 4.29: The CLC of (16959) using only the second night's data

4.4.6 (32910) 1994TE15

	El.	Ph.	V	rate(arcsec/min)
13-08-2010	168.1	7.1	15.7	0.5
15-08-2010	168.0	7.2	15.7	0.5
16-08-2010	167.8	7.3	15.7	0.5

Table 4.10: (32910) Ephemeris

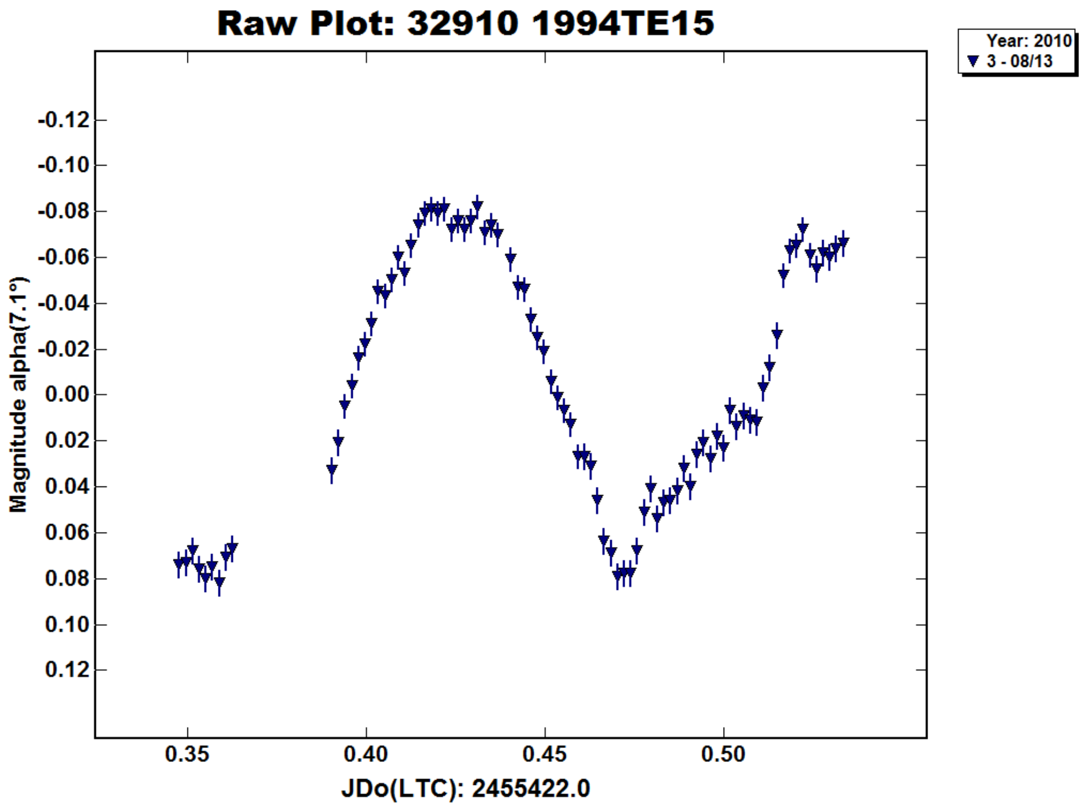

Figure 4.30: Raw plot of 13-08-2010

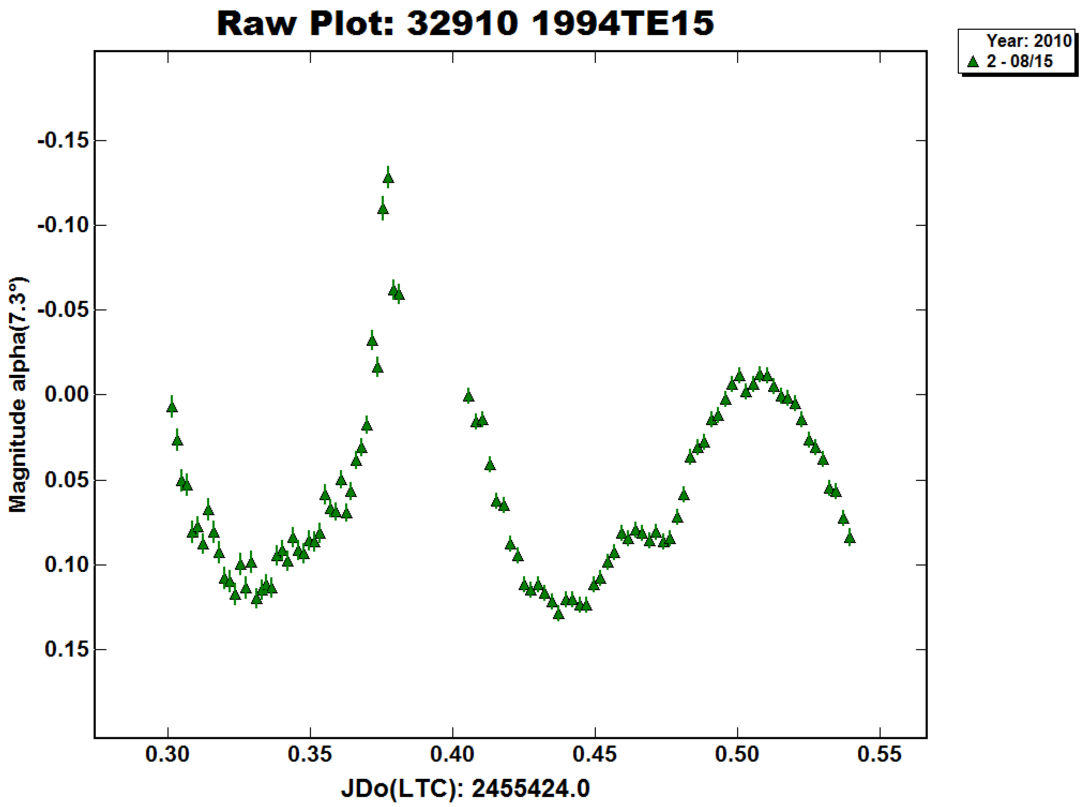

Figure 4.31: Raw plot of 15-08-2010

The target was observed for 3 nights (Figures 4.30-4.32). The amplitude of the light-curve is A = 0.13 mag and the period was calculated as P = 5.559 ± 0.0249 h (Figure 4.33).

The inner Main Belt is very chaotic. This is caused by the mean motion resonances with Mars and three-body resonances, Mars-Jupiter-asteroid, which are combined so that the asteroid's orbit slowly migrate in eccentricity. This chaotic diffusion leads many bodies to become Mars-crossers. (32910) 1994 TE15 was selected because it has close encounters with Mars. The trajectory of the asteroid was numerically integrated using the swift-whm and swift-rmvs3 routines from the *SWIFT package* [Levison and Duncan, 1994]. The eight planets were considered in the integrations. As we can understand, from the changes of its semi-major axis versus time (Figure 4.34), it has close encounters with Mars, but not so strong in order for it to be ejected from the main belt (Figures 4.35-4.36).

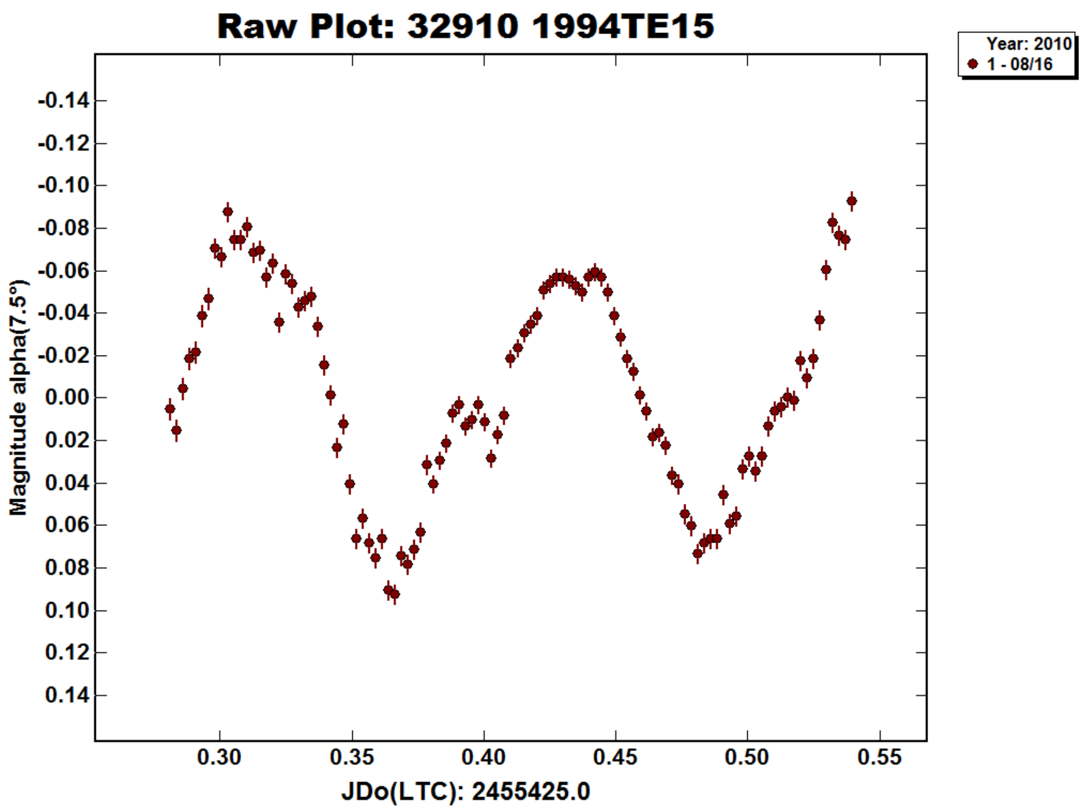

Figure 4.32: Raw plot of 16-08-2010

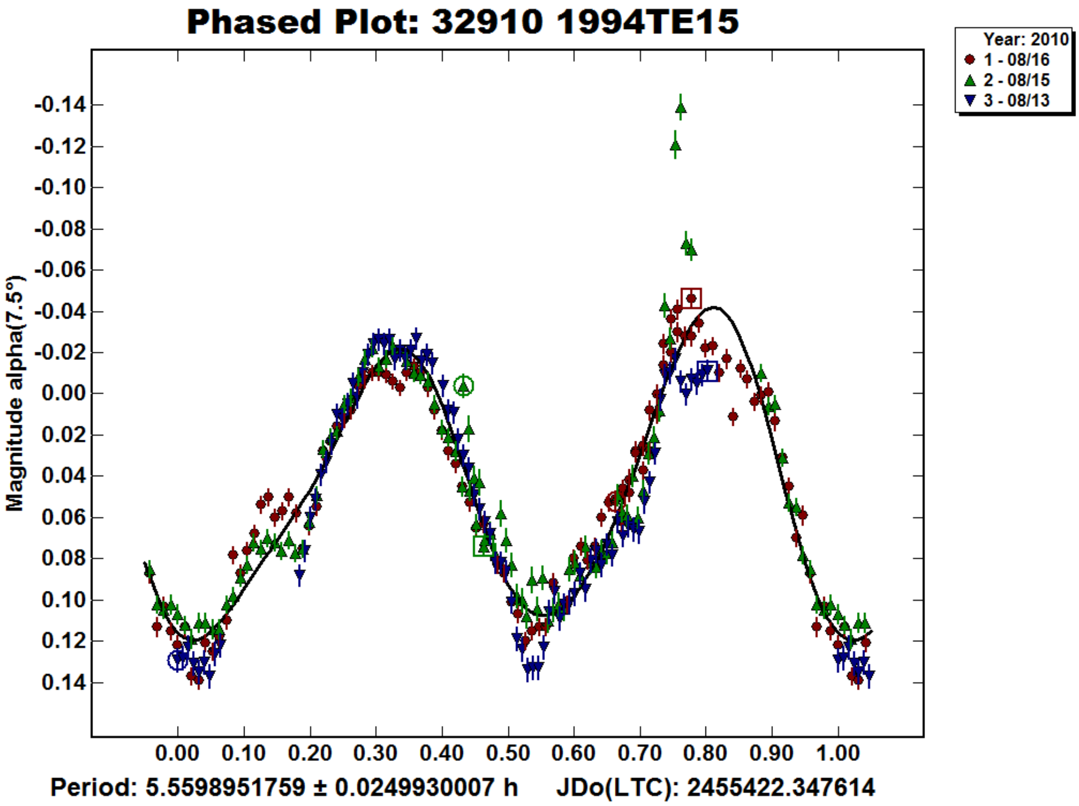

Figure 4.33: The CLC of (32910)

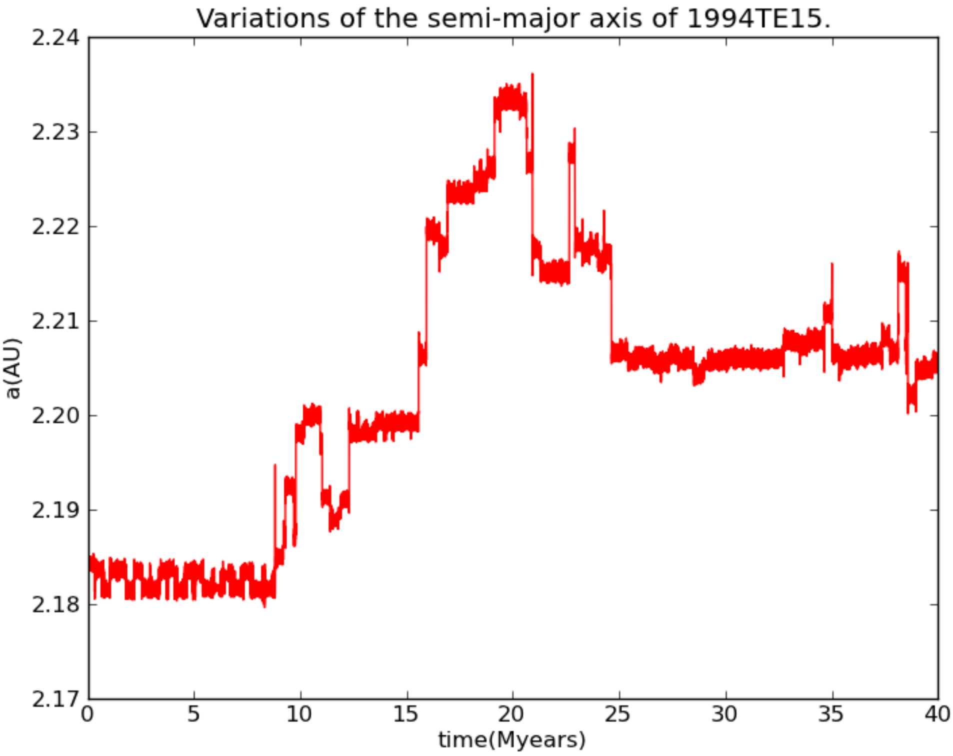

Figure 4.34: Variations of the semi-major axis of (32910)

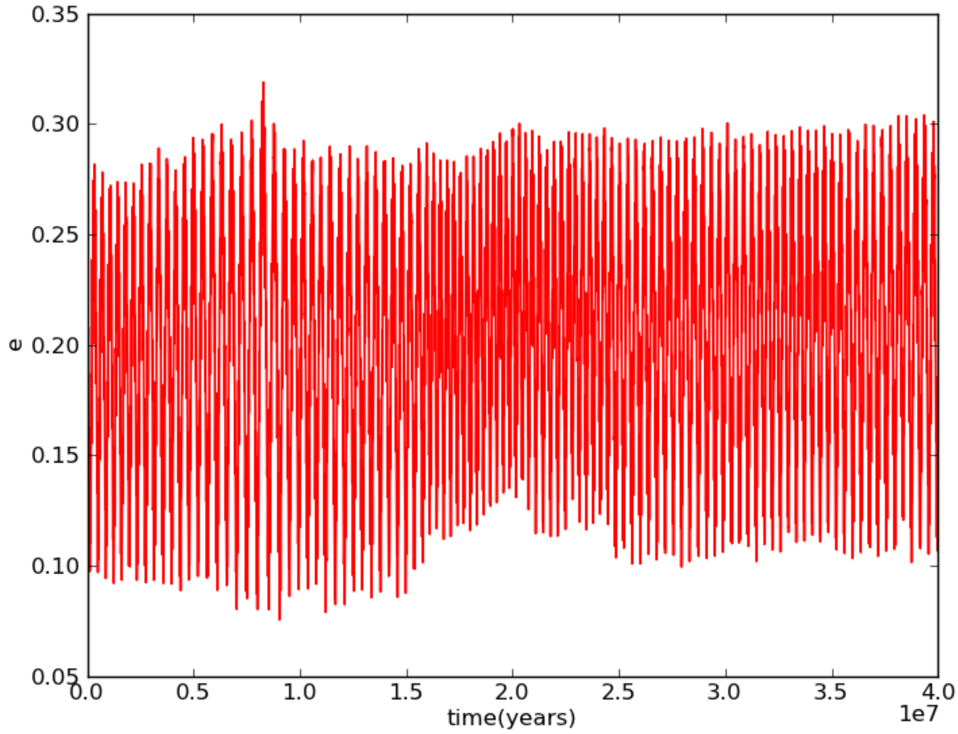

Figure 4.35: Variations of the eccentricity of (32910)

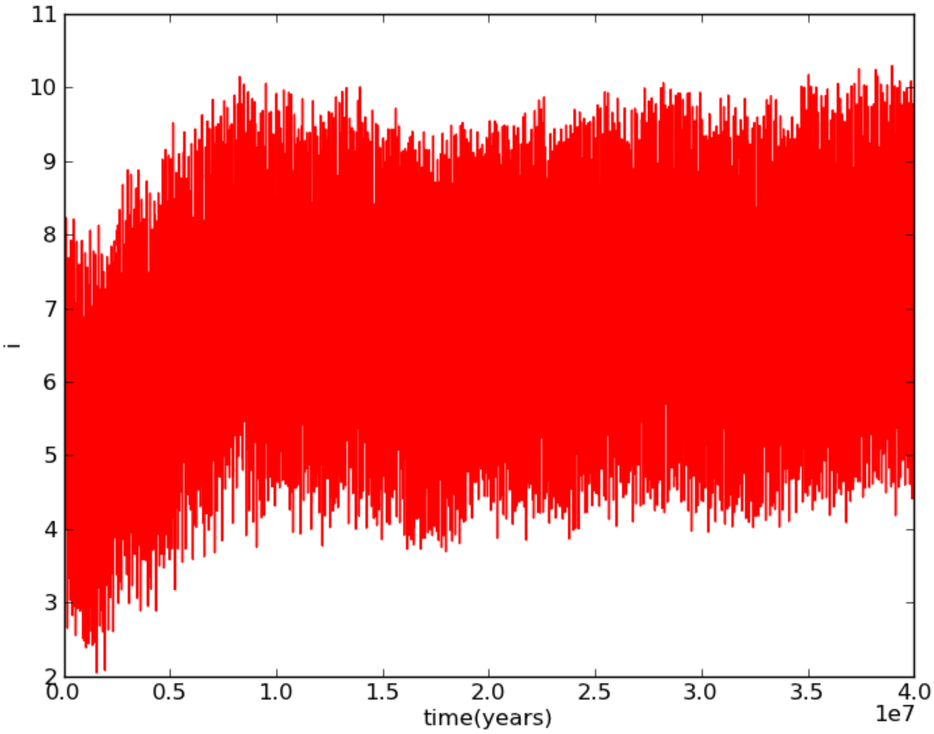

Figure 4.36: Variations of the inclination of (32910)

Chapter 5

Conclusions

The initial intention of the project was the calculation of the rotation period of some main belt asteroids but also the extraction of their shape and the determination of the orientation of their spin axis. We focused on relatively bright targets with either unknown or short rotation periods. Unfortunately, we were not able to finish the whole procedure. Many reasons contributed to this result. The main factor for not observing more targets or not re-observe the same was the weather conditions, like humidity or wind. Another one is the maximum apparent magnitude limitations from the instrumentation. In addition, the location of the telescopes disabled the all-night observations due to the natural obstacles in the area, like the trees in the West or a few road lights in the East.

Despite all the difficulties that appeared at times, we managed to have the total phase diagram of the three of the targets. Together we calculated the rotation period of them. The rotation period of (266) Aline was found almost the same with previous observations. The rotation period of (16959)1998QE17 was found the half of the previous observation, however we ended up to the conclusion that our observations and data analysis was more accurate than the past. Further simultaneous observations of another team confirmed ours. (32910) 1994TE15 is an interesting object as it belongs to Mars-crossers group and we were the first who gave its light-curve in public and confirmed the rotation period with Pravec's announcement in JPL (Jet Propulsion Laboratory) .

From this project came of some publications. First of all there was a presentation in a workshop at California Institute of Technology in July 2011. After that the period of (32910) 1995TE15 was mentioned in JPL's small-body database [JPL, 2011]. Two months later in September 2011, two posters were submitted in the 10^{th} Conference of the Hellenic Astronomical Society [10th Hel.A.S Conference Ioannina, 2011a], [10th Hel.A.S Conference Ioannina, 2011b]. In March 2012 a paper which presented the total work on asteroids was submitted in Minor Planet Bulletin and published on 25^{th} of June 2012 in issue 39-3 [MPB, 2012].

Hopefully this work is going to continue at least for the next year when more new targets will be observed. Most of the difficulties that we faced the previous years do not exist any more. So the project is very promising to give more and more accurate results.

References

10th Hel.A.S Conference Ioannina. Calculation of the rotational period of the 'mars crosser' asteroid (32910) 1994te15, 2011a. URL `http://www.helas.gr/conf/2011/posters/S_1/avdellidou.pdf`. 120

10th Hel.A.S Conference Ioannina. Aristotle university astronomical station at mt.holomon, 2011b. URL `http://www.helas.gr/conf/2011/posters/S_5/avdellidou.pdf`. 120

L. Alvarez, W. Alvarez, and S. Klint. Asteroid-Caused Extinctions. *Science News*, 117:22, 1980. 37

P. Bendjoya, E. Slezak, and C. Froeschle. The wavelet transform - A new tool for asteroid family determination. *aap*, 251:312–330, November 1991. 51

W. F. Bottke, Jr., D. Vokrouhlický, D. P. Rubincam, and D. Nesvorný. The Yarkovsky and Yorp Effects: Implications for Asteroid Dynamics. *Annual Review of Earth and Planetary Sciences*, 34:157–191, May 2006. doi: 10.1146/annurev.earth.34.031405.125154. 16

S. J. Bus and R. P. Binzel. Phase II of the Small Main-Belt Asteroid Spectroscopic SurveyA Feature-Based Taxonomy. *icarus*, 158:146–177, July 2002. doi: 10.1006/icar.2002.6856. 55

B. Carry. Density of asteroids. *ArXiv e-prints*, March 2012. xiii, 63, 64

A. Cellino, P. Tanga, A. Dell'Oro, and D. Hestroffer. Asteroid science with Gaia: Sizes, spin properties, overall shapes and taxonomy. *Advances in Space Research*, 40:202–208, 2007. doi: 10.1016/j.asr.2007.03.011. 61

L. M. Close, W. J. Merline, D. Tholen, T. Owen, F. Roddier, and C. Dumas. Adaptive Optics Imaging of Pluto-Charon and the Discovery of a Moon aroun d the Asteroid 45 Eugenia: The Potential of Adaptive Optics in Planetary Astrono my. In *Bulletin of the American Astronomical Society*, volume 31 of *Bulletin of the American Astronomical Society*, page 1585, December 1999. 59

F. DeMeo and R. P. Binzel. Comets in the near-Earth object population. *Icarus*, 194:436–449, April 2008. doi: 10.1016/j.icarus.2007.10.011. 22

J. Durech, V. Sidorin, and M. Kaasalainen. DAMIT: a database of asteroid models. *aap*, 513:A46, April 2010. doi: 10.1051/0004-6361/200912693. 72

A. Ferrero. Lightcurve Determination at the Bigmuskie Observatory from 2011 July-December. *Minor Planet Bulletin*, 39:65–67, April 2012. 107

R. Gomes, H. F. Levison, K. Tsiganis, and A. Morbidelli. Origin of the cataclysmic Late Heavy Bombardment period of the terrestrial planets. *Nature*, 435:466–469, May 2005. doi: 10.1038/nature03676. 17

K. Hirayama. Groups of asteroids probably of common origin. *aj*, 31:185–188, October 1918. doi: 10.1086/104299. 50

JPL. Jpl small bodies database, 2011. URL `http://ssd.jpl.nasa.gov/sbdb.cgi`. 120

H. F. Levison and M. J. Duncan. The long-term dynamical behavior of short-period comets. *icarus*, 108:18–36, March 1994. doi: 10.1006/icar.1994.1039. 112

H. F. Levison, A. Morbidelli, C. Vanlaerhoven, R. Gomes, and K. Tsiganis. Origin of the structure of the Kuiper belt during a dynamical instability in the orbits of Uranus and Neptune. *Icarus*, 196:258–273, July 2008. doi: 10.1016/j.icarus.2007.11.035. 14

S. C. Lowry, A. Fitzsimmons, P. Pravec, D. Vokrouhlický, H. Boehnhardt, P. A. Taylor, J.-L. Margot, A. Galád, M. Irwin, J. Irwin, and P. Kusnirák. Direct Detection of the Asteroidal YORP Effect. *Science*, 316:272–, April 2007. doi: 10.1126/science.1139040. 21

A. Milani, M. Carpino, G. Hahn, and A. M. Nobili. Dynamics of planet-crossing asteroids - Classes of orbital behavior. *Icarus*, 78:212–269, April 1989. doi: 10.1016/0019-1035(89)90174-7. 26

A. Morbidelli, H. F. Levison, K. Tsiganis, and R. Gomes. Chaotic capture of Jupiter's Trojan asteroids in the early Solar System. *Nature*, 435:462–465, May 2005. doi: 10.1038/nature03540. 16

MPB. Minor planet bulletin, 2012. URL `http://www.minorplanet.info/MPB/MPB_39-3.pdf`. 120

E. M. Shoemaker. Asteroid and comet bombardment of the earth. *Annual Review of Earth and Planetary Sciences*, 11:461–494, 1983. doi: 10.1146/annurev.ea.11.050183.002333. 25

D. J. Tholen. *Asteroid taxonomy from cluster analysis of Photometry.* PhD thesis, Arizona Univ., Tucson., September 1984. 54

K. Tsiganis, R. Gomes, A. Morbidelli, and H. F. Levison. Origin of the orbital architecture of the giant planets of the Solar System. *Nature*, 435:459–461, May 2005. doi: 10.1038/nature03539. 15

D. Vokrouhlický and D. Nesvorný. Pairs of Asteroids Probably of a Common Origin. *aj*, 136:280–290, July 2008. doi: 10.1088/0004-6256/136/1/280. xiii, 67

V. Zappala, A. Cellino, P. Farinella, and Z. Knezevic. Asteroid families. I - Identification by hierarchical clustering and reliability assessment. *aj*, 100: 2030–2046, December 1990. doi: 10.1086/115658. 51